MODELLING ENGINE PERFORMANCE AND EMISSIONS FUELED BY BIODIESEL BLENDS FOR OPTIMAL OPERATION

VITALIS KIBIWOT NGELECHEI

A Thesis Submitted to the Graduate School in Partial Fulfillment of the Requirements for the Doctor of Philosophy Degree in Agricultural Engineering of Egerton University

EGERTON UNIVERSITY

SEPTEMBER 2024

DECLARATION AND RECOMMENDATION

Declaration

I declare that this thesis is my original work and that it has not been wholly or in part presented for an award of any degree in Egerton University or any University known to me.

Signature: 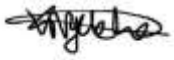 Date: September 9th 2024

Vitalis Kibiwot Ngelechei

BD11/41506/15

Recommendation

This thesis has been submitted with our approval as the University Supervisors;

Signature: _ 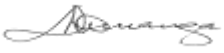 Date: September 9th 2024

Prof. Daudi M. Nyaanga, PhD

Department of Agricultural Engineering

Egerton University

Signature:  Date: September 9th 2024

Dr. Musa R. Njue, PhD

Department of Agricultural Engineering

Egerton University

Signature:  Date: September 9th 2024

Prof. George O. Owino, PhD

Department of aerospace Engineering

Technical University

COPYRIGHT

DEDICATION

This work is dedicated to Almighty father, my beloved children and in honor of my late wife. To you, my late wife, Alexia Walegwa (for sure you were looking forward to seeing me graduate), receive my special dedication, through the Lord, for your understanding, support, loyalty, and love for it shall never be forgotten. Forgive my offences to you. Rest in peace 'my love', till we meet again and may your spirits live within our entire family forever.

ACKNOWLEDGEMENTS

I would like to thank the Almighty God for His Grace throughout my academic journey to this extent. Thanks to the African Development Bank (AfDB) for funding the study in collaboration with Egerton University through the efforts and stewardship of Prof J. Onyando. Thanks to Jomo Kenyatta University of agriculture and technology (JKUAT) for her provision of engine test equipment. Special appreciation to my supervisor, Prof D. Nyaanga, Dr M. Njue and Prof. G. O. Owino, for their invaluable support, encouragement, detailed review of the manuscripts at every stage to ensure successful completion of the study.

I wish to also express my special thanks to my colleagues in the postgraduate programme, especially Dr M. Korir of the Faculty of engineering Egerton University for their invaluable assistance and constructive contributions throughout the compilation of this thesis. Appreciation to Sally Kiplagat of Library, Egerton University, for assistance in guidance in the literature search engines and in addition, to emotional support, co-operation, friendship, occasional humour, and social interactions, which enabled me to stay focused in the final stages of this study.

Sincere thanks to my family for the kind support. Big thank you to my dear beloved late wife, Alexia Waleghwa Mwashigadi (gone but not forgotten), for her continuous moral support and encouragement throughout my PhD journey (left us in the final stages of the study). To my father, the late Kiptarus Arap Ngelechei, your support for my education has made me go this far. To you Mama Teresia Tarus, my beloved mother, for her kind support and encouragement throughout my study journey and particularly, during my difficult time of loss of my wife. To my children (Maryann Jemutai, David Kiprop, Moses Kibet, Scolastica Jepchumba, John Kangogo, and Jayden Kiptum) and siblings for their understanding, patience, and encouragement throughout this journey. To John Mwashigadi's family (In-laws), I am short of words to express my greatest appreciation for the moral support and wishing me well and your desire to see me continue with my studies, particularly after my wife's demise.

Finally, thanks to all of you not directly mentioned, for the assistance rendered during the study.

I salute you all.

ABSTRACT

Engines fueled by diesel play a pivotal role in today's economy, especially in agriculture and transport sectors. However, concerns over diesel-related greenhouse gas (GHG) emissions and its depletion of reserves has spurred interest in biodiesel as an alternative fuel. Biodiesel blends were introduced to address reduced engine power and efficiency due to poor fuel atomization. However, determining optimal biodiesel blend level for engine performance has proven a challenge due to their diverse properties and combustion behaviors since they are sourced from different oils. This research aims to model engine performance and emission fueled by biodiesel blends to optimize the engine operation. Use of biodiesels blends could significantly reduce dependence on imported oil, stimulate the economy by creating jobs and reduce vulnerability and decreasing reliance on global oil. The research developed mathematical models using Buckingham pi-theorem for brake thermal efficiency (Bte), specific fuel consumption (Sfc), carbon monoxide (CO) emissions and nitrogen oxides (NOx) emission for an engine fueled by different biodiesel blends. The performance and emission tests were carried out using a 3.5 kW one cylinder four stroke engine on a test rig connected to an eddy current electric dynamometer. The fuels used for experiments were WVO, canola, oleander, sunflower and coconut biodiesels blended at 10%, 15%, 20%, 25% and 30% with diesel, to run the engine operated at speeds of 1500 rpm and loaded at 0, 3, 6, 9 and 12 kg. Finally, the Non-Dominated Sorting Genetic Algorithm II (NSGA II) method was used to determine the biodiesel blending for optimal engine operation. The study established that biodiesel; densities ranged between 872 to 925 kg/m^3; kinematic viscosity of 4.2 to 5.2 mm^2/s and Lower heat value from 36200 to 39400 kJ/kg The results observed lower Bte and CO emissions, while Sfc and NOx emission were higher for engine fueled with biodiesel blends as compared those of diesel fuel. The developed mathematical model predicted Bte, Sfc, CO and NOx with error margins of 1.65%, 15.98%, 4.69% and 2.78 % respectively as compared to the experimental results. The study successfully developed a mathematical model to predict Bte, Sfc, NOx, and CO emissions for CI engines fueled by biodiesel blends. It also identified optimal blend levels to be 22.5, 21.9, 20.6, 19.98 and 19.6 percent for biodiesel; WVO, canola, oleander, sunflower and oleander which gave the Bte as 21.9, 23.6, 23.3 23.7 and 23.0 while NOx as 139.0, 135.3, 135.9, 134.9 and 136.5 respectively. While the model provides a foundation for simulating biodiesel blend combustion in CI engines, future studies should expand its inputs to cover a broader range of biodiesel properties, engine types, and real-world operating conditions is essential, enhance the model's accuracy and reliability, making it a more versatile tool for optimizing biodiesel blends.

TABLE OF CONTENTS

LIST OF TABLES

LIST OF FIGURES

LIST OF PLATES

LIST OF ACRONYMS AND SYMBOLS

AF	: Air-Fuel Ratio
ANOVA	: Analysis of Variance
ASTM	: American Standard Test and Measurement
B0	: Diesel
B10	: Blend of 10% Biodiesel 90% Diesel
B100	: Pure biodiesel
B15	: Blend of 15% Biodiesel 85% Diesel
B20	: Blend of 20% Biodiesel 80% Diesel
B25	: Blend of 25% Biodiesel 75% Diesel
B30	: Blend of 30% Biodiesel 70% Diesel
BMEP	: Brake Mean Effective Pressure
Bp	: Brake power
Bte	: Brake Thermal Efficiency
CAD	: Crank-shaft advance
CI	: Compression Ignition
Cv	: Lower Heating Value
DICI	: Direct Injection Compression Ignition
e-constraint	: epsilon constraint
ECU	: Electrical control unit
EGR	: Exhaust Gas Recirculation
EN	: European Nations standard
EPA	: Environmental Protection Agency
ES	: Evolutionary Strategies
FAME	: Fatty acid methyl ester
FEA	: Finite Element Analysis
FFA	: Free Fatty Acids
GA	: Genetic algorithm
GHG	: Greenhouse gases
HC	: Hydrocarbons
HHV	: Higher Heating Value

ICE : Internal Combustion Engine

IEAI : International Energy Agency

Ip : Indicated power

JKUAT : Jomo Kenyatta University of Agriculture and Technology

KIRDI : Kenya Industrial Research and Development Institute

KNBS : Kenya national bureau of statistics

KPC : Kenya Pipeline Company

SEM : Least Significant Difference

MOPSO : Multi-objective particle swarm optimization

NEMA : National environmental management association

NOx : Nitrogen Oxides

NSGA II : Non-Dominated Sorting Genetic Algorithm II

PM : Particulate matter

PSO : Particle swarm Optimization

Rpm : Revolution per minute

SEM : Standard Error of the Mean

Sfc : Specific Fuel Consumption

SOC : Start of combustion

SOI : Start of injection

SPEA2 : Strength Pareto based genetic algorithm

SPH : Smoothed-particle hydrodynamics

USEM : Ultra-low Sulphur diesel

VCR : Variable compression reactions

WVO : Waste Vegetable Oil

Cv : Calorific value

ρ : Density

v : Kinematic viscosity

CHAPTER ONE
INTRODUCTION

1.1 Background information

Energy remains a crucial driver for economic development, enhancing quality of life, overall human welfare, and other socio-economic advancements (Hussain *et al*., 2020). The industrial revolution, which began in the late 18th and early 19th centuries, sparked a massive increase in demand of energy across all the sectors especially in transportation, manufacturing, and agriculture (Bereczky *et al*., 2014). During the 19th century, global energy consumption was primarily characterized by the extensive use of biomass and the introduction of coal fueled industrialization. Fossil fuels (crude oils), natural gas, and nuclear energy becoming predominant as technological progress and economic growth accelerated in the 20th century. In the 21st century, there was been a shift towards renewable energy sources such as biofuels, natural gas, and hydropower, driven by environmental concerns (Ghazali *et al*., 2015). For example, studies of Menga (2022) illustrated that petroleum fuels (crude oil) accounted for approximately 31.6 percent of global energy consumption by 2022, in contrast to renewable energy sources, which contributed 7.5 percent. Petroleum fuels were a significant primary energy source for engines due to their plentiful supply, affordability (Abed *et al*., 2019), high combustion efficiency, reliability, adaptability, and ease of handling (Mahmudul *et al*., 2017). However, in recent years, the supply of petroleum has decreased while the demand for petroleum fuels has significantly risen. For example, in the past few decades, global petroleum fuel consumption has grown from 93 million barrels per day in 2018 to over 100 million barrels per day (Aydin *et al*., 2020; Mahmudul *et al*., 2017). This increase led to significant depletion of crude oil reserves in oil-producing countries, with World Bank forecasting a 75% reduction in crude oil reserves by 2050 (Ağbulut & Sarıdemir, 2021). Petroleum fuels are burned in the cylinders of internal combustion (IC) engines to generate mechanical power. IC engines are classified based on the type of fuel it uses into, spark ignition (SI) engines and compression ignition (CI) engines (Heywood, 1988). CI engines were primarily designed to run optimally on diesel fuel and have for a long time been used predominantly in heavy machinery, transportation, agriculture, and light industries due to their high thermal efficiency and low fuel consumption (Al-manea *et al*., 2022; Zheng et al., 2009). However, these engines emit significant amounts of greenhouse gases (GHG) from their exhausts, including carbon dioxide (CO_2), carbon monoxide (CO), unburned hydrocarbons (HC), nitrogen oxides (NOx), and particulate matter (PM) (Lindstad & Rialland, 2020; Menga, 2022; Ni *et al*., 2020). For instance, burning one (1) kg of diesel

in a CI engine produces approximately three point two (3.2) kg of CO_2, contributing to about twenty five (25) percent of global CO_2 emissions (Leach *et al*., 2020). The focus on GHG emissions has increased in recent years due to their negative impacts on environmental pollution, global warming, and human health (Burchart-Korol & Folęga, 2019; Strezov & Cho, 2020). Consequently, environmental regulations have imposed stricter standards to control emission levels (; Elumalai *et al*., 2021; Lindstad & Rialland, 2020). To address these challenges, researchers have explored various renewable energy options including biodiesel, producer gas, hydrogen and butanol.

In recent years, biodiesel has emerged as a promising substitute for fossil diesel globally due to its reliability and compatibility with existing diesel engines thus requiring little/no modification and its ability to reduce greenhouse gas emissions (Aydin, 2020; Soudagar *et al*., 2021). Additionally, biodiesel utilizes locally available resources and improves diesel engine lubricity, leading to reduced wear and longer engine life (Al-manea *et al*., 2022). Biodiesel is a renewable, non-toxic fuel composed of long-chain fatty acids and mono-alkyl esters, derived from the triglycerides in vegetable oils or animal fats through a process called transesterification (Bajpai *et al*., 2006; Barnwal & Sharma, 2005). Biodiesel is derived from vegetable oils produced mainly from crops such as sunflower, soybeans, mustard, canola, peanut, cotton, *Jatropha curcas*, croton, castor seeds, coconuts, palm, and various locally available odiferous vegetation (Verma & Singh, 2018). Biodiesel has similar fuel properties (lower heating value, flash point, and cetane number) to diesel. Additionally, it is a renewable fuel, less toxic, and biodegradable, thus environmentally friendly when used to run engines. The use of biodiesel as a fuel is not a new development; it is as old as the diesel engine itself. Rudolph Diesel, the inventor of the diesel engine in 1892, used peanut oil to run one of his engines at the Paris Exposition (Senda *et al*., 2004). As depicted in figure 1.1 below, the biodiesel cycle, often referred to as the "carbon neutral cycle," highlights how CO_2 emissions are absorbed by oil plants through photosynthesis. These plants are subsequently harvested and processed into biodiesel. When biodiesel is burned, it releases CO_2 back into the atmosphere, which is then reabsorbed by new plants, thus completing the cycle, thus theoretically results in net-zero additional CO_2 emissions. The lifecycle of CO_2 emissions demonstrates that biodiesel can reduce emissions by 50-80% compared to petroleum diesel. The figure below highlights the benefits of using biodiesel.

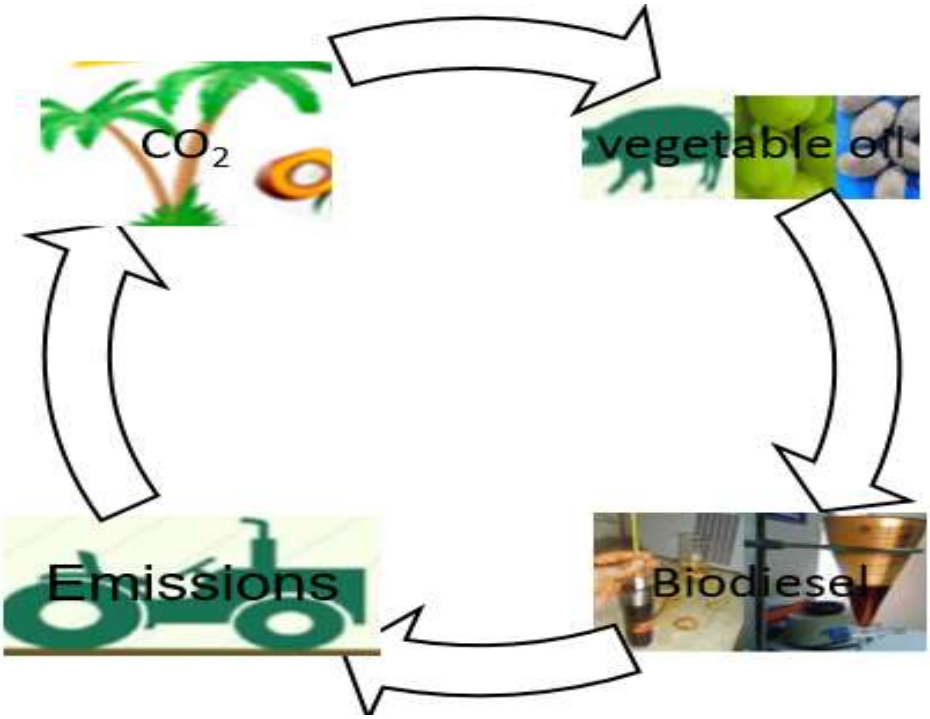

Figure 1.1: Biodiesel cycle

Currently, the use of biodiesel in CI engines has been reported in several countries, particularly where government support exists (Tveit, 2015). According to the International Energy Agency (IEA), the biodiesel industry has experienced rapid growth, with global production increasing tenfold from 2000 to 2008 (Verma & Singh, 2014). Biodiesel (methyl esters) fuel has been the preferred substitute for diesel engines because it possesses characteristics like diesel (Knothe & Razon, 2017), allowing for direct application with little or no engine modification while reducing greenhouse gas emissions (Ashok, 2017; Hoekman *et al*., 2012; Mofijur, 2019; Ogunkunle, 2020). Additionally, biodiesel contains oxygen in its structure, which helps improve combustion in engines compared to diesel fuel (Janaun & Ellis, 2010). For instance, Kenya's vegetable oil production in 2021 was approximately 160,000 metric tons (Nyakundi, 2022), from several types of vegetable oils including sunflower, coconut, jatropa and cottonseed. The country still falls short of satisfying domestic demand, relying on supplies of imports (Vadivelu *et al*., 2022), a great concern on the viability of biodiesel production, however in response, the government has introduced policies aimed at increasing domestic production and promoting sustainable practices.

Engines running on biodiesel fuel, unfortunately, have been associated with reduced performance, brake power, thermal efficiency, and increased fuel consumption (Verma & Singh, 2014;

Vadivelu *et al*., 2022). The reduced performance was attributed to biodiesel's lower heat value and higher viscosity as compared with diesel since a fuel with a lower heat value results in low brake power, in contrast, higher viscosity leads to poor atomization, both leading to power loss in an engine (Peterson *et al.*, 1990). A low cetane number implies the energy release is reduced, as reported by studies by Gupta *et al.* (2007). Conditions that ensure good fuel economy and complete combustion typically lead to higher in-cylinder temperatures, which, unfortunately, create better conditions for the oxidation of nitrogen, thus increasing its oxides emissions (Mueller *et al*., 2009; Zhang *et al*., 2015). Biodiesel blends have been used as a trade-off to achieving reduced toxicity of exhaust emission s and improved engine performance (Myo, 2008). However, the influence of biodiesel blends on engine performance and vary depending on the quality and origin of biodiesel (Chaichan *et al*., 2013; Ghazali *et al*., 2015; Humphreys *et al*., 2021; Senda *et al*., 2004). Thus, it was imperative to comprehensively evaluate, explore and account for the properties of the biodiesels.

The major challenge, however, was to determine the optimal biodiesel-diesel blend ratios for different feedstock's that maximize the performance of CI engines. Earlier studies have reported variability in engine performance and emission characteristics for blends with similar fuel parameters (Lapuerta *et al*., 2008). These differences are attributed to the fact that biodiesel is produced from various vegetable oil feedstock's, which possess different physical and chemical properties (Powell *et al*., 2010; Tveit, 2015). These properties affect combustion processes and mechanisms differently (Krishnakumar *et al*., 2021), significantly impacting diesel engine performance. The fatty acid composition, higher oxygen content, and chemical stability of biodiesel blends compared to petroleum diesel result in improved combustion, reduced emissions, and decreased energy content (Soudagar *et al*., 2021; Vadivelu *et al*., 2022). The fatty acid composition of biodiesel affects its properties, such as viscosity and energy content, which in turn impact engine performance due to the presence of unsaturated fatty acids. However, Agarwal *et al*. (2017) noted that efficiency strongly depends on the biodiesel feedstock, with sources high in unsaturated fats generally showing better performance. Similar conclusions were reached by Humphreys *et al*. (2021) who experimentally tested jatropha, neem, and mahua biodiesel blends in a diesel engine.

Knowledge on the blending of biodiesel is crucial for ensuring its viability as an alternative to polluting diesel. Therefore, to comprehend the effects of operational fuel properties, it was imperative to employ experimental setups to accurately determine the relationship between blend levels and brake thermal efficiency of biodiesel blends. Unfortunately, this necessitated setting up numerous

experimental investigations aimed at quantifying changes in engine performance when fueled by biodiesel blends compared to diesel. These studies were essential for advancing knowledge about the interaction between properties of biodiesel blends and the intricate combustion processes in engines, thereby enhancing understanding of their environmental benefits and efficiency potentials (Tveit, 2015). Conducting experiments at varying fuel parameter levels to observe their effects on engine performance and emission characteristics can be costly and time-consuming due to the need to generate a vast number of experimental conditions. One of the challenges in developing accurate models for biodiesel blends is accounting for the wide variation in fuel properties depending on the feedstock and production process. To address this, researchers have developed methods to incorporate fuel property variations into their models. Macor *et al.* (2011) proposed a methodology to adapt existing diesel engine simulation models for use with biodiesel blends by introducing correction factors based on fuel properties such as cetane number, oxygen content, and lower heating value. An alternative approach involved using analytical methods, although these have been shown to be less precise (Lapuerta *et al*., 2008). Buckingham Pi theorem offers a structured and efficient approach to developing semi-empirical models for predicting engine performance and emissions parameters. By leveraging dimensional analysis, it provides a powerful tool for simplifying complex engine mechanical and thermodynamics systems to enhance predictive accuracy. Modeling and simulation approaches have proven effective in simulating engine operations by isolating one variable at a time and providing output results based on variations in other variables (Tveit, 2015). Thus, modeling and simulation serve as useful tools for studying engine performance and emission trends of biodiesel/blend-fueled engines, as they are more precise in predicting the outcomes of specific tests and can easily highlight cause-effect relationships between input and output variables. While current engine simulation application is limited due to high-capacity computers.

Biodiesel have emerged as promising alternative to diesel due to its potential to reduce greenhouse gas emissions and enhance energy security, aimed to determine the optimal blend ratios essential for achieving efficient and clean combustion in engines, considering their specific properties. The approach involved using optimization techniques to balance engine performance and emission trade-offs for the blend to offer valuable insights for developing effective and sustainable fuel solutions. The study has filled the critical knowledge gaps of promote integration of biodiesels, crucial for informing government policy decisions regarding future its usage, particularly considering growing

environmental concerns and the necessity to diversify energy sources into existing CI engines through the development of simple and cost-effective models.

1.2 Statement of the problem

The transition towards using biodiesel as a potential substitute for diesel in compression ignition engines has garnered significant attention, driven by concerns over environmental sustainability, health issues, and dwindling reserves. However, operating engines with biodiesel presents challenges due to its inferior properties compared to diesel fuel. Blending biodiesel with diesel has emerged as a promising strategy to improve fuel properties and reduce greenhouse gas emissions. Yet, there remains a lack of understanding regarding the complex interactions between different biodiesel blend properties and their effects on engine performance characteristics (Kalaimurugan *et al*., 2020). Previous research has shown that different biodiesel feedstock sources yield varying engine performance results, reflecting the diverse nature of feedstock oils (Ghazali *et al*., 2015). Experimental studies have attempted to correlate specific fuel properties with engine performance parameters (Sagar, 2022), but often struggle to isolate the interrelationships between simultaneous changes in these properties (Soudagar *et al*., 2021; Vadivelu *et al*., 2022). Furthermore, efforts to employ empirical models have produced less accurate results, while commercial simulation software, though accurate, poses computational complexity and expense challenges (Khan, 2020). The study shall model to predict the performance and emission characteristics of biodiesel fueled engines, to ultimately contributing to environmental sustainability.

1.3 Objectives

1.3.1 Broad objective

To model the performance and emission characteristics of a compression ignition engine fueled by biodiesels' blends to maximize fuel efficiency and minimization emissions.

1.3.2 Specific objectives

The specific objectives of this research were to:

i. Analyze the effect of blending biodiesels and diesel on the fuel properties
ii. Determine the effect of the biodiesels' blends on engine performance and emissions.
iii. Develop mathematical models to predict the effects of biodiesel blends engine performance and emissions.
iv. Establish the biodiesels' blends level for optimal engine operation.

1.4 Research Questions

The research questions for this study were:

i. How does blending of biodiesel with diesel affect its fuel properties?
ii. How do the biodiesels' blends affect engine performance and emissions characteristics?
iii. How does the model predicted engine performance and emissions fueled by biodiesel blends compare to the experimental results?
iv. What are the optimal blend levels for the different biodiesel to give best engine operations?

1.5 Justification of the study

Biodiesel usage could significantly reduce dependence on imported oil, thereby enhancing national security and narrowing the trade deficit. For example, Kenya currently loses 20 to 25 percent of the national import bill of foreign exchange to petroleum; for instance, it imported 5.2 million tons in 2019 (Nyakundi, 2022). Moreover, biodiesel production would support decentralized energy sourcing and provide employment opportunities to foster rural development, while also decreasing reliance on global oil markets and reducing vulnerability to price spikes amid a projected 75% global reduction in crude oil reserves by 2050 (Nyakundi, 2022, Osawa *et al*., 2015). Such initiatives not only address energy concerns but also revitalizes the agricultural sector and promotes rural development while mitigating environmental impact by reducing greenhouse gas emissions estimated at 37 billion tons of CO2 from engines (Aakko-Saksa, 2023; World Bank, 2021).

The study shall provide valuable information on biodiesel to inform government policy decisions regarding future its development. As the world seeks to reduce dependence on fossil fuels and mitigate the environmental impact of transportation, biodiesel remains an important part of the solution, albeit one requiring careful continued refinement.

The study focused on determining optimal blend levels for various biodiesel feedstock, thereby supporting an agile industry constantly seeking cost-effective and reliable new sources. Furthermore, it will develop a mathematical model to simulate engine performance with biodiesel blends, offering researchers with economical method to optimize engine operating conditions improving efficiency while achieving lower emissions through informed blend level trade-offs.

1.6 Scope and Limitations

1.6.1 Scope

The study aimed to characterize various biodiesel blends obtained from local outlets based on density, kinematic viscosity and lower heating value. These biodiesel blends were then tested for their performance and emissions characteristics using a single-cylinder, four-stroke engine at a constant speed of 1500 rpm under varying loads. Key parameters evaluated for optimizing engine performance included brake thermal efficiency, specific fuel consumption, nitrogen oxides and carbon monoxide. To model engine performance and emissions, semi-empirical mathematical models were developed using the Buckingham Pi theorem, experimental data, and MATLAB. Optimization of the engine performance and emissions was carried out using a non-dominated sorting genetic algorithm II (NSGA II). Below is the figure illustrating the theoretical framework.

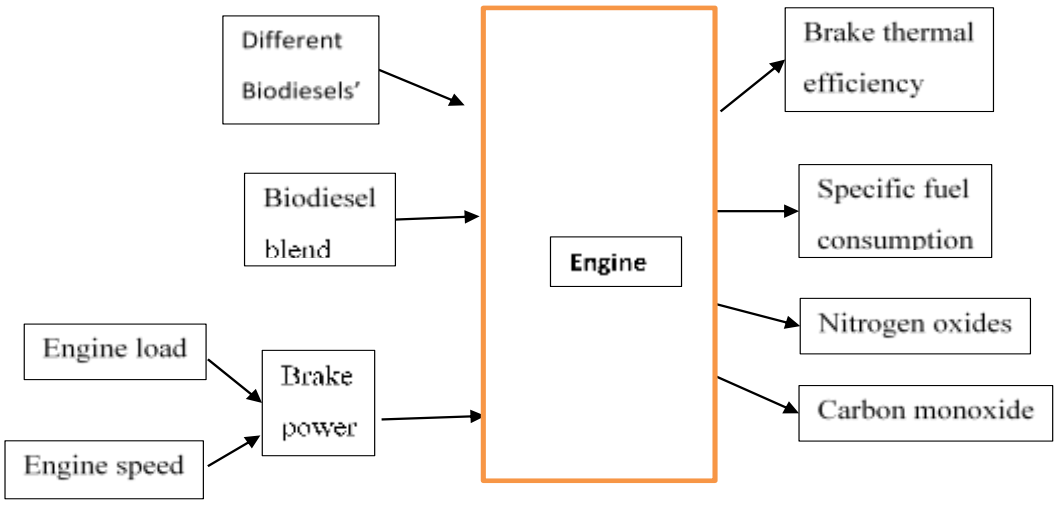

Figure 1.2: Theoretical framework of the engine process

1.6.2 Limitations

The model was developed for a single-cylinder, four-stroke CI engine operated at constant speed of 1500 rpm; compression ratio was set 17.5 and ignition timing of 25.125^{o}C, probably, not fully capturing the performance and emissions characteristics of multi-cylinder engines commonly used in real-world applications. Additionally, biodiesel used was locally sourced and blended at 10 to 30%. Moreover, experiments are conducted in controlled laboratory settings and may not accurately represent real-world engine operating conditions.

1.7 Definition of terms

Biodiesel	:Biodiesel is a non-toxic, long chain fatty acids and mono-alkyl esters produced from triglycerides of vegetable oils or animal fats through the process of trans-esterification
Biodiesel Blends	: Per cent mixture of biodiesel and diesel by volume. "B" factor to state the amount of biodiesel in any fuel mix, such as 20% biodiesel, 80% diesel, is labelled B20.
Biofuel	: Refers to fuel derived from biomass of any known biological matter such as plants and animal fats; solid, liquid, or gaseous.
Brake power	: Power delivered by an engine to the load.
Combustion	: Burning fuel in the presence of air (oxidizer) to produce power and heat while emitting water vapor and greenhouse gases.
Compression Ignition (CI)	: Diesel or compression ignition (CI) is an internal combustion (IC) engine modelled on diesel cycle thermodynamics processes where the fuel mix with air to ignite itself, at sufficient pressure and temperature.
Engine emission	: Greenhouse gases are emitted from engine as a by-product of combustion through exhaust pipe to the environment.
Engine operating conditions	: Engine settings that affect its performance include speed, load, ignition angle, Injection timing, air intake pressure, and fuel injection pressure.
Engine Performance	: Indicator parameters are used to rate the effectiveness of an engine in converting the chemical energy of fuel into useful power and its associated exhaust emissions.
Greenhouse gases	: Polluting gases produced by human activities include carbon dioxide, nitrogen oxides, hydrocarbons, carbon monoxide.
Least Significant Difference (SEM)	: The analysis used in conjunction with ANOVA to compare the means between each pair of groups and there I significant
Mathematical Modelling	: Mathematical modeling is a method of representing real-world systems, or processes using mathematical equations and relationships, to allow for the analysis, prediction, and simulation of its behavior.
Non-premixed combustion	: The presence of sufficient pressure and temperature, a fuel may ignite to allow combustion before it is properly mixed with an air.

Premixed combustion	: Occurs when an ignitable mixture of fuel and air burns very quickly during the ignition delay.
Steady running	: Means continuous operation at the required speed and power output with normal exhaust gas temperature (EGT).
Standard error of mean	: Expected measures of how much the sample mean vary from population mean, that is the amount of variability we would anticipate in calculating sample mean if we repeatedly sampled from the same populations.
Tran-esterification	: Base-catalyzed chemical reaction process at low temperatures and pressures using alcohol (methanol or ethanol) in the presence of a catalyst, such as sodium hydroxide or potassium hydroxide, to chemically break the molecule of raw renewable oil into methyl or ethyl esters
Transient operations	: Includes starting, warming up, and changing from one speed to another, especially during acceleration and deceleration. It is the probability that the observed differences between groups are due to random chance.
Tukey's HSD Letters (a, b, c, d, e, f)	: These letters represent groups that are significantly different from each other. If two groups share the same letter, there is no significant difference between them. The letters are assigned based on the magnitude of the difference between group means.

CHAPTER TWO
LITERATURE REVIEW

2.1 General overview

The literature review provides a comprehensive analysis of biodiesel blends, detailing their properties and their effects on engine performance. The review assesses the environmental, technological, and economic impacts of biodiesel use. Additionally, it offers insights into predicting engine performance and emissions by evaluating various modeling methods and their operational optimization when using biodiesel blends. Presently, extensive research is conducted to identify viable vegetables for biodiesel production and ultimately contributing to the advancement of biodiesel utilization and enhance environmental sustainability.

2.1.1 Biodiesels and their properties

Biodiesel is a liquid fuel composed of mono alkyl esters and fatty acids derived from vegetable oils through a process of transesterification (Aybek *et al*., 2011; Fayyad *et al*., 2010; Knothe & Steidley, 2005). Transesterification is a base-catalyzed chemical reaction process conducted at low temperatures and pressures, using alcohol (methanol or ethanol) in the presence of a catalyst, such as sodium hydroxide or potassium hydroxide, to chemically break the vegetable oil molecule into methyl or ethyl esters, with glycerol as a by-product (Atabani *et al*., 2012). The vegetable oils are derived from edible and non-edible plant seeds or fruits. Edible sources include palm, soybean, canola, mustard, sunflower, and linseed (Atabani *et al*., 2014; Goodrum & Geller, 2005; Yuan *et al*., 2022) while non-edible oil sources include Jatropha, Karanja, Mahua, Castor, and Croton (Kumar *et al*., 2007). Vegetable oils are esters of three-carbon trihydric alcohol, glycerine, and straight-chained monocarboxylic acids known as fatty acids (Kumar *et al*., 2007). Biodiesel is commonly produced through the transesterification of vegetable oil to improve its fuel properties, including viscosity, volatility, cold flow properties, and oxidative stability (Leung *et al*., 2010; Issariyakul & Dalai, 2014). Compared to diesel, vegetable oils have higher density, flash points and cetane numbers, with lower heating values (Kafuku & Mbarawa, 2010; Rao *et al*., 2006).

The primary sources of vegetable oil for biodiesel production include various plants with distinct characteristics and benefits. Among these is the oleander (*Cocos nucifera*) a shrub or small tree from the sub-family Apocynoideae of the dogbane family, cultivated globally in temperate and subtropical areas as an ornamental and landscaping plant (Patel *et al*., 2016). *Croton megalocarpus* is also known for its high oil yields, this plant can be cultivated on marginal lands unsuitable for food

crops (Mbarawa *et al*., 2011). Moreover, Jatropha (*Jatropha curcas*) a hardy tropical plant with low water requirements, adaptable to various climatic conditions, including semi-arid and marginal lands often unsuitable for traditional food crops and its seeds have a high oil content of about 30% making it a promising biodiesel feedstock (Mutune *et al*., 2018; Nzila *et al*., 2013). Sunflower is well-suited for warm to hot climates with full sunshine (Ilkılıç, 2011, Skorić, 2012). The plant is pressed to extract vegetable oil (Teixeira *et al*., 2010) and is valuable as a biodiesel feedstock (Leung *et al*., 2010). Coconut (*Nerium Coconut*) on the other hand, typically grows at heights above 750m in temperate regions and up to 1300m in tropical coastal areas (Takase, 2022). Additionally, coconut oil contains about 70% more fatty acids than other vegetable oils (Caballero *et al*., 2003; Harries *et al*., 2004; Osawa *et al*., 2015;). The benefit of soybean as the leading global source of vegetable oil due to its enhanced biodegradability, increased flash point, reduced toxicity, and increased lubricity (Bhattacharya, 2007; Hoekman *et al*., 2012). It is also favored for its high oil content and higher crop yield per acre (Kafuku & Mbarawa, 2010; Osawa *et al*., 2015). Canola is another commercially farmed crop rich in oil (Ndegwa *et al*., 2011). Another plant producing edible oil is the linseed (*Linum usitatissimum*) which is an annual crop with a plant height of 30-100 cm and blue flowers (Saroha *et al*., 2022). It grows best in moderate to cool temperatures in well-drained, fertile, medium, and heavy soils, especially silty loam, clay loam, and silty clay (Shahidi, 2005). The seeds are bright, reddish-colored, unscented, tasty, and oily (Zhang *et al*., 2012), used in dyeing, linoleum production, the nutrient industry, and animal feed (Saroha *et al*., 2022). Recently, it has been used for biodiesel production due to its high linolenic acid content, which improves cold flow properties important in colder climates (Moser & Vaughn, 2010).

The fuel properties include density, kinematic viscosity, flash point, cloud point, iodine value, pour point, acid value, cold filter plugging point, heating value, cetane number, oxygen content, and oxidation stability (Adhikesavan & Ganesh, 2021). These properties are critical in determining the engine efficiency and amount of energy from the fuel (Mofijur *et al*., 2012). The different biodiesels exhibit significant variations in their properties mainly due the feedstock used in its production (Sharma *et al*., 2020), resulting into differences in ignition quality, stability, cold flow property and combustion charcteristics (Adhikesavan & Ganesh, 2021), but are generally similar as compared to diesel (Sharma *et al*., 2020). Table 2.1 shows properties of some sample biodiesels.

Table 2.1: Biodiesels properties

Fuel Property	Units	ASTM D6765	EN 14214	palm FAME	Oleander FAME	sunflower FAME	soybean FAME
Density	kg/m^3	880	900	864.4	807.3	880	913.8
Kinematic Viscosity	mm^2/s	6	5	4.5	2.726	4.439	4.039
Cloud Point	^oK	-3 to-12	-	16	0	3.4	9
Iodine Number	no.	-	max120	54	-	-	142
Cetane Number	no.	min.47	min.51	54.6	-	49	37.9
Lower heat value	MJ/kg	-	35	40	38.5	39.8	39.76
Acid Value		max 0.50	max 0.5	0.24	0.106	0.027	0.266
Pour Point	^oK	-15	-	15	-	-	2
Flash Point	^oK	100-170	20	135	114.8	160	76
Sulfur	%	max.0.05	10	0.003	3.2	0.2	0.8

Source: Aybek *et al*. (2011)

Biodiesel, derived from various oil sources, exhibits unique physical and chemical properties. These properties can vary significantly depending on the feedstock used, impacting the overall performance and environmental benefits of the biodiesel, for instance, the ignition quality of biodiesel, often measured by the cetane number, can vary significantly with different feedstock. Despite these differences, biodiesels generally possess properties comparable to those of diesel (Sharma *et al*., 2020), making the suitable alternative fuels as shown the table below.

Table 1.2: Typical properties of biodiesel compared to diesel

Properties	Biodiesel	Diesel
Density at 15^0C (Kg/M^3)	840-950	820-845
Cetane Number	51-62	44-49
Kinematic Viscosity at 40^0C (mm^2/s)	3.5-5.0	1.3
Flash Point ^0C	≥120	>55
Molecular Weight	292	200
Sulphur content	0%	0.05%
Lower heating Value ($MJKg^{-1}$	37.1	42.7

Source: Palani *et al.* (2022)

Biodiesels are produced to meet stringent recommended standards, ASTM (American standard testing and measurement) D6751 and EN (European standard)14214 (El-Dalatony *et al.,* 2017; Harabi *et al.,* 2019; Muanruksa *et al.,* 2020; Su *et al.,* 2018), ensuring that their performance aligns closely with that of diesel fuels. The physicochemical properties of most biodiesel are specified using ASTM D6751 and the EN 14214 (Adhikesavan & Ganesh, 2021). Fuel properties of biodiesel blends as reported in the literature, are discussed below;

a. Density

The density of a fuel is a critical property that influences various aspects of engine performance and combustion characteristics. The density directly affects the mass of fuel injected, which in turn impacts the air-fuel ratio and the energy content of the injected fuel (Agarwal, 2007; Mofijur *et al.,* 2012). However, it is essential to note that fuel density also plays a role in fuel atomization and spray formation (Suh *et al.,* 2011). Higher density fuels generally atomize less effectively, potentially leading to incomplete combustion. This is because denser fuels exhibit higher inertial forces during injection, promoting smaller droplet sizes and poor dispersion within the combustion chamber (Küçükosman *et al*., 2022). Consequently, higher density fuels tend to reduce particulate matter (PM) and smoke emissions, as well as improve engine efficiency (Lee *et al.,* 2005). Whereas biodiesels typically have higher densities than conventional diesel, it is crucial to consider the impact of variations in density among different biodiesel feedstock's (Hoekman *et al.,* 2012).

The degree of saturation and the length of the hydrocarbon chains in the fatty acid composition of the feedstock influence the density of the resulting biodiesel (Hoekman *et al.,* 2012; Knothe & Steidley, 2005). This variation can lead to differences in fuel injection characteristics, combustion behavior, and emissions profiles (Giakoumis, 2013; Ramírez-Verduzco *et al.,* 2011). Denser fuels require higher thus necessitate adjustments in fuel system components to accommodate the increased mass flow rates. Furthermore, fuel density is temperature-dependent, and its impact on engine performance may vary under different operating conditions (Van Gerpen, 2004).

b. Kinematic Viscosity

Kinematic viscosity is a key property that measures a fluid's resistance to flow (Knothe & Steidley, 2005). This property greatly affects the fuel's ability to atomize and vaporize into a fine mist in diesel engines. According to Hoang *et al*. (2021), biodiesel exhibits higher viscosity than petroleum diesel, which decreases its efficiency in flowing through the fuel system. However, blending biodiesel

with diesel can lower the overall viscosity compared to pure biodiesel (Imdadul *et al.*, 2015). Higher viscosity can result in poorer fuel atomization (Tesfa *et al.*, 2010), leading to larger droplet sizes, insufficient vaporization, narrower injection spray angles, and deeper cylinder penetration of the fuel spray (Knothe & Steidley, 2005). This higher viscosity produces larger droplets during injection, causing incomplete combustion, reduced engine performance, and increased emission levels (Palani *et al*., 2022). Imdadul *et al*. (2015) also found that the higher viscosity of biodiesel causes it to vaporize earlier and ignite more easily, potentially increasing nitrogen oxide (NOx) emissions.

Additionally, the higher viscosity of biodiesels compared to diesel, can lead to thickening, causing improper flow in fuel lines, potentially resulting in issues such as injector nozzle blockage and incomplete combustion within the cylinder, particularly at low temperatures (Knothe & Steidley, 2005; Ramírez-Verduzco *et al.,* 2011). Conversely, at higher temperatures, the increased viscosity of biodiesel may improve engine performance by providing better control over the fuel spray, thereby reducing emissions (Imdadul *et al.,* 2015). However, the higher viscosity of biodiesel, which reduces fuel spray penetration, has been used to explain the recovery of power for biodiesel fuels (Xue *et al.*, 2011). This improved air-fuel mixing due to enhanced spray penetration can potentially compensate for the power losses associated with higher viscosity. However, it is important to note that the higher viscosity can also decrease combustion efficiency due to poor fuel injection atomization, ultimately leading to power losses (Soudagar *et al.,* 2021; Xue *et al.,* 2011). Therefore, the kinematic viscosity of a fuel plays a crucial role in determining its atomization and combustion characteristics, thereby affecting engine performance, emissions, and overall efficiency. While higher viscosity can provide certain benefits, such as improved fuel spray penetration and air-fuel mixing, it is essential to strike a balance to ensure optimal fuel injection, atomization, and combustion processes (Demirbas, 2009; Soudagar *et al.,* 2021).

c. Flash Point

The flash point is the temperature and pressure at which a fuel begins to evaporate and form an ignitable mixture (Chandra & Kumar, 2007; Hoffman *et al.,* 2011). It is a crucial property of fuels as it affects their ability to be stored and transported safely (Mofijur *et al.,* 2015). Biodiesels typically have higher flash points (typical values are over 160°C at 0.85 bar) compared to conventional diesel (Knothe & Steidley, 2005), making them less flammable and safer to store and transport (Fan *et al.*, 2018). However, the higher flash point of biodiesel can also pose challenges in terms of ignition and vaporization, potentially resulting in reduced engine performance at low temperatures (Mofijur *et al.,*

2015). This is because a higher flash point indicates a higher temperature requirement for the fuel to vaporize and form an ignitable mixture, which may lead to incomplete combustion or misfiring, especially in cold-start conditions (Ramírez-Verduzco *et al.*, 2011).

The flash point of a fuel is influenced by its chemical composition and structure. Biodiesels derived from feedstocks with longer carbon chain lengths and higher degrees of saturation tend to have higher flash points (Knothe & Steidley, 2005; Soudagar *et al.*, 2021). Additionally, the presence of impurities in the biodiesel can lower the flash point, potentially increasing the risk of flammability (Demirbas, 2009). To address the potential drawbacks of high flash points, blending biodiesel with diesel can be an effective strategy. Blending increases the flash point of the fuel mixture, improving safety, enhancing compatibility with existing fuel systems, and potentially improving combustion efficiency (Azizul *et al.*, 2020). The optimal blend ratio can be determined based on factors such as the desired flash point, engine operating conditions, and emission requirements.

Furthermore, advances in engine design and fuel injection systems can help mitigate the challenges associated with higher flash points of biodiesels. Strategies such as preheating the fuel, adjusting injection timing, and implementing advanced combustion techniques can improve the vaporization and ignition of biodiesels, thereby enhancing engine performance and efficiency (Hoekman *et al.*, 2012; Tan *et al.*, 2014). The flash point is a crucial property that affects the safe handling, storage, and transportation of fuels, as well as their ignition and combustion characteristics. While biodiesels generally have higher flash points than conventional diesel, blending and advancements in engine technology can help overcome the potential challenges associated with this property, enabling the safe and efficient use of biodiesels in various applications.

d. Low heating value

The heating value determines the amount of heat energy generated from a given quantity of fuel. The low heating value (Cv) of a fuel is a measure of the energy content of a fuel when it undergoes complete combustion, and the products of combustion are cooled to the temperature of the combustion air (Nguyen & Pham, 2015). The CV measures the fuel's ability to release energy through combustion and has a direct influence on the engine power output and fuel usage. A lower energy content causes lower engine power compared to diesel (Xue *et al.*, 2011). Due to the lower energy density of biodiesels (Usu & Aydin, 2020), a larger quantity needs to be consumed to achieve the same power output in an engine compared to diesel. This lower energy content of biodiesels can be attributed to chemical composition, which consists of long-chain fatty acid esters with oxygen content (Soudagar *et al.*,

2021). Conversely, diesel, being derived from petroleum, has higher energy density than biodiesel (Gad & Jayaraj, 2020), making it an attractive fuel for use in engines.

The lower heating value of a fuel is directly related to its chemical composition and structure. Fuels with higher hydrogen-to-carbon ratios and lower oxygen content generally exhibit higher C_V (Demirbas, 2009). Additionally, the degree of saturation and chain length of the fatty acid components in biodiesels influence on Cv, with saturated and shorter-chain biodiesels having slightly higher C_V (Knothe & Steidley, 2005). It's important to note that while Cv of biodiesels can result in lower engine power output, other factors such as combustion efficiency, injection characteristics, and engine modifications can partially compensate for the energy density difference (Tan *et al.,* 2014). Furthermore, the environmental benefits of biodiesels, such as lower greenhouse gas emissions and renewability, make them attractive alternatives to conventional diesel (Hoekman *et al.,* 2012).

Generally, the low heating value (Cv) is a critical parameter that directly impacts engine power output and fuel consumption. Biodiesels generally have lower Cv compared to conventional diesel due to their chemical composition, necessitating the consumption of larger quantities to achieve equivalent power outputs. However, ongoing research on biodiesels formulations aim to mitigate this limitation while leveraging the environmental issues (Ramírez-Verduzco *et al.,* 2011).

e. Cetane Number

The cetane number measures the ignition quality of fuel, indicating its readiness to auto-ignite and the smoothness of combustion within the cylinder (Celik & Bayindirli, 2022). This characteristic is crucial for diesel fuel as it directly influences engine performance, emissions, and overall efficiency. Biodiesels generally have higher cetane numbers compared to conventional diesel fuel (Huang *et al*., 2020), resulting in improved engine startability, reduced engine noise, enhanced power output, lower fuel consumption, and reduced emissions (Aleme & Barbeira, 2012; Sharma *et. al.*, 2020). The cetane number of biodiesels can vary based on the feedstock type and fatty acid composition (Kumar *et al*., 2020; Mishra *et al*., 2016; Wang, 2001). Typically, biodiesels from feedstocks with higher saturated fatty acid content exhibit higher cetane numbers compared to those with higher unsaturated fatty acid content (Knothe & Steidley, 2005; Ramírez-Verduzco *et al*., 2011). While higher cetane numbers are generally desirable for improved combustion and reduced engine knock, leading to increased power output and better engine performance and high cetane numbers (Sharma *et. al.*, 2020). High cetane number contribute to increased nitrogen oxide (NOx) emissions due to advanced injection timing and higher combustion temperatures (Soudagar *et al*., 2021).

Blending biodiesel with diesel has been used as an effective approach to address the potential trade-off between emissions and performance parameters (Azizul *et al*., 2020). helps optimize the cetane number, and lubricity. Moreover, blending, in addition to advances in engine design and fuel injection systems has helped optimize cetane numbers, with other fuel properties such density and viscosity, to enhancing combustion efficiency and reduce emissions (Hoekman *et al*., 2012; Tan *et al*., 2012). The cetane number of biodiesels can also be influenced by the production process and the presence of additives or impurities, which can be controlled through implementing proper quality control measures to meet specific engine requirements (Pullen *et al*., 2012; Yaakob *et al*., 2014). The cetane number is crucial in determining the ignition quality, combustion characteristics, and overall performance of diesel fuels, including biodiesels.

f. Oxidation Stability

Oxidation stability is the ability of a fuel to resist oxidation and the formation of deposits in the engine (Maithomklang *et al.,* 2022). Biodiesels typically have a lower level of oxidation resistance (less oxidative stability) compared to petroleum diesel (Maithomklang *et al.,* 2022), leading to reduced engine performance and increased emissions (Kumar *et al.,* 2020). The oxidation instability of biodiesels is primarily caused by the unsaturation of the fatty acid chains (Pullen *et al.,* 2012; Yaakob *et al.,* 2014). The presence of double bonds in the fatty acid chains of biodiesels makes them more susceptible to oxidation reactions, particularly in the presence of air, heat, and catalytic materials (Soudagar *et al.,* 2021; Knothe & Steidley, 2005). Oxidation can lead to the formation of insoluble gums, sediments, and other deposits within the fuel system, clogging filters, injectors, and combustion chambers, ultimately affecting engine performance and increasing emissions (Demirbas, 2009). The degree of oxidation stability is influenced by several factors, including the fatty acid composition of the biodiesel, the presence of antioxidants or impurities, and storage conditions such as temperature, exposure to air, and light (Yaakob *et al.,* 2014). Biodiesels derived from feedstocks with higher degrees of unsaturation, such as those from vegetable oils, tend to exhibit lower oxidation stability compared to those from more saturated feedstock, like animal fats (Knothe, 2005; Ramírez-Verduzco *et al.,* 2011).

To improve the oxidation stability of biodiesels, several strategies can be employed. One approach is to blend biodiesel with conventional diesel, which can enhance the overall oxidation resistance of the fuel mixture (Azizul *et al.,* 2020). Additionally, the incorporation of antioxidant additives, such as synthetic or natural antioxidants, can help inhibit oxidation reactions and prolong

the fuel's shelf life (Pullen *et al.,* 2012). Proper storage and handling practices, such as minimizing exposure to air, light, and high temperatures, can significantly improve the oxidation stability of biodiesels (Knothe, 2005). Advances in biodiesel production techniques, including the use of more stable feedstocks or the modification of fatty acid compositions, can also contribute to enhancing oxidation stability (Hoekman *et al.,* 2012; Tan *et al.,* 2012).

g. Chemical structure

The chemical structure of biodiesels defines the arrangement of the carbon, hydrogen and other element in its structure (Kilaz & Šimáček, 2018). Generally, structure affects the fuel combustion, for example, higher fuel oxygen content in the structure often present in biodiesels, leads to complete combustion process and lower emissions, while also leads higher flame temperature hence higher NOx emissions. Biodiesel blends have unique chemical properties compared to diesel fuel, which makes them significant replacements for conventional diesel due to their positive impact on the engine's performance (Hoang *et al.* 2021; Kilaz & Šimáček, 2018) noted that the chemical composition of biodiesel blends was influenced by the type of biodiesel and its percentage the blend. On the positive side, biodiesel contains oxygen, which promotes combustion and helps reduce emissions of hydrocarbons (HC), carbon monoxide (CO), and particulate matter (PM) (Adhikesavan & Ganesh, 2021). Biodiesel is essentially sulphur free, although some biodiesel produced from used cooking oils has been shown to have as much as 30 ppm sulphur (Knothe & Steidley, 2005).

2.1.2 Engines performance indicators

The compression ignition (CI) engine have two main operations namely; The thermodynamics processes produces power by burning fuel with air inside the cylinder, and; the mechanical operation of the moving parts to transmit the produced power whereby the hot gases pushes the piston to rotate the crankshaft (Keating, 2007). The thermodynamics processes of a CI engine were modelled according to the diesel cycle developed by Rudolf and followed four strokes, namely, Intake, compression, power, and exhaust (see Figure 2.1), separated by piston movement inside the cylinder. During the intake stroke (0^o to 180^o CAD), air is taken in at ambient conditions and compressed at the compression stroke (180^o to 360^o CAD) to around 40 bars (typical compression ratios ranging from 15:1 to 22) and temperatures of 40^oC. The highly atomized fuel is then injected by the nozzles to the highly compressed air in the cylinders, at about 40^o CAD, to initiate the power stroke (0^o to 180^o CAD). Thus mixture evaporates, ignite, and burn (combustion) to release energy at high pressures and temperatures and heat as summarized in Equation 2.1 (Heywood, 1988).

$$nC_xH_yO_z + mO_2 \rightarrow nCO_2 + qH_2O + nNO_x + H + E \quad \text{..... (2.1)}$$

Where;

n, m, q are coefficients	$C_xH_yO_z$ is hydrocarbon fuel	H is heat
E is Energy	NO_x is nitrogen oxides	

Finally, the combustion products are released during the exhaust stroke (180^o to 360^o CAD). The figure below shows the working principles of an engine.

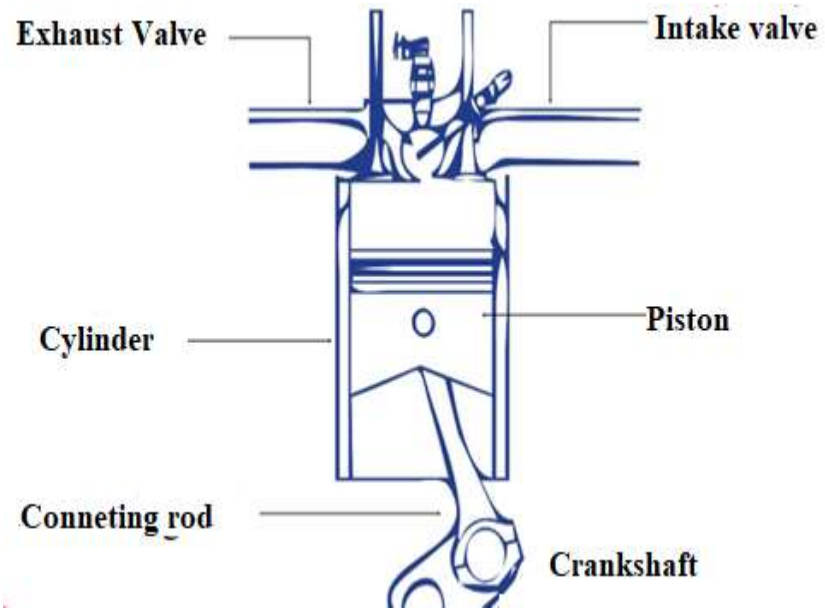

Figure 1.1: Engine working principles (Heywood, 1988)

During the cycle processes, pressure, volume, temperature, and phase variations occur. It's important to understand that combustion processes involve complex chemical-kinetic reactions, including the formation of intermediate chemical species that determine engine emissions and performance (Eriksson & Nielsen, 2014). Modern engines are generally designed to run on biodiesel without any modifications (Rastogi *et al*., 2021; Uslu & Aydin, 2020). Engine performance encompasses various aspects that affect its efficiency, power output, and emissions (Agarwal *et al*., 2013). The impact of biodiesel blends on four-stroke, single-cylinder engines can vary depending on the specific properties of the fuel (Chandran, 2020). Four-stroke engines are generally more compatible with biodiesel blends since they are designed to handle a wider range of fuel properties. In contrast, two-stroke engines require specific fuel properties to function properly, and using biodiesel blends may negatively impact their performance (Palani *et al*., 2022), as noted;

a. Brake power

Brake power (BP) is a critical parameter in understanding the performance of an engine, as it represents the rate at which work is performed by the engine's output shaft. BP is crucial for evaluating the effectiveness of an engine under various operating conditions. Essentially, it is the measurable power that an engine delivers to perform mechanical work, excluding losses due to friction and other inefficiencies within the engine. The relationship between brake power, engine speed, and load is foundational to the operation of diesel engines. As engine load increases, the amount of fuel injected into the combustion chamber rises, which in turn produces more power output. This is because the additional fuel allows for a more intense combustion process, releasing more energy and thus increasing the torque produced by the engine. Consequently, the brake power increases with the load, as the engine can perform more work. Engine speed also significantly influences brake power. At low speeds, although the torque might be relatively high, the power output is limited because power is the product of torque and speed. As the engine speed increases, both torque and power rise to a certain point. This trend continues until the engine reaches a speed where the mechanical and thermal stresses begin to limit further increases in power. The peak brake power typically occurs just below the engine's maximum speed, where the balance between fuel combustion efficiency, mechanical efficiency, and heat dissipation is optimal (Heywood, 1988). The interplay between speed and load is well-documented in the literature. For instance, Bayraktar *et al.* (2023) note that the power output of a diesel engine increases with both engine speed and load, achieving peak power under near full-load conditions. At these conditions, the engine operates at its most efficient state, where the air-fuel mixture is optimally burned and converted into mechanical energy to give useful work.

However, the increase in power does not continue linearly with speed indefinitely. At very high speeds, the engine may experience reduced volumetric efficiency, as the time available for the intake of the air-fuel mixture becomes insufficient. This can result in incomplete combustion and increased thermal and frictional losses, ultimately reducing the engine's efficiency and power output (Lakshminarayanan *et al.*, 2010). Engine design and technology are crucial in determining how brake power is influenced by speed and load. Modern diesel engines employ advanced technologies such as turbocharging, intercooling, and electronic fuel injection systems to optimize combustion and improve power output across a wide range of operating conditions. These technologies help maintain higher torque and power at varying speeds and loads, thereby enhancing the overall performance of the engine.

b. Brake thermal efficiency

Brake thermal efficiency (Bte) measures an engine's ability to convert the fuel's thermal energy into mechanical power. Bte decreases rapidly with increasing engine speed due to rising mechanical friction. Diesel engine efficiency generally increases with load, peaking between 75-90% of maximum load (Heywood, 1988). The relationship between Bte and engine speed is crucial in engine performance analysis. As engine speed increases, mechanical friction within the engine rises, leading to greater energy losses. This frictional loss primarily results from the increased velocity and frequency of the moving parts, which generate more heat and resistance. Consequently, Bte decreases rapidly with increasing engine speed because a larger portion of the fuel's thermal energy is dissipated as heat rather than being converted into useful mechanical work. The heat is generated by friction.

Diesel engine efficiency typically shows a different trend concerning engine load. Efficiency generally improves with increasing load. At higher loads, the combustion process is more complete, and the proportion of energy losses due to heat transfer and friction is lower relative to the total energy input. According to Heywood (1988), Bte reached its peak between 75% and 90% of the engine's maximum load. This peak efficiency occurs because, at these load levels, the engine operates in an optimal range where the air-fuel mixture is burned efficiently, and the mechanical components work within their designed stress limits. However, beyond this peak efficiency range, Bte starts to decline due to the rising rate of heat losses compared to the increase in power output.

Engine operates at higher temperatures at low loads, which increases heat transfer to the surroundings and reduces the net energy available for conversion into mechanical power. Additionally, the increased stress on engine components leads to higher frictional losses, further reducing overall efficiency. Several factors influence the brake thermal efficiency of diesel engines, including engine design, fuel quality, the air-fuel mixture ratio, and the presence of advanced technologies like turbocharging and intercooling. Modern diesel engines are equipped with features that enhance fuel atomization and combustion efficiency, helping to maintain higher Bte across a broader range of operating conditions.

c. Specific fuel consumption

Specific fuel consumption (Sfc) measures an engine's fuel efficiency by quantifying the amount of fuel consumed to produce a specific amount of power, typically expressed in grams per kilowatt-hour. A lower Sfc indicates better fuel efficiency, meaning the engine requires less fuel to generate a given amount of power. As engine load increases, Sfc generally improves, indicating enhanced

efficiency. This improvement occurs because, at higher loads, the engine burns fuel more completely and efficiently, operating closer to its optimal range where the air-fuel mixture is ideal, leading to better combustion and energy conversion. In diesel engines, as the load increases, fuel consumption rises proportionally because more fuel is needed to produce the additional power required to handle the higher load. However, the relationship between fuel consumption and engine speed is more complex and depends on the engine's operating range. At moderate speeds, Sfc improves because the engine runs more efficiently. However, at very high speeds, Sfc worsens significantly due to airflow restrictions and incomplete combustion. At these high speeds, the engine struggles to intake sufficient air, leading to inefficient combustion and higher fuel consumption (Jindal, 2010).

Near the peak torque range, where the engine produces its maximum torque, Sfc is at its best. This range represents the engine's most efficient operating point. The air-fuel mixture is optimal, combustion is complete, and mechanical losses are minimized. Therefore, engines are typically tuned to operate near this range to maximize fuel efficiency during normal driving conditions. However, at very high engine speeds, Sfc deteriorates. This decline occurs because airflow restrictions become more pronounced at high speeds, and the engine has less time to draw in and mix air with fuel properly, leading to incomplete combustion. Consequently, higher speeds result in greater frictional losses within the engine components, increasing overall fuel consumption. As a result, the engine becomes less efficient, and Sfc increases, indicating poorer fuel efficiency.

d. Engine Torque

Engine torque is a measure of the twisting force produced by an engine, typically expressed in Newton-meters (Nm). Torque is crucial for determining a vehicle's ability to accelerate and handle heavy loads, such as hauling and towing. Essentially, torque represents the rotational force available at the engine's crankshaft, which is then transmitted to the wheels to propel the vehicle. The torque produced by an engine varies with engine speed (rpm). Generally, torque increases with engine speed up to a certain point, where it reaches a peak. This peak torque is typically achieved at mid-range engine speeds. At this point, the engine operates in its most efficient range, where the air-fuel mixture is optimal, and combustion is most effective. As the engine speed continues to increase beyond this peak, the torque curve begins to flatten and eventually decline. This flattening occurs because the engine's ability to intake and burn fuel efficiently diminishes at higher speeds. Airflow limitations become more pronounced, restricting the amount of air that can enter the combustion chambers. With less air available, combustion process becomes less efficient, and more torque despite the higher rpm.

Engine's performance at high speeds is affected by increased frictional losses and mechanical stresses. These factors contribute to a reduction in the engine's overall efficiency, causing the torque to drop off. This is why, although brake power (Bp), a product of torque and RPM, continues to increase with engine speed to a certain extent, the rate of Bp increase slows down as the engine reaches its RPM upper limit. For instance, in passenger cars, a flat and broad torque curve ensures smooth acceleration and better drivability across different speeds. In contrast, for heavy-duty trucks and towing vehicles, higher torque at lower rpm's is preferable for better hauling capability and efficient operation under load.

e. Brake mean effective pressure

Brake mean effective pressure (Bmep) is the average pressure exerted on the pistons during the combustion process over a complete engine cycle. This measure provides insights into the efficiency and effectiveness of the combustion process. Bmep is particularly useful because it allows for the comparison of different engines and their performance under various operating conditions, independent of their size or design (Heywood, 1988).

As engine speed increases, Bmep typically rises, reaching its peak at an optimal speed before it starts to decline. This trend occurs because higher engine speeds can enhance the combustion process, leading to increased pressure and, consequently, more power output. However, this relationship only holds up to a certain point. Beyond the engine's optimal speed, factors such as increased frictional losses and decreased time for effective combustion can reduce the efficiency, causing Bmep to drop (Mustayen *et al*., 2022).

Understanding the relationship between engine speed and Bmep allows for better design and tuning of engines to achieve maximum efficiency and performance. For instance, in the development of biodiesel blends, analyzing how these fuels influence Bmep at various engine speeds can help in determining the most efficient fuel formulations and engine settings (Knothe, 2015).

f. Volumetric efficiency

Volumetric efficiency is defined as the ratio of the actual volume of air drawn into the engine cylinder during the suction stroke to the swept volume of the piston. Essentially, it measures how effectively the engine fills its combustion chamber with the air-fuel mixture during the intake stroke. Higher volumetric efficiency implies better engine performance since it indicates that the engine is taking in a larger amount of the air-fuel mixture, which is necessary for combustion. Volumetric

efficiency can be influenced by several factors, including engine speed. At higher speeds, the volumetric efficiency typically increases because the rapid movement of the piston creates a high vacuum at the intake port. This vacuum helps to draw in a larger volume of air into the cylinder, consequently, the higher air flow rate leads to better filling of the combustion chamber, enhancing the engine's ability to burn more fuel and thus produce more Bp. On the hand, at lower volumetric efficiency when reduced produces less Bp.

However, this relationship holds true only up to a certain point. At excessively high speeds, volumetric efficiency can decrease due to various limitations such as insufficient time for the air to fill the cylinder completely, valve timing issues, and increased frictional losses. Therefore, achieving an optimal balance is crucial for maintaining high volumetric efficiency across a range of operating conditions. Volumetric efficiency is an important performance parameter because it directly affects the power output of the engine. Higher volumetric efficiency means that more air-fuel mixture is available for combustion, resulting in greater power production. This is why engineers strive to design engines with high volumetric efficiency, using technologies like turbocharging, variable valve timing, and optimized intake and exhaust systems to maximize air intake and enhance overall engine performance (Feneley *et al.*, 2017).

g. Mechanical efficiency

Mechanical efficiency represents the effectiveness of an engine in converting the power developed in the combustion chamber to useful work. It is defined as the ratio of brake power (the usable power output of the engine) to indicated power (the total power generated within the combustion chamber). Essentially, mechanical efficiency measures how well an engine converts energy produced during combustion into useful power (Heywood, 1988).

Mechanical efficiency is influenced by various factors, including friction losses, heat losses, and mechanical losses within the engine. Friction losses occur due to the resistance between moving parts, while heat losses converted into work (Mustayen *et al*., 2022). Higher mechanical efficiency indicates a more efficient engine, where a greater proportion of the power generated in the combustion chamber is converted into useful work. Conversely, a lower mechanical efficiency implies that a significant amount of the generated power is lost due to inefficiencies within the engine. Improving mechanical efficiency is a key objective in engine design and development, as it directly impacts fuel economy and overall performance (Leach *et. al*., 2020).

h. Air fuel ratio

The air-fuel ratio (AF) is a critical parameter in internal combustion engines, defined as the ratio of the mass of air to the mass of fuel inducted into the engine. This ratio significantly influences the combustion process, engine performance, fuel efficiency, and emissions. Properly managing the air-fuel ratio is essential for optimizing engine operation under various conditions (Heywood, 1988). As engine speed increases, the air-fuel ratio typically decreases, especially under different engine loads. This decrease is primarily due to the increased amount of fuel being delivered to the engine cylinders to meet the higher power demand. At higher engine speeds, the engine requires more fuel to maintain performance and generate the necessary power output. Consequently, the proportion of air relative to fuel decreases, resulting in a lower air-fuel ratio (Mustayen *et al*., 2022).

The decrease in air-fuel ratio with increased engine speed can have several effects. For instance, a richer mixture (lower air-fuel ratio) can lead to more complete combustion and higher power output, but it can also result in higher fuel consumption and increased emissions of pollutants such as carbon monoxide and unburned hydrocarbons. Conversely, a leaner mixture (higher air-fuel ratio) can improve fuel efficiency and reduce emissions, but it may also lead to issues like knocking and reduced power output (Leach *et. al*., 2020). This balance is particularly important when using alternative fuels such as biodiesel blends. Researchers can study the effects of these fuels on the air-fuel ratio at various engine speeds and loads to optimize engine performance and minimize environmental impact (Knothe, 2015). According to Ondimu *et al.* (2019), engines running on biodiesel blends exhibit comparable performance to those running on conventional diesel, with the added benefits of reduced engine wear and longer maintenance intervals. This is attributed to biodiesel's higher lubricity compared to diesel.

2.1.3 Engine emissions

Engine emissions are greenhouse gases are emitted from engine as a by-product of combustion through exhaust pipe to the environment. Exhaust emissions from vehicles typically consist of a variety of gases, some of which can have environmental and health impacts. The composition of exhaust gases varies mainly, depending on the type of fuel and engine technology. Some common exhaust emission gases include the following:

i. **Carbon Monoxide (CO):** A colourless, odourless gas that forms when carbon-containing fuels are not completely burned. It is poisonous and can have adverse health effects.
ii. **Carbon Dioxide (CO_2):** Exhaust gas produced by burning fuels contribute to climate change.

iii. **Nitrogen Oxides (NOx):** Includes nitrogen monoxide (NO) and nitrogen dioxide (NO_2). NOx is formed during combustion at high temperatures and contributes to air pollution and smog.

iv. **Sulfur Dioxide (SO_2):** Produced when fuels containing sulfur are burned. It contributes to air pollution and can have respiratory and environmental effects.

v. **Particulate Matter (PM):** Small particles, including soot and other fine particles, released into the air during combustion. PM can have respiratory and cardiovascular health effects.

vi. **Hydrocarbons (HC):** Unburned organic compounds that contribute to smog.

Emission standards and acceptable limits are typically set and enforced by the environmental regulatory agency, for instance in Kenya, it is national environmental management agency (NEMA), while in the USA, environmental protection agency (EPA). The agency regulate different specific emission standards/limits tailored to their activities for the different industries and sectors, such as; transportation, manufacturing, and power generation. The EPA emission recommended limits using compression ignition (CI) engines are; Nitrogen Oxides (NOx) = 140 ppm, Sulphur oxides (SOx) = 191ppm, PM = 180 ppm, CO=100 ppm and CO_2 = 150 ppm (Lakshminarayanan *et al.*, 2010).

The transition to renewable energy sources is critical in addressing global environmental challenges, particularly climate change and air pollution. Biodiesel, has garnered significant attention as an alternative to conventional fossil fuels. The primary environmental benefits of biodiesel is its ability to significantly reduce GHG emissions compared to traditional diesel. According to Masime *et al.* (2021), the lifecycle GHG emissions of biodiesel are substantially lower, primarily due to the carbon sequestration properties of the feedstock's used in its production. This reduction is crucial for Kenya, which is increasingly vulnerable to the impacts of climate change. Air quality improvement is another significant environmental benefit associated with biodiesel. Studies have shown that biodiesel combustion results in lower PM, CO and SOx (Feneley *et al.,* 2017). This reduction in air pollutants can lead to improved public health outcomes, particularly in urban areas where air pollution is a major concern. Additionally, biodiesel's lower aromatic hydrocarbon content further contributes to its cleaner combustion profile, thus it promotes sustainable waste management practices. In Kenya, there is a growing interest in producing biodiesel from waste vegetable oils and animal fats, which are otherwise disposed of improperly, leading to environmental contamination (Kedir *et al.,* 2022). By converting waste oils into biodiesel, not only is the burden on waste disposal systems reduced, but the environmental also minimized.

2.1.4 Challenges in adoption of biodiesels

The adoption of biodiesels as an alternative fuel for engines has gained significant attention in recent years due to concerns over fossil fuel depletion and environmental impacts, unfortunately it faces several technological and economic challenges. These include issues related to engine performance, cold flow properties, material compatibility, production costs, and feedstock price volatility. However, ongoing research and development efforts have led to various solutions, such as engine optimization, improved production processes, and the use of alternative feedstock. This literature review examines the technological and economic challenges associated with biodiesel adoption in engines, as well as potential solutions to these challenges.

The primary technological challenges in biodiesel adoption is its impact on engine performance, for instance, Lapuerta *et al.* (2008) established that use of biodiesel's lead to changes in engine combustion characteristics. Changes in combustion result into reduced engine power and torque. Biodiesel tends to have a higher cloud point and pour point compared to petroleum diesel, which can lead to fuel gelling and engine starting issues in cold weather conditions (Sharma, 2016). This limitation can restrict the use of biodiesel in colder climates or require the use of fuel heating systems. Biodiesel's higher viscosity can also pose challenges for fuel injection systems. Agarwal (2013) reported that the increased viscosity of biodiesel can lead to poorer fuel atomization, potentially resulting in incomplete combustion and increased emissions of certain pollutants. Furthermore, some studies have shown that biodiesel can degrade certain rubber and plastic components in fuel systems, leading to leaks and premature wear (Haseeb *et al*., 2011). Improvements in biodiesel production processes enhance fuel quality, for instance, the use of advanced catalysts and reactor designs help improve its cold flow properties (Ambat *et al.,* 2018, Masime *et al.,* 2015)

On the economic perspective, one of the main challenges in biodiesel adoption is its higher production cost compared to petroleum diesel. Silitonga *et al.* (2013) highlighted that the cost of biodiesel feedstock account for up to 75% the total production cost, affecting its economic viability. The feedstock prices volatility poses another economic challenge. Biodiesel production relies heavily on agricultural crops, which are subject to price fluctuations due to factors such as weather conditions, crop yields, and global demand (Avagyan *et al.,* 2019). Infrastructure requirements for biodiesel production, distribution, and storage also present economic challenges. Adapting existing infrastructure to handle biodiesel or building new dedicated facilities requires significant investment (Mäki *et al.,* 2018). Government policies and incentives play a crucial role in promoting biodiesel use

such as; tax incentives, and subsidies can help offset the higher production costs of biodiesel and encourage its adoption (Avagyan *et al.*,2019). Diversification to use non-edible oils, waste cooking oils, and algal oils of feedstock sources is another strategy to address economic challenges (Atabani *et al.,* 2012). Improvements in production technology such as the advanced production methods, such as supercritical transesterification and enzymatic processes, have shown potential in reducing energy consumption and improving yields in biodiesel production (Ambat *et al.,* 2018). Also, supportive government policies and continued are crucial in overcoming the challenges and promote biodiesel adoption.

To address the performance and durability issues associated with biodiesel use, researchers have explored various technological solutions. One approach is the optimization of engine parameters for biodiesel operation. Xue *et al.,* (2011) demonstrated that adjusting injection timing and pressure can help mitigate some of the negative effects of biodiesel on engine performance and emissions. To address material compatibility issues, the development of biodiesel-resistant materials for fuel system components has been an area of focus. Haseeb *et al.* (2011) use of certain elastomers and surface treatments can improve the durability of engine components exposed to biodiesel. Biodiesel production technology has seen significant improvements, enhancing the efficiency and cost-effectiveness of the production process. The development of transesterification processes, which convert oils and fats into biodiesel, has become more refined and accessible.

Kenya presents various opportunities and challenges integration of biodiesel. Technological advancements in biodiesel production, engine modification, and fuel distribution are critical factors influencing the adoption and efficiency of biodiesel use. indicates that localized, small-scale biodiesel production units are becoming increasingly viable, providing a sustainable energy source for rural. Engine technology is another critical area influenced by biodiesel adoption. While biodiesel can be used in existing diesel engines with minimal modifications, ongoing research focuses on optimizing engine performance and longevity when using biodiesel blends. The distribution and infrastructure for biodiesel also play a crucial role in its adoption. Establishing a reliable supply chain for biodiesel involves developing adequate storage facilities, distribution networks, and retail outlets (Kedir *et al.,* 2022). As Kenya continues to pursue sustainable energy solutions, biodiesel stands out as a promising option that aligns with the nation's environmental and technological goals. However, ongoing research and investment are essential to fully realize these benefits and address the challenges associated with biodiesel integration

2.2 Properties of biodiesel blends

The fuel properties of biodiesels impact engine performance in several ways. For example, biodiesels have lower heat values compared to diesel leading to reduced engine power and torque while increased specific fuel consumption (Sharma *et al.*, 2020; Tesfa *et al.*, 2010). In contrast, biodiesels with higher densities can enhance power output by allowing more fuel mass delivery (Lee *et al.*, 2005; Silitonga *et al.*, 2013). Additionally, biodiesels with low kinematic viscosities can improve combustion through enhanced atomization (Lee *et al.*, 2005; Silitonga *et al.*, 2013). Bari *et al*. (2002) observed that palm oil biodiesel showed lower brake thermal efficiency compared to petroleum diesel, likely due to differences in fuel properties. Thus, variances in biodiesel fuel parameters from conventional diesel can affect engine performance metrics in both positive and negative ways. Biodiesel has a higher viscosity than traditional diesel, which can lead to increased fuel power output (McCarthy *et al*., 2011). It is due to the use of special additives or the blending of biodiesel with traditional diesel fuel. In addition, the high volatility of biodiesel overcomes cold-start problems in engines, hence the appropriate fuel heating systems (Brahma *et al*., 2022). Biodiesel in engines is compatible with engine components and increases power output. Some older engines may not be designed to handle biodiesel, and the materials used in these engines may not be compatible with the fuel, furthermore, modern CI engines are designed to handle the use of biodiesel. Below are discussions on effects blending on biodiesel properties.

2.2.1 Density

Density measures the mass of a fluid per unit volume. A key reason it is an important property for fuels is that diesel engine fuel injection systems meter fuel by volume. Density directly impacts the mass and energy content per injection. Van Gerpen (2004) found that biodiesel has a higher density than petroleum diesel, and that density increases in a linear fashion with increasing biodiesel content in blends. Numerous other studies have confirmed this linear relationship between biodiesel blending ratio and fuel density (Aydin, 2017; Fattah *et al.*, 2014; Lapuerta *et al.*, 2008). The higher density with increased biodiesel content has implications for engine performance. He *et al.* (2003) and Knothe & Steidley (2005) reported that fuel injection timing should be advanced as the biodiesel fraction increases to account for the higher cetane number and density.

Biodiesel density can vary depending on the feedstock. Biodiesel from palm oil tends to have a higher density than biodiesel from canola or soybean oils (Ramírez-Verduzco *et al.*, 2012). Laplace *et al.* (2021) observed density differences between 1% and 7% depending on feedstock when testing

eight biodiesels. They concluded that accurate fuel density values should be used in engine calibration based on the type of biodiesel being blended. Temperature is another variable impacting density. Like other liquids, biodiesel density decreases linearly with increasing fuel temperature (Van Gerpen, 2004; Alptekin, 2008). Fuel temperature can fluctuate significantly so this needs consideration in engine calibration. Seasonal ambient conditions can also alter density (Jain & Sharma, 2010). Ramrez-Verduzco *et al.* (2011) while examining the effects of blending on density, found out that they were higher compared to diesel but lower the biodiesel, depending on the ratio's (Alptekin & Çanakçı, 2008).

2.2.2 Kinematic viscosity

Kinematic viscosity is a measure of a fluid's resistance to flow under the influence of gravity. In the context of biodiesel fuels, this property plays a crucial role in determining the efficiency and performance of an engine. Tat and Van Gerpen (2004) conducted extensive tests on various biodiesel fuels and discovered that viscosity increases linearly with rising blend levels when mixed with ultra-low sulfur diesel (USEM). This linear trend has been corroborated by other studies, which have consistently shown that biodiesel blends exhibit higher viscosity as the proportion of biodiesel increases (Giakoumis, 2013; Knothe & Steidley, 2005; Refaat, 2009). The higher viscosity observed in biodiesel is attributed to the larger molecular sizes and stronger intermolecular binding forces compared to petroleum diesel. These characteristics lead to increased resistance to flow, which can negatively impact engine performance. Specifically, excessively high viscosity can result in poor fuel atomization, incomplete combustion, and the formation of engine deposits (Mofijur *et al.*, 2016). For instance, Knothe *et al.* (2005) reported approximately a 66% increase in viscosity.

Most engine manufacturers approve blends containing up to 20% biodiesel. Beyond this limit, the high viscosity of biodiesel can cause damaging effects on the engine, necessitating modifications to the injection timing, pressure, and duration to handle the increased viscosity (Mofijur *et al.*, 2016). Feedstock with higher saturation levels tend to exhibit lower viscosity, making them more suitable for blending with diesel (Knothe & Steidley, 2005). Temperature is a factor affecting biodiesel viscosity. The viscosity of biodiesel changes exponentially with temperature, as noted by Van Gerpen (2004). This sensitivity to temperature requires careful consideration in engine design and operation, especially in colder climates where fuel viscosity can increase significantly.

Blending biodiesel with diesel has been shown to improve kinematic viscosity. Aworanti *et al.* (2012) demonstrated that mixing biodiesel with diesel can enhance fuel flow properties, which is

essential for achieving optimal atomization. Proper atomization is vital for efficient combustion and overall engine performance. Lee *et al.* (2005) emphasized the importance of considering the atomization capabilities of the fuels being mixed to ensure that the resulting blend provides optimal atomization and fuel flow. Compression ignition engines typically require fuels with a kinematic viscosity ranging between 3.5 and 5.0 mm^2/s at 40°C (Knothe *et al.*, 2005). For specific biodiesel blends, such as sunflower oil biodiesel-diesel, the kinematic viscosity ranges from 4.5 to 5.8 mm^2/s, while palm oil biodiesel-diesel blends exhibit viscosities between 3.2 and 4.5 mm^2/s (Palani *et al.*, 2022). These values highlight the importance of selecting appropriate feedstock and blending ratios to meet engine specifications and ensure efficient operation.

In addition to viscosity, some engines equipped with fuel injectors may require modifications to the fuel system to accommodate the higher viscosities associated with biodiesel blends. Such modifications can include changes to injector design, fuel pump calibration, and fuel line adjustments to ensure consistent and reliable fuel delivery. By carefully selecting feedstock, blending ratios, and considering temperature effects, it is possible to develop biodiesel blends that meet engine requirements and enhance fuel efficiency. Ongoing research and development in this field will continue to play a vital role in advancing the use of biodiesel as a sustainable alternative to diesel.

2.2.3 Low heat value

Lower heating value (CV) represents the amount of heat released when fuel undergoes complete combustion with oxygen, excluding the heat of vaporization of water. Multiple researchers have shown that the lower heating value of fuel linearly declines with increasing biodiesel percentage in diesel blends (Carraretto *et al.,* 2004; Hoekman *et al.,* 2012; Lapuerta *et al.,* 2008). This is primarily due to the higher oxygen content in biodiesel, which reduces the proportion of carbon and hydrogen compared to the hydrocarbons present in petroleum diesel. Consequently, pure biodiesel can have up to 12% lower energy content per gallon compared to diesel fuel (McCormick *et al.,* 2006). The presence of oxygen in biodiesel contributes to its lower heating value because it reduces the overall energy density of the fuel. This reduction necessitates a greater volume of biodiesel in blends to achieve the same energy output as diesel during combustion (Xue *et al.,* 2011). Thus, for applications requiring a specific energy output, more biodiesels must be consumed compared to diesel, which can affect fuel economy and performance.

The feedstock used to produce biodiesel significantly impact properties like the lower heating value. Different feedstock contains varying amounts of carbon, hydrogen, and oxygen, leading to

differences in energy content. For instance, Bodisco *et al.* (2021) found that palm oil methyl esters had an 8% lower energy content compared to rapeseed methyl esters. This variability highlights the challenge of characterizing the heating value of biodiesel without knowing the specific feedstock used in a blend. Additionally, the quality of biodiesel can degrade over time due to oxidation and contamination, further impacting its lower heating value. Oxidation occurs when biodiesel reacts with oxygen, leading to the formation of peroxides and other compounds that reduce its energy content. Contamination from water, particulate matter, or other impurities can also adversely affect the fuel's heating value and performance (Sharma *et. al.,* 2010). The lower heating value of biodiesel and its blends is crucial for optimizing engine performance and fuel efficiency. This requires careful consideration of the feedstock used, the potential for oxidation and contamination, and the specific energy needs of the application. By selecting appropriate feedstock and maintaining fuel quality, it is possible to maximize the energy output and performance of biodiesel blends.

2.3 Effects of biodiesel blends on engine performance and emissions

Compression ignition (CI) engines are designed to run on diesel fuel can run on biodiesel with little or no modification (Rastogi *et al*., 2021). The diesel contains higher levels of sulfur compared to biodiesel, leading to the formation of harmful emissions such as sulfur oxides. Thus, improving combustion with low sulfur content, which reduces emissions of harmful pollutants such as sulfur dioxide and particulate matter, thus, reducing the risk of water contamination (Neupane, 2022). Thus, using biodiesel in engines leads to lower emissions of harmful pollutants than petroleum diesel improves air quality and reduces the health impact caused by diesel engines. Biodiesel blends are considered a cleaner-burning alternative to traditional diesel fuel, as they produce fewer harmful emissions, including particulate matter, unburned hydrocarbons, carbon monoxide, and sulfur oxides. The biodiesel used in engines has been the subject of numerous studies with varying results for example, some studies have found that biodiesel can improve engine performance by increasing fuel efficiency, reducing emissions (Sharma *et. al.,* 2020). However, one of the key factors affecting the fuel efficiency of biodiesel in engines is its physiochemical properties (Usu & Aydin, 2020). The engine efficiency depends on several properties namely, flash point, pour point, cetane number, density, kinematic viscosity, heating value, and lower heat value. Biodiesel as a fuel for CI engines impact performance in terms of power output, fuel efficiency, and emissions depending on the engine design, operating conditions, and the biodiesel's properties. However, the biodiesel running an engine result in lower power output (Usu & Aydin, 2020) explained by its lower energy density than

traditional diesel {meaning that it contains less energy per unit volume}. It is important to note that the exact effect on power output depends on the engine design, operating conditions, and the biodiesel's properties.

The CI engine can run on biodiesel and diesel with a few adjustments, mainly in the engine management system, to ensure optimal performance and efficiency. Compared to diesel fuel, Biodiesel in CI engines can produce lower emissions of carbon monoxide (Hussain *et al*., 2020). The choice between biodiesel and diesel as a fuel for CI engines will depend on the engine application's specific requirements and emissions goals. Explain that while both fuels have advantages and disadvantages, they can be used in a common rail CI engine, a type of internal combustion engine that uses high-pressure fuel injection. Among the key advantages of biodiesel fuels is the aspect of being developed from renewable resources, which is important in reducing dependence on petroleum and lowering greenhouse gas emissions (Neupane, 2022). Further, biodiesel fuel has a higher lubricity than diesel fuel, which helps reduce wear and tear on the engine components, leading to improved performance and longevity (Abdelrazek *et al*., 2023; Wood *et al.*, 2015). Consequently, the fuel produces fewer emissions than diesel fuel, leading to a cleaner environment and improved air quality (Mofijur *et al.*, 2015). The biodiesel has a lower energy density than diesel fuel, reducing fuel efficiency and increased fuel consumption (Abed *et al*., 2019), oxygen content in the structure to enhance combustion to improve its efficiency (Mahmudul *et al.*, 2015; Monirul *et al.*, 2015; Tasic *et al.*, 2019).

The biodiesel use as a fuel for engines can have a positive impact on performance in terms of power output, fuel efficiency, and emissions (Niculescu *et al.*, 2019). However, the exact effect will depend on their operating conditions and properties of the biodiesel being used (Ghazali *et al.*, 2015). Thus, as the demand for biodiesels' blends continues to grow (Rastogi *et al*., 2021), it is important to investigate on engine performance to ensure effectiveness in reducing emissions and improving engine performance. The fatty acids in biodiesel vary in their carbon chain length, which affects engine performances and exhaust emissions (Xue *et al*., 2011).

The most important performance characteristics of CI engines when fueled by biodiesel blends are discussed in sub-sections below;

2.3.1 Brake thermal efficiency

Brake thermal efficiency (Bte) is an important engine performance key parameter which measures the ability of an engine to convert the fuel thermal energy to mechanical power, calculated as "the ratio between engine brake power to the power obtained based on lower heating value of the

fuel" (Prabu, 2019). This essentially represents how effectively the chemical energy content of fuel gets converted to mechanical power output and largely depends on their physiochemical aspects of fuels (Kohse-Höinghaus, 2021; Maithomklang *et al*., 2022). Many research studies have assessed the influence of biodiesel usage on the brake thermal efficiency of compression ignition engines, with varying results. (Sharma *et. al*., 2020) found that the use of biodiesel can lead to increase engine performance due to the elimination of issues such as injector clogging, increased deposits on engine parts. However, one of the key factors affecting Bte of CI engines fueled by biodiesel are its chemical composition (Usu & Aydin, 2020). Biodiesel is composed of long-chain fatty acid esters, which can be challenging in diesel since presence of impurities, such as free fatty acids, moisture, and contaminants, can also affect the performance of biodiesel in engines (Murugesan *et al.,* 2009). To overcome these problems, biodiesel must be processed to meet strict quality standards, such as the American Society for Testing and Materials (ASTM) specification D6751 (Van Gerpen, 2004).

The effects of biodiesel on diesel engine performance and Bte have been studied extensively over the past two decades. Agarwal (2007) conducted a comprehensive review of prior biodiesel research, finding that most biodiesels resulted in improved brake thermal efficiency compared to regular diesel fuel. He attributed this to the higher oxygen content and cetane number of biodiesels, which improve the combustion process. They observed that brake thermal efficiency increased with biodiesel percentage across all sources. However, jatropha biodiesel showed higher efficiencies, which was correlated to its degree of unsaturation. Demir *et al.* (2019) specifically examined waste cooking oils as a biodiesel feedstock. Their results aligned with the previous studies, demonstrating steadily increasing brake thermal efficiency with biodiesel blends up to 20%. Xue *et al*. (2011) while researching on rapeseed oil biodiesel found out that it; had higher efficiency compared to diesel, especially at higher loads. Fuels with higher kinematic viscosity may experience poor atomization and mixing with air, leading to incomplete combustion and lower Bte. On the other hand, fuels with lower viscosity can promote better combustion efficiency, resulting in higher Bte. However, the influence of kinematic viscosity on Bte may be less direct compared to its effects on other engine parameters. According to Ghazali *et al.* (2015) who tested biodiesels from varying feedstock's including linseed, soybean, corn, and sunflower oils. It is concluded that biodiesels with higher olefin and saturation content like linseed showed improved engine efficiency. Aydin (2011) looked at blend optimization and found that efficiency peaked at B20 for soybean biodiesel, aligning. However, the precise optimal blend likely depends on the specific fuel properties.

The reduction in efficiency with increasing blend level has also been widely reported by Demir *et al.* (2019) in their work with waste cooking oil biodiesel. They attributed the decrease predominantly to the lower energy density causing a reduction in power as evidenced in these results of these research. As noted by Agarwal *et al.* (2011), biodiesels with a higher degree of unsaturation tend to show higher engine efficiency. In this dataset, WVO and Oleander contain higher percentages of unsaturated fats compared to the saturated fat-rich Coconut biodiesel. The consistently higher brake thermal efficiencies for WVO and Oleander blends concur with other researcher's observations (Agarwal *et al.,* 2013). Mofijur *et al*. (2016) note that using low biodiesel blends up to B20 has "little effect on the brake thermal efficiency" and may even slightly improve it in some cases. However, at higher blends like B50 or pure biodiesel (B100), a noticeable reduction in brake thermal efficiency has been reported across investigations. In a study of a diesel generator engine, Prabu (2019) observes a 3.64 % decrease in brake thermal efficiency while using B100 compared to standard diesel operation. The reasons attributed include biodiesel's "slightly lower Lower heat value than diesel which directly affects the brake thermal efficiency value" (Mofijur *et al*., 2016,) as well as differences in fuel physical properties which impact injection characteristics and combustion. Usage of additives, adjustments to engine operating parameters as well as optimization of injection timing have demonstrated potential to "negate this low brake thermal efficiency issue with biodiesel to some extent" (Prabu, 2019). Overall, compression ignition engines can often use lower biodiesel blends without significantly compromising brake thermal efficiency, but higher blends require careful configuration to counter possible efficiency declines (Lapuerta *et al*., 2008).

Recent studies have examined the effects of biodiesel blends on engine performance parameters compared to diesel. Raman *et al.* (2016) reported that a B25 biodiesel blend used in a CI engine without modification achieved acceptable Bte, however, some biodiesel blends have demonstrated lower Bte compared to diesel fuel (Vadivelu *et al.,* 2022). This reduction in Bte has been attributed to the higher kinematic viscosity of biodiesel and the lower heating value of biodiesels derived from feedstock like beef tallow (Vadivelu *et al.,* 2022). Investigations into the performance of moringa oil methyl ester blends likewise found lower brake thermal efficiency resulting from greater viscosity, lower heating value, and density compared to diesel (Lapuerta *et al*., 2008). observed a 5% reduction in efficiency with palm oil diesel blends due to their 10% higher fuel consumption stemming from a lower heat value, however, combustion improved over diesel alone due to the oxygen content in palm oil diesel.

2.3.2 Specific fuel consumption

Specific fuel consumption (Sfc) is a key measure of an engine's fuel efficiency, expressed as fuel consumption per unit of power output. A lower SFC indicates better fuel efficiency, meaning less fuel is needed to generate a specific amount of power. The effects of biodiesel blends on Sfc vary depending on the biodiesel source, engine operating conditions, and blend level. Biodiesel blends in compression ignition (CI) engines have been widely studied due to their potential as a renewable fuel source. Biodiesel typically increases Sfc compared to conventional diesel fuel. Recent research consistently shows that biodiesel blends lead to higher Sfc in CI engines. For instance, Ashok *et al*. (2017) reported that Sfc increased by 2.9%, 6.3% and 9.8% for B20, B40 and B60 blends, respectively, compared to diesel fuel. This trend is mainly due to the lower heating value of biodiesel, which requires a higher fuel flow rate to maintain the same power output.

The increase in Sfc is generally proportional to the biodiesel percentage in the blend. Örs *et al*. (2019) observed that B10, B20, and B50 blends increased Sfc by 1.37%, 2.77%, and 6.94%, respectively. However, the exact impact varies based on engine design, operating conditions, and biodiesel feedstock. Several studies have explored reasons for the increased Sfc with biodiesel blends. Gad *et al*. (2021) attributed the higher Sfc to the combined effects of biodiesel's lower heating value, higher density and viscosity compared to diesel. The properties affect fuel atomization, evaporation, and combustion characteristics, influencing engine efficiency and fuel consumption.

Despite the increase in Sfc, biodiesel blends often demonstrate improved combustion characteristics. Subramani *et al*. (2021) reported that while Sfc increased with biodiesel content, thermal efficiency improved due to better combustion properties. It's worth noting that engine optimization of mitigate negative effects on Sfc for biodiesel blends (Subramani *et al.,* 2018), since biodiesel blends generally increase Sfc in CI engines, the extent of this increase depends on various factors. Ongoing research focuses on optimizing engine parameters and improving biodiesel properties to minimize fuel consumption impacts while leveraging the environmental benefits of this renewable fuel source. Biodiesel's higher viscosity and lower energy density than diesel fuel result in lower specific fuel efficiency (Abdelrazek *et al*., 2023). Increased friction from higher viscosity leads to higher engine pumping losses. Rastogi *et al*. (2021) showed that biodiesel's lower energy density could be offset by improved combustion properties, resulting in a net increase in fuel efficiency. Biodiesel's higher cetane number, a measure of ignition quality, leads to more complete combustion, reducing fuel consumption and increasing (Wood *et al*., 2015).

Sfc increases when using biodiesel compared to diesel (Ehsan, 2007). Zheng *et al*. (2009) reported 2%-12% higher SFC values for biodiesel compared to diesel. The brake thermal efficiency of an engine is not significantly affected by using low levels of biodiesel blends (Xue *et al*., 2011). Zhang *et al*. (2015) found that increasing biodiesel proportions in fuel mixes led to SFC increases of 1.1%, 2.3%, and 3.3% for soybean blends B10, B20, and B30, respectively.

2.3.3 Carbon monoxide emissions

Carbon monoxide (CO) emissions result from incomplete fuel combustion due to limited oxygen in the mixture, especially in the inner layers of the diffusion flame, where there is a rich mixture (more fuel) (Abdelrazek *et al*., 2023). CO concentration in exhaust gas mainly depends on the air/fuel mixture (Resitoglu *et al*., 2014). Although, lean fuel mixtures also produce CO, the concentration reduces with decreasing combustion temperatures (Leach *et. al*., 2020). CO production in diesel engines with lean fuel mixtures results from too large fuel droplets or inadequate turbulence in the ignition chamber (Resitoglu *et al*., 2014). Gad and Jayaraj (2020) noted that diesel fuel in CI engines produces higher emissions of CO, as compared to biodiesel, due to its lower aromatic, oxygen content and higher cetane number, which leads to more efficient combustion (Agarwal & Rajamanoharan, 2009). Biodiesel produces higher CO_2 emissions compared to diesel, explained by the higher energy content of diesel

Research consistently shows that biodiesel can reduce certain harmful emissions, particularly carbon monoxide (CO). Chandran (2020) demonstrated that biodiesel use in CI engines results in lower CO levels compared to diesel. This reduction is attributed to the higher oxygen content in biodiesel, which promotes more complete fuel combustion (Xue *et al*., 2011). Improved combustion efficiency reduces CO formation and helps oxidize existing CO into CO2 more effectively. Diesel's higher energy density means more carbon is available for combustion per unit volume, potentially leading to increased CO_2 formation ((Xue *et al*., 2011). Additionally, use of diesel's results in more oxidized, producing more CO and partially oxidized species instead of CO_2 (Mofijur *et al*., 2016).

While biodiesel reduces CO, PM, UHC, and SOx emissions, it faces challenges in controlling nitrogen oxide (NOx) emissions. Biodiesel blends often have higher NOx emissions compared to diesel (Agarwal, 2007). This increase is due to the higher oxygen content of biodiesel, leading to higher combustion temperatures that promote NOx formation through thermal mechanisms (Hoekman *et al*., 2012). The trade-off between reduced CO and increased NOx emissions presents a challenge for engine designers and policymakers. Strategies to mitigate NOx increases with biodiesel use include exhaust

gas recirculation (EGR), advanced injection timing, and additives Zhang *et al*. (2015). Biodiesel's emissions characteristics vary depending on the feedstock, blend ratio, and engine design and operating conditions. For instance, Mosarof *et al*. (2015) found that different biodiesel feedstock like palm, jatropha, and waste cooking oil showed varying degrees of emission reductions compared to diesel.

Biodiesel blends, where biodiesel is mixed with conventional diesel in various proportions, offer a compromise between emission reductions and engine performance. Lower blend ratios (e.g., B20, with 20% biodiesel) can provide some emission benefits while minimizing negative impacts on engine durability and performance (Lapuerta *et al*., 2008). Biodiesel use in CI engines presents a complex picture of environmental benefits and challenges. While it offers significant advantages in reducing CO, PM, UHC, and SOx emissions, the increase in NOx emissions remains a concern. Ongoing research focuses on optimizing engine parameters, improving biodiesel properties, and developing engine technologies to maximize benefits and mitigate drawbacks.

Research indicates that biodiesel combustion releases lower CO emissions compared to petroleum diesel due to its higher oxygen content, promoting more complete combustion (Lapuerta *et al*., 2008; Resitoglu *et al*., 2014). The absence of sulfur in biodiesel also contributes to lower CO emissions, as sulfur can interfere with the combustion process (Uslu and Aydin, 2020; Travis, 2012). Additionally, CO emissions depend on cetane number since it affects premixed combustion and diffusion flame combustion (Abdelrazek *et al*., 2023).

CO emissions decrease when using biodiesel blends compared to diesel fuel in conventional CI engines. Zheng *et al*. (2009) found that under CI conditions, uniform fuel distribution in the cylinder, including crevice and boundary layer regions, where incomplete oxidation occurs, results in high CO emissions. Alptekin *et al*. (2008) noticed that while biodiesel increased CO2 and NOx, it emitted lower CO than diesel fuel. Blends with bioethanol slightly reduced CO emissions compared to B20 (20% biodiesel, 80% diesel). Lapuerta *et al*. (2008) tested a diesel engine with waste olive oil biodiesel and reported a 21% drop in CO emissions at high load, with a 10% biodiesel blend reducing CO by 16.4%. These CO reductions align with previous findings.

Biodiesel properties impact engine CO emissions. Biodiesels with a lower carbon-to-hydrogen ratio and higher oxygen content compared to conventional diesel generally lead to lower CO emissions (Hoekman *et al.,* 2012). The oxygen in biodiesel fuels facilitates more complete combustion, reducing CO production. However, biodiesels with higher viscosities and lower volatility can increase CO emissions due to poor fuel atomization and incomplete combustion (Lapuerta *et al*., 2008; Szybist *et*

al., 2007). The chemical structure of biodiesels also, influence CO emissions, with biodiesels containing more unsaturated compounds have low viscosity, demonstrating lower CO levels (Hoekman *et al.,* 2012).

Table 2.3: Emissions for CI engine running on biodiesel and diesel

Exhaust Gas Components	Biodiesel	Diesel
NOx	350-1000 ppm	100-4000ppm
HC	50-330 ppm	500-5000ppm
CO	300-1200 ppm	1000-6000ppm
PM	65 mg/m^3	0 mg/m^3
O_2	10-15%	0.2-2%

Source: Tveit (2015)

2.3.4 Nitrogen oxides emissions

Nitrogen oxides (NOx) are mainly formed during combustion when oxygen and nitrogen react at high temperatures in the combustion chamber, especially in premixed combustion, where the temperature is high and there is a lot of oxygen present (Resitoglu *et al*., 2014). In diesel engines, most of these NOx emissions are nitrogen molecules, which will further oxidize to NO_2 (Pandey and Sharma, 2021). Nevertheless, modern diesel engines with advanced emission control systems can effectively mitigate the increase in NOx emissions from biodiesel. Using biodiesel in engines reduces emissions of harmful pollutants, though there may be an increase in NOx emissions (Riyadi *et al*., 2023). Advanced emission control systems can effectively mitigate this increase. NOx was reduced by 35% and 52%, respectively. When used in engines, it produces fewer harmful emissions than traditional diesel fuel. Biodiesel has been found to decrease emissions of particulate matter, hydrocarbons, and carbon monoxide. However, biodiesel emissions may contain higher nitrogen oxide (NOx) levels than traditional diesel. Biodiesel has a higher oxygen content, which can lead to increased combustion temperatures and higher NOx formation (Sharma, 2021). Using biodiesel also reduces nitrogen oxide (NOx) emissions, contributing to smog and acid rain formation (Ogunkunle & Ahmed, 2021). NOx emissions from diesel engines result from high combustion temperatures and are influenced by engine

design and operating conditions. Rastogi *et al*. (2021) explained found biodiesels to increase NOx emissions compared to diesel, while in some engines, decrease.

Studies have found that biodiesels increase NOx emissions compared to conventional diesel (Lapuerta *et al.,* 2008). The higher oxygen content in biodiesels results in a more complete combustion process with higher combustion temperatures, which promotes NOx formation (Hoekman *et al.,* 2012) Biodiesels also tend to have lower aromatic content compared to diesel, and aromatics help limit NOx production by lowering flame temperatures (Hoekman *et al.,* 2012). However, some biodiesels with higher densities and viscosities can reduce NOx emissions through delayed combustion and reduced combustion temperatures (Szybist *et al.,* 2007). The degree of unsaturation present in the biodiesel's chemical structure also affects NOx, with more unsaturated biodiesels showing lower NOx emissions (Hoekman & Robbins, 2012). Overall, factors like oxygen content, aromatic content, density, viscosity, and degree of unsaturation have been shown to influence NOx emissions when substituting biodiesels for conventional diesel.

NOx is a harmful pollutant that contributes to smog and acid rain. The higher NOx emissions from biodiesel are believed to be due to the higher oxygen levels in the fuel, which leads to higher combustion temperatures and the formation of NOx. Abed *et al*. (2019) denote that the higher oxygen content of biodiesel can result in higher NOx emissions. In another research by Rastogi *et al*. (2021), findings revealed that Nitrogen oxides (NOx) are a group of gases contributing to air pollution and the formation of smog and acid rain. Biodiesel is associated higher combustion temperatures leading to increase NOx emissions compared to diesel. However, the increase in NOx emissions from biodiesel is typically lower than the reduction in emissions of other pollutants, such as CO and PM. The study by Sharma *et. al.* (2020) noted that advanced engine technologies and emission control systems could be used to mitigate the increase in NOx emissions associated with biodiesel use.

2.4 Engine performances and emissions models

The literature review explores various mathematical models used in the studies of engine performance and emissions. Modeling and simulation are essential tools to study and analyze internal combustion (IC) engines, to gain insights into the complex in-cylinder processes of engines (Agarwal *et al.,* 2013; Rakopoulos *et al.,* 2016; Tveit, 2015). The mathematical models have widely been used in engine calibration and control systems, for example, modern engines use model-based control strategies that rely on empirical equations to adjust fuel injection timing and air-fuel, to optimize

performance and reduce emissions. Mathematical models are categorized as; analytical, empirical, semi-empirical and numerical (Tveit, 2015), are reviewed below;

2.4.1 Analytical mathematical models

Dimensional analysis is an effective method to develop analytical mathematical model to investigate engines processes (Deshmukh *et al.,* 2019;), through reduction of the number of independent parameters involved in modeling and experimental engineering problems. The analysis applies dimensionless groups, which represent ratios of important physical quantities involved in the problem, some of which may be constants and simplifies the solution and enables the generalization of the results of engineering models and experiments (Padmavat *et al.,* 2017; Temizer *et al.,* 2020). The dimensionless groups, researchers gain insights into the relative importance of different factors and their interactions, enabling more efficient experimental design and data analysis (Demirbas, 2009; Soudagar *et al.,* 2021; Tan *et al.,* 2012). Dimensional analysis has been extensively used by researchers to identify and analyze the key dimensionless groups that govern various aspects of engine operation and combustion processes (Chun & Muk, 2019; Deshmukh *et al.,* 2019; Hoekman *et al.,* 2012; Padmavat *et al.,* 2017). For example, the Reynolds number, which represents the ratio of inertial forces to viscous forces and is crucial in understanding fuel atomization and air-fuel mixing (Knothe, 2005; Ramírez-Verduzco *et al.,* 2011, Xue *et al.,* 2011).

Dimensional analysis has, also, been instrumental in developing correlations and empirical models that relate engine performance parameters, such as brake power, fuel consumption, and emissions, to the relevant dimensionless groups (Pullen *et al.,* 2012; Yaakob *et al.,* 2014). These correlations help in predicting engine behavior and optimizing operating conditions without the need for extensive experimental data numerical simulations (Gad & Jayaraj, 2020; Kumar *et al.,* 2020).

2.4.2 Empirical mathematical models

Empirical mathematical models are equations derived from experimental data to describe and predict real-world systems. These models are indispensable across many domains, providing insights into complex phenomena when first-principles theoretical models may be intractable or unknown (Kumar *et al.,* 2020). A significant advantage of empirical models is their ability to reveal correlations and relationships directly from experimental observations or measurements without requiring detailed knowledge of underlying processes (Cox, 2021; Kareem, 2014; Young *et al.,* 2019). Empirical modeling has used traditional methods such as linear and nonlinear regression remain staples in, while

modern approaches such as artificial neural networks and support vector machines have emerged as powerful tools (Solomatine & Ostfeld, 2008), significantly broadened its scope and capabilities. Beranova and Higgins (2017) employed multiple linear regression to correlate manufacturing process parameters to optimize manufacturing processes by identifying key factors that influence product quality. Similarly, Sagar *et al.* (2022) utilized artificial neural networks to estimate solar radiation values based on meteorological measurements. Empirical models may not always provide the comprehensive insights offered by theory-based counterparts, their practical usefulness for characterization, prediction, and decision support is undeniable (Young *et al.,* 2019), but, their ability to extract meaningful insights from data provide researchers help with understanding and predicting of the real-world phenomena.

Empirical models for engine performance often focus on parameters such as brake specific fuel consumption (Bsfc) and brake thermal efficiency (Bte). The equation helped in understanding the relationship between fuel consumption and engine load. Another important empirical model is the performance map, which is a graphical representation of engine efficiency and power output as functions of engine speed and load. Also, for studying emissions, empirical models often focus on pollutants such as nitrogen oxides (NOx), carbon monoxide (CO), unburned hydrocarbons (HC), and particulate matter (PM). One common approach is to use regression analysis to develop empirical equations that predict emission levels based on engine operating parameters.

2.4.3 Semi-empirical mathematical models

Semi-empirical models combine theoretical principles with empirical correlations to predict engine performance and emissions. These models often provide a good balance between accuracy and computational simplicity. The models have been greatly used since they combine the ability to deal with the complexity of engine systems and the different in the biodiesel variety of biodiesel feedstock's increase, researchers are also exploring hybrid modeling approaches that combine different types of models. For example, Al-Manea *et al.* (2022) proposed a hybrid model that combined a thermodynamic engine cycle simulation with an artificial neural network to predict the performance and emissions of a diesel engine fueled with crude palm oil and its blends. This approach allowed them to leverage the strengths of both modeling techniques, resulting in improved prediction accuracy. The application of semi-empirical mathematical models in the analysis of biodiesel blends has garnered significant interest due to their balance of theoretical rigor and empirical adaptability. These models integrate foundational scientific principles with observed data, enabling the prediction of complex behaviors in

biodiesel-fueled engines. The discussion elucidates the role of semi-empirical models in understanding the physicochemical properties and engine performance of biodiesel blends. Semi-empirical mathematical models blend theoretical principles with experimental data, offering a practical approach to understanding complex systems. These models are particularly useful when pure theoretical models are too complex or when purely empirical models lack explanatory power Brakora *et al.* (2011). The development of semi-empirical models often begins with a theoretical framework based on fundamental principles, which is then adjusted or calibrated using experimental data to improve its accuracy and applicability to real-world scenarios. The resulting model retains the explanatory power of theory while benefiting from the precision of empirical observations (Brown, 2018). One key advantage of semi-empirical models is their ability to bridge the gap between theory and practice. They can provide insights into underlying mechanisms while still producing reliable predictions. This makes them valuable tools in fields such as climate science, materials engineering, and pharmacokinetics (Taylor *et al*., 2019). For instance, in climate science, semi-empirical models have been used to predict sea level rise. These models combine theoretical understanding of the factors influencing sea levels with historical data on sea level changes. Vermeer and Rahmstorf (2009) developed a semi-empirical model that linked global mean temperature to sea level rise, providing projections that have been widely cited in climate policy discussions.

In materials engineering, semi-empirical approaches are used to predict the properties of new materials based on their composition and structure. Zhang and Li (2023) developed a semi-empirical model to estimate the thermal conductivity of Nano-fluids, combining theoretical heat transfer principles with experimental data. In pharmacokinetics, semi-empirical models help researchers understand how drugs behave in the body. These models often incorporate theoretical concepts of drug absorption, distribution, and elimination, fine-tuned with experimental data from clinical trials. This approach allows for more accurate predictions of drug efficacy and safety (Johnson, 2017).

Despite their usefulness, semi-empirical models have limitations. They may not perform well when extrapolating beyond the range of data used for calibration. Additionally, the empirical components of the model may mask underlying physical processes, potentially limiting their explanatory power (Kumar *et al.,* 2020). Researchers must also be cautious about overfitting when developing semi-empirical models. Overfitting occurs when a model is too closely tailored to the calibration data, reducing its ability to generalize to new situations. Techniques such as cross-validation can help mitigate this risk (Davies & Thompson, 2018).

Machine learning techniques are increasingly being used to develop hybrid models that combine theoretical knowledge with data-driven approaches (Lee *et al.*, 2023). Semi-empirical mathematical models offer a valuable compromise between purely theoretical and purely empirical approaches. They provide a flexible framework for understanding complex systems, bridging the gap between theory and observation. While they have limitations, their ability to combine explanatory power with predictive accuracy makes them essential tools in many scientific fields. Karra and Kong (2010) proposed a semi-empirical model for predicting NOx emissions from biodiesel-fueled engines:

2.4.4 Numerical mathematical models

Numerical mathematical models are powerful tools used to represent and analyze physical systems through computational methods rather than relying on analytical solutions. These models consist of sets of equations that describe complex phenomena, enabling the study of real-world behaviors in scenarios where finding closed-form formulaic solutions is either challenging or impossible (Liu & Quek, 2013). The application of numerical models has significantly expanded in engineering, largely due to their ability to incorporate nonlinear dynamics, stochastic parameters, multidimensional spaces, and discrete time-steps, often necessary to accurately model real-world systems (Kutz, 2013). Different numerical modeling approaches are developed to meet various application needs, depending on the scale and precision required by the governing theory formulations. For instance, finite element analysis (FEA) is a prominent technique that involves the discretization of space and time, allowing for detailed simulations of structural behavior under various conditions (Liu & Quek, 2013). With advancements in high-performance computing, numerical models have grown exponentially in sophistication and scale, such as computational fluid dynamics (CFD) for simulating fluid flows. These advancements have made numerical models' indispensable tools in scientific research and engineering applications, providing insights that were previously unattainable.

The study conducted by Zhang *et al.* (2016), numerical modeling was used to investigate the combustion and emission characteristics of a four-stroke diesel engine when fueled with biodiesel as an alternative to conventional diesel fuel. This study focused on key parameters such as cylinder pressure, heat release rate, cylinder temperature, brake thermal efficiency, brake-specific fuel consumption, and emissions of nitrogen oxides (NOx), soot, carbon monoxide (CO), and hydrocarbons (HC). The researchers employed AVL-Fire software in conjunction with the CHEMKIN code to create a detailed model of the diesel engine cylinder. This model aimed to simulate the injection and combustion processes of biodiesel using a kinetic mechanism that included 106 species and 263

reactions. The simulation model was validated against experimental data under 100% and 50% load conditions and was subsequently used to simulate the combustion processes diesel, biodiesel, and biodiesel–diesel blends containing 10%, 20%, and 30% biodiesel by volume.

However, the reliability of numerical models is highly dependent on the accuracy with which they represent the input phenomena and the parameters used in their solution algorithms (Oreskes *et al*., 1994). Therefore, multi-objective verification and validation procedures are critical in comparing model predictions to experimental data. This rigorous approach helps in building confidence in the model's predictions, making it a robust tool for scientific inquiry and practical applications. By continuously refining these models and validating them against empirical data, researchers enhance their predictive capabilities and contribute to advancement of knowledge across various domains.

One of the primary approaches in modeling engine performance and emissions with biodiesel blends is the use of computational fluid dynamics (CFD) models. CFD models simulate the complex fluid flow, heat transfer, and combustion processes within the engine cylinder. These models typically solve the governing equations of fluid dynamics, including conservation of mass, momentum, and energy, along with additional equations for species transport and chemical reactions.

Researchers have adapted existing CFD models originally developed for conventional diesel fuel to account for the unique properties of biodiesel blends. For example, Liu and Quek (2013) developed a modified version of the KIVA-3V CFD code to simulate the combustion of palm oil biodiesel blends in a direct injection diesel engine. Their model incorporated adjustments to fuel properties such as density, viscosity, and surface tension, as well as modifications to the spray breakup and evaporation sub-models to account for the different physical characteristics of biodiesel.

Another important aspect of modeling biodiesel combustion is the representation of chemical kinetics. Detailed chemical kinetic mechanisms have been developed to capture the complex reactions occurring during biodiesel combustion. These mechanisms can be integrated into CFD models to provide more accurate predictions of combustion behavior and emissions formation. For instance, Brakora *et al.* (2011) proposed a reduced chemical kinetic mechanism for biodiesel surrogates, which was implemented in a multi-dimensional engine simulation code to predict NOx and soot emissions from biodiesel combustion. In addition to CFD models, researchers have also developed phenomenological models to study engine performance and emissions with biodiesel blends. These models use simplified representations of physical and chemical processes, often based on empirical correlations or semi-empirical equations. While less detailed than CFD models, phenomenological

models can provide faster computation times and are particularly useful for parametric studies and optimization tasks. Hamze *et al.* (2015) developed a two-zone thermodynamic model to predict the performance and emissions of a diesel engine fueled with biodiesel blends. Their model divided the combustion chamber into burned and unburned zones and used semi-empirical correlations to calculate heat release rates and emissions formation. The model showed good agreement with experimental data for various biodiesel blends and engine operating conditions.

Neural network models have also gained popularity in recent years for predicting engine performance and emissions with biodiesel blends. These models use machine learning techniques to establish complex relationships between input parameters (such as fuel properties, engine design, and operating conditions) and output variables (like power, efficiency, and emissions). Aydin (2011) developed an artificial neural network (ANN) model to predict the performance and exhaust emissions of a diesel engine running on waste cooking oil biodiesel blends. Their model demonstrated high accuracy in predicting brake specific fuel consumption, brake power, and CO and NOx emissions for various blend ratios and engine speeds

2.5 Optimization of engine performances

Aydin (2011) looked at blend optimization and found that efficiency peaked at B20 for soybean biodiesel, aligning with the downward trend after B20 seen here for canola biodiesel. However, the precise optimal blend likely depends on the specific fuel properties. The reduction in efficiency with increasing blend level has also been widely reported, including by Demir *et al*. (2019) in their work with waste cooking oil biodiesel, they attributed the decrease predominantly to the lower energy density causing a reduction in power as evidenced in these results of the research. As noted by (Agarwal *et al.,* 2011), biodiesels with a higher degree of unsaturation tend to show higher engine efficiency. In this dataset, WVO and oleander contain higher percentages of unsaturated fats compared to the saturated fat-rich coconut biodiesel. Consistently higher brake thermal efficiencies for WVO and oleander blends concur with other researcher's observations (Agarwal *et al.*, 2011). Researchers have studied engine performance for decades, and their work has contributed to developing more efficient and environmentally friendly engines. Some of the key focus areas in these studies have been engine optimization, combustion processes, and the development of alternative fuels. Important area of study has been engine optimization, which involves using computer simulations and experiments to determine the optimal operating conditions for an engine (Hoang *et al.,* 2021). This research has focused on improving fuel efficiency and reducing emissions while maintaining or improving engine

power output. Another area of interest has been combustion processes, including studying various fuels and additives that can improve engine performance. These fuels can potentially reduce engine emissions and improve fuel efficiency, making them a promising area for future research. Many studies and reviews have been published on engine performance, and some of these studies provide a good starting point for further research on engine performance. They can be a valuable resource for those looking to understand the current state of knowledge in this field.

The studies by Patel *et al*. (2016) explored the application of the Grey Taguchi method on use to guarantee are both fuel efficiency and reduction of greenhouses gases (GHG) emissions of internal combustion (IC engines). Therefore, it has paramount to optimization of engine performance characteristics running on fuels. involve solutions to the conflicting objective problem of maximizing engine output power, torque and efficiency, while minimizing fuel consumption and emissions (Leach *et al*., 2020; Stein, 2014). Several research such as Atashkari (2007), have attempted to solve the conflicting objective problems the engine output using the non-Dominating Sorting Genetic Algorithm (NSGA-II). In another study, D'Errico (2011), a multi-objective optimization of output torque and NOx emissions was carried out for a single-cylinder gasoline engine for a motorcycle using a 1D fluid-dynamics model, was used for the multi-objective optimization process.

Multi-objective optimization has become increasingly important in the field of internal combustion engines, particularly for biodiesel-fueled engines. As the automotive industry strives to balance performance improvements with stringent emission regulations, researchers are turning to advanced optimization techniques to find optimal solutions that satisfy multiple, often conflicting objectives. Biodiesel, derived from renewable sources such as vegetable oils and animal fats, has gained attention as an alternative fuel due to its potential to reduce greenhouse gas emissions and dependence on fossil fuels. However, the use of biodiesel in engines can lead to changes in performance characteristics and emission profiles compared to diesel, thus need optimization to ensure that biodiesel-fueled engines meet both performance and emission targets.

Non-Dominated Sorting Genetic Algorithm II (NSGA-II) has emerged as a powerful tool for multi-objective optimization in this context. Developed by Deb *et al*. (2002), NSGA-II has become one of the most widely used evolutionary algorithms for multi-objective optimization problems due to its efficiency and effectiveness in finding diverse Pareto-optimal solutions. Recent studies have applied NSGA-II to optimize various aspects of biodiesel-fueled engines. For instance, Dewangan *et al.* (2023) used NSGA-II to optimize injection parameters for a diesel engine running on biodiesel-diesel blends,

with the objectives of maximizing brake thermal efficiency while minimizing NOx and smoke emissions. The study demonstrated the algorithm's ability to find a set of Pareto-optimal solutions that effectively balanced these conflicting objectives. Another significant application of NSGA-II in this field was presented by Sakthivel *et al*. (2020). They employed the algorithm to optimize the composition of a ternary biodiesel blend and engine operating parameters simultaneously. The objectives included maximizing brake thermal efficiency and minimizing brake-specific fuel consumption, CO, HC, and NOx emissions. Results showed that NSGA-II effectively navigate the complex solution space and identifying optimal blend compositions.

The effectiveness of NSGA-II in handling multiple objectives is particularly valuable in engine optimization problems, where trade-offs between performance and emissions are common. For example, measures that improve fuel efficiency often led to increased NOx emissions, while strategies to reduce particulate matter can result in higher fuel consumption. NSGA-II's ability to generate a diverse set of Pareto-optimal solutions allows engineers to understand these trade-offs and make informed decisions based on specific requirements or constraints. One of the key advantages of NSGA-II is its elitist approach, which ensures that the best solutions found so far are always retained in the population. This feature, combined with its fast non-dominated sorting procedure and crowding distance calculation, allows NSGA-II to converge quickly to the Pareto-optimal front while maintaining diversity among solutions.

Recent research has also focused on enhancing NSGA-II's performance for specific engine optimization problems. For instance, Zhang *et al*. (2012) proposed an improved NSGA-II algorithm incorporating a novel crossover operator and adaptive mutation strategy. They applied this modified algorithm to optimize the combustion chamber geometry of a biodiesel-fueled engine, aiming to maximize power output and thermal efficiency while minimizing emissions. The improved algorithm demonstrated faster convergence and better solution quality compared to the standard NSGA-II. One of the challenges in applying Grey Taguchi to engine optimization problems is the computational cost associated with evaluating objective functions, especially when complex engine simulations are involved. To address this, researchers have explored surrogate modeling techniques in conjunction with NSGA-II. These surrogate models were then used within the NSGA-II framework to optimize engine parameters for a biodiesel-fueled, significantly reducing the computational time.

The integration of NSGA-II with other computational tools and techniques has further enhanced its applicability in engine optimization. For example, Mishra *et al*. (2023) combined NSGA-

II with response surface methodology (RSM) to optimize the performance and emissions of a diesel engine fueled with a novel biodiesel blend. The RSM was used to develop mathematical models relating engine parameters to performance and emission characteristics, which were then optimized using NSGA-II. This hybrid approach allowed for a more comprehensive exploration of the design space and led to improved optimization results. As research in this field progresses, there is growing interest in incorporating more objectives into the optimization process. While NSGA-II has traditionally been applied to problems with two or three objectives, recent studies have explored its effectiveness in handling a larger number of objectives. For instance, Rao *et al*. (2006) applied a modified version of NSGA-II to optimize a biodiesel-fueled engine considering five objectives simultaneously: brake power, brake-specific fuel consumption, and emissions of CO, HC, and NOx.

Despite its widespread use and success, NSGA-II is not without limitations. As the number of objectives increases, the algorithm's performance can degrade due to the increasing number of non-dominated solutions. This has led to the development of alternative algorithms for many-objective optimization problems, such as NSGA-III and MOEA/D. However, for the typical number of objectives encountered in biodiesel engine optimization, NSGA-II remains a robust and effective choice. NSGA-II has proven to be a powerful tool for multi-objective optimization of performance and emissions in biodiesel-fueled engines. Its ability to handle complex, conflicting objectives and generate diverse sets of Pareto-optimal solutions makes it well-suited for addressing the challenges in this field. Recent research has demonstrated its effectiveness in optimizing various aspects of biodiesel engines, from operational parameters to component design. As the automotive industry continues to push for cleaner and more efficient engines, non-sorting generic algorithm (NSGA-II) and its variants are likely to play an increasingly important role in development and optimization of biodiesel-fueled engines.

The multi-objective optimization was carried out by comparing the performance of the ε-constraint and the NSGA-II algorithm optimization methods. It was found in the study D'Errico (2011) that the multi-objective optimization solution for the NSGA-II algorithm was better than that of the ε-constraint method. In the work of Martinez-Morales *et al*. (2013), artificial neural networks were used for the non-linear identification of a gasoline engine to evaluate objective functions used within an optimization framework involving the use of the NSGA-II algorithm and the Multi-Objective Particle Swarm Optimization (MOPSO) algorithm, are outlined below:

2.5.1 Pareto-based multi-objective optimization

The Pareto principle asserts that in a multi-objective problem, there is often a trade-off between objectives, making it improbable to find a single solution that optimizes all objectives simultaneously. Pareto-based methods aim to identify a set of solutions known as the Pareto frontier or Pareto optimal solutions. These solutions represent the best compromises between conflicting objectives. Algorithms like the Non-Dominated Sorting Genetic Algorithm (NSGA-II) and the Strength Pareto Evolutionary Algorithm (SPEA2) are commonly used for Pareto-based multi-objective optimization. The successful application of NSGA-II and other multi-objective optimization techniques in biodiesel engine research requires accuracy of the mathematical models, the appropriate selection of objective functions and constraints and real-world operating conditions (Pandian *et al*., 2019; Xue *et al*., 2011).

a. Weighted sum method

This method involves assigning weights to each objective to convert a multi-objective problem into a single-objective problem. By assigning appropriate weights, the objectives can be combined into a single aggregated objective function, where the weights reflect the relative importance of each objective. The aggregated objective function can then be optimized using traditional optimization techniques, such as linear or quadratic programming.

In this approach, each objective of the multi-objective problem, is assigned a weight w_i representing its relative importance or priority compared to other objectives. These weights are typically normalized to ensure that the aggregated objective function accurately reflects the overall objectives of the problem. The traditional optimization techniques like linear programming (LP), quadratic programming (QP), or evolutionary algorithms are applied to find the optimal solutions that minimizes or maximizes the objectives. The simplicity and flexibility of the weighted sum method make it applicable across various domains, including engineering, finance, logistics, and resource allocation. For instance, in engineering design, practitioners use this method to balance conflicting design criteria such as cost, performance, and reliability.

According to Multi-Objective Optimization the principles and Case Studies (Springer, 2015), the weighted sum method provides decision-makers with a clear and structured approach to handle trade-offs between competing objectives. This foundational text emphasizes the method's effectiveness in transforming complex multi-objective problems into manageable single-objective formulations. However, the weighted sum method solution heavily relies on the accurate assignment of weights, which can be subjective and context dependent. Moreover, the method assumes linear relationships

between models thus oversimplifying complex real-world interactions and trade-offs of the parameters affecting the system.

Recent advancements in multi-objective optimization research have focused on addressing these limitations. For instance, researchers have explored hybrid approaches that combine the weighted sum method with metaheuristic algorithms like genetic algorithms or particle swarm optimization to improve solution quality and robustness. These advancements aim to enhance the method's applicability in handling nonlinear relationships and complex decision landscapes. While the weighted sum method remains a foundational tool in multi-objective optimization, ongoing research continues to refine and extend its capabilities. By critically assessing its theoretical underpinnings, practical applications, and recent advancements, this approach provides decision-makers with valuable insights and methodologies to navigate and optimize complex decision.

b. Constraint on the conflicting objective

Constraint on the conflicting objectives is often referred to as the ε-constraint method. It is a prominent approach in multi-objective optimization, offers a structured way to handle conflicting objectives by transforming a multi-objective problem into a single-objective one (Mavrotas & Florios, 2013). This method designates one objective as primary while converting others into constraints, allowing decision-makers to focus on optimizing a key objective while ensuring other objectives meet specified thresholds (Ehrgott & Ruzika, 2008). The process involves setting upper or lower limits on the constrained objectives, effectively defining the acceptable trade-off space. This approach is particularly valuable in scenarios where there's a clear hierarchy among objectives or when stakeholders need to ensure minimum performance levels across multiple criteria (Bérubé *et al.,* 2009). For instance, in environmental management, one might maximize economic benefit while constraining environmental impact to an acceptable level (Ehrgott & Ruzika, 2008). The flexibility of adjusting constraint values enables a systematic exploration of the Pareto front, providing insights into the relationships between objectives and the consequences of different trade-offs (Mavrotas & Florios, 2013). This exploration is crucial in fields such as engineering design, where understanding the trade-offs between cost, performance, and reliability is essential (Marler & Arora, 2004).

One of the key advantages of the ε-constraint method is its ability to handle non-convex Pareto fronts, a limitation of some other methods like the weighted sum approach (Chankong & Haimes, 2008). This makes it particularly useful in complex real-world problems where the relationship between objectives may not be straightforward or linear. However, the method is not without

challenges. It can be computationally intensive, especially when dealing with many objectives or complex constraints (Purshouse & Fleming, 2007). Additionally, the selection of appropriate constraint requires careful consideration to avoid infeasibility of the solutions (Mavrotas & Florios, 2013).

Despite these challenges, the ε-constraint method remains a widely used and effective tool in various fields. Its application ranges from supply chain optimization (Guillén-Gosálbez & Grossmann, 2009) to portfolio management (Ehrgott & Ruzika, 2008) and urban planning (Cao *et al.*, 2011). In each of these areas, the method's ability to provide direct control over objective trade-offs makes it invaluable in complex decision-making processes. The method's versatility is further enhanced by its potential for integration with other optimization techniques. For example, it can be combined with evolutionary algorithms to improve solution diversity and convergence in multi-objective problems (Deb *et al.*, 2000). The ε-constraint method offers a robust framework for addressing multi-objective optimization problems, particularly when there's a need to prioritize objectives or ensure minimum performance levels. Its ability to generate a diverse set of Pareto-optimal solutions while handling non-convex fronts makes it a powerful tool in the decision-maker's arsenal. As optimization problems in various fields continue to grow in complexity, the ε-constraint method, along with its variants and hybrid approaches, is likely to remain a key technique in balancing multiple, often conflicting, goals in complex systems and decision-making processes.

c. Lexicographic method Constraint on the conflicting objective

The lexicographic method is a distinctive approach to multi-objective optimization that addresses conflicting objectives by establishing a strict hierarchy of importance. In this method, objectives are ranked in order of priority, and the optimization process unfolds sequentially, focusing on one objective at a time. The process begins by optimizing the highest-priority objective without considering the others. Once this primary objective is optimized, its optimal value becomes a constraint for the next stage, where the second-highest priority objective is optimized. This stepwise procedure continues, with each subsequent optimization constrained by the optimal values of all higher-priority objectives, until all objectives have been addressed. The lexicographic method is particularly useful in scenarios where there is a clear and indisputable ordering of objective importance, such as in certain engineering design problems or in decision-making processes with well-defined hierarchical goals. While this approach ensures that higher-priority objectives are never compromised for the sake of lower-priority ones, it can sometimes lead to suboptimal solutions for lower-ranked objectives. Despite this limitation, the lexicographic method remains valuable in many practical applications, especially

where maintaining the integrity of critical objectives is paramount, offering decision-makers a structured way to navigate complex multi-objective problems with clearly defined priorities.

d. Evolutionary algorithms

Evolutionary Strategies (ES) have also been employed, although to a lesser extent, for optimizing biodiesel engine parameters. ES methods, inspired by principles of natural evolution, explore the solution space and aim to find a set of optimal or near-optimal solutions (Bhaskar & Benjamin, 2019). These techniques have demonstrated their effectiveness in multi-objective optimization problems involving biodiesel-fueled engines, effectively balancing trade-offs between performance, emissions, and other conflicting objectives.

One notable example is the study by Bhaskar and Benjamin (2019), where they applied a hybrid ES technique for the multi-objective optimization of a cotton seed biodiesel-fueled engine. The results showed that ES could effectively optimize engine parameters, such as injection timing, fuel injection pressure, and exhaust gas recirculation (EGR) rate, to achieve improved performance and reduced emissions simultaneously. The choice of optimization method depends on various factors, including problem complexity, the number of objectives, the preferences of the decision-maker, and the trade-offs involved (Johnson, 2016). To determine the most suitable approach for a specific situation, it may be helpful to assess the problem requirements and consult with experts in optimization or decision-making techniques.

In the context of biodiesel engine optimization, the constraint method has emerged as a valuable technique for optimizing combustion characteristics, such as ignition timing and air-fuel ratio, specifically tailored for biodiesel combustion (Johnson, 2016). This method incorporates constraints related to biodiesel properties and emissions, enabling the identification of optimal engine configurations that achieve better performance and reduced emissions when using biodiesel as fuel.

The constraint method considers the unique properties of biodiesel fuels, such as their higher density, viscosity, and cetane number, as well as their impact on combustion processes and emissions formation (Knothe &, 2005; Ramírez-Verduzco *et al.,* 2011). By incorporating these constraints, the optimization algorithm can explore the feasible solution space more effectively, leading to engine parameter settings that maximize performance while adhering to emissions regulations and other operational constraints (Hoekman *et al.,* 2012; Tan *et al.,* 2012).

Furthermore, the constraint method can be combined with other optimization techniques, such as GA, ES, or hybrid approaches, to enhance the overall optimization process and improve the quality of

the solutions obtained (Pullen *et al.,* 2012; Yaakob *et al.,* 2014). This integration of domain-specific knowledge and constraints with powerful optimization algorithms can facilitate the development of more efficient and environmentally friendly biodiesel engine systems.

2.5.2 Grey Taguchi Method

The Grey Taguchi method combines the robustness of the Taguchi method with grey relational analysis, providing a mechanism to handle uncertainties in optimization. It excels in situations where imprecise data or variations are present. Grey Taguchi gives a simultaneous optimization of multiple parameters considering the interdependencies among performance metrics. Also, facilitates trade-off analysis, helping identify Pareto optimal solutions where no single objective can be improved without degrading others. This approach is crucial for achieving a well-balanced improvement in engine performance, efficiency, and emissions (Deb *et al*., 2002). The Grey Taguchi method This is essential for making informed decisions in the presence of conflicting objectives (Deb, 2011). The Grey Taguchi method is adept at handling uncertainties and variations in the optimization process. It incorporates grey relational analysis, enabling robust optimization in the presence of imprecise or uncertain data, a common scenario in engine parameter tuning (Lin *et al*., 2017). The optimization contributes to efficiency improvement which is crucial for sustainable engine operation, aligning with global efforts to reduce fuel consumption and carbon footprint (Kumar *et al*., 2019).

The efficiency of the Grey Taguchi method in handling multi-objective optimization translates to time and resource efficiency. Compared to exhaustive search methods, the Grey Taguchi method offers a computationally efficient solution, making it practical for real-world engineering applications (Montgomery *et al*., 2017). The Grey Taguchi method's practicality and ease of implementation make it attractive for industrial applications. Its adoption in optimizing CI engines aligns with the need for practical solutions in the automotive industry, where quick and effective parameter tuning is essential (Niu *et al*., 2020). The Grey Taguchi method's versatility allows it to be applied across various engine types, including CI engines. Its adaptability to different operational conditions and engine configurations enhances its value as a widely applicable optimization tool (Pulko *et al*., 2018). Meeting stringent emission standards is a significant challenge for automotive industries. Simultaneous optimization using the Grey Taguchi method aids in achieving emission reduction goals without compromising other aspects of engine performance, ensuring compliance with environmental regulations (Patel *et al*., 2016)).

2.5.3 Genetic Algorithms

Genetic Algorithms (GA) have been applied to optimize biodiesel engine parameters like injection timing, intake pressure, nozzle hole diameter, etc. for objectives like reduced emissions, improved efficiency and performance. Sivaramakrishnan and Ravikumar (2021) used a GA to optimize a diesel engine fueled with fish oil biodiesel. Kannan and Anand (2012) employed a GA to study combustion of biodiesels from various feedstock's. GA has shown good performance in optimizing biodiesel combustion. Xue *et al.* (2011) applied GA successfully to optimize the effects of performance and emissions on an engine fueled by waste cooking biodiesel. Pandian *et al.* (2019) enhanced a GA for optimizing the injection system of an engine ran on mahua biodiesel.

Genetic Algorithms (GA) have emerged as a powerful optimization technique for tackling complex and multivariable problems in the field of biodiesel engine research. These bio-inspired algorithms mimic the principles of natural selection and evolution, allowing for the exploration of a vast solution space and identifying optimal combinations of engine parameters for objectives such as reduced emissions, improved efficiency, and enhanced performance (Kannan & Anand, 2012; Sivaramakrishnan & Ravikumar, 2021).

The application of GA in biodiesel engine optimization has shown promising results, demonstrating its ability to effectively navigate the intricate trade-offs and interdependencies between various engine parameters and performance metrics (Xue *et al.,* 2011; Pandian *et al.,* 2019). By encoding potential solutions as "individuals" or "chromosomes" and subjecting them to iterative processes of selection, crossover, and mutation, GA can efficiently converge towards optimal or near-optimal solutions (Demirbas, 2009; Soudagar *et al.,* 2008). The key advantages of GA is its capability to handle multiple objectives simultaneously, making it well-suited for optimizing engines fueled by biodiesels derived from diverse feedstock's (Kannan & Anand, 2012). Each feedstock's unique fuel properties, such as density, viscosity, and cetane number, can significantly influence engine performance and emissions (Knothe, 2005; Ramírez-Verduzco *et al.,* 2011). GA can effectively balance these trade-offs and identify the most favorable engine parameter settings for a given biodiesel.

Moreover, GA has been successfully applied to optimize various engine subsystems and components, including injection systems, combustion chambers, and exhaust after-treatment systems (Hoekman *et al*., 2012; Pandian *et al.,* 2019; Tan *et al.,* 2012;). By optimizing parameters such as injection timing, nozzle geometry, and exhaust gas recirculation (EGR) rates, GA can enhance fuel-air mixing, combustion efficiency, and emissions reduction for biodiesel-fueled engines.

Researchers have also explored hybrid approaches that combine GA with other optimization techniques, such as response surface methodology (RSM) or artificial neural networks (ANNs), to further improve the accuracy and efficiency of the optimization process (Pullen *et al.*, 2012; Yaakob *et al.*, 2014). These hybrid methods leverage the strengths of different algorithms, enabling more robust and reliable optimization solutions for biodiesel engine applications. It is important to note that the successful implementation of GA in engine optimization requires careful problem formulation, appropriate selection of objective functions, and proper tuning of algorithm parameters (Gad & Jayaraj, 2020; Kumar *et al.*, 2020). Additionally, incorporating domain knowledge and constraints from engine design and operational requirements can further enhance the practicality and relevance of the optimized solutions.

2.5.4 Particle Swarm Optimization (PSO)

This is an evolutionary, population-based optimization algorithm inspired by the social behavior of organisms like bird flocking or fish schooling originally developed by Kennedy and Eberhart (1995). It works by initializing a population of candidate solutions dubbed "particles" that collaborate to move toward the optimal region of a multi-dimensional search space. Particles evaluate their positions relative to the best global values to determine suitable trajectories (Ling *et al.*, 2022).

Multi-Objective Optimization Studies Researchers have leveraged PSO for optimizing engine performance with biodiesel usage because it can readily handle the disconnect between objectives like maximizing power output while simultaneously minimizing emissions or fuel consumption. For instance, Al-Manea *et al.* (2022) used PSO to optimize injection timing, rail pressure, and pilot ratio for a diesel engine fueled by crude palm oil methyl esters. Brake specific fuel consumption improved 2.2% while nitric oxide emissions declined 14%. Similarly, Ling *et al.* (2022) adopted a version of PSO dubbed Adaptive Particle Swarm Optimization to calibrate injection settings and EGR rates in a diesel engine using biodiesel, successfully lowering fuel consumption by 7.3% and smoke opacity 25.4%.

2.6 Summary/Closure of literature review

Density, kinematic viscosity and low value heating value fuel properties () play a crucial role for engine performance and emissions (Fan *et al.*, 2018; Giakoumis & Sarakatsanis, 2018; Hoekman *et al.*, 2012; Pereira *et al.*, 2019). However, the understanding of the intricate interactions between the different biodiesel blends' properties and their impact on engine performance characteristics remains

lacking (Ghazali *et al*., 2015; Kalaimurugan, 2020). Thus, research is required to establish the effects of the different biodiesels and their blends on fuel properties.

While significant progress has been made in modeling engine performance and emissions with biodiesel blends, there are still areas that require further research is required to develop computationally efficient models that can simulate the entire engine system, to ease studying the complex performances parameters, without costly physical testing.

Engines have numerous inputs and outputs parameters which affect the combustion characteristics of an engine. The parameters are whose shown in table below

Table 2.4: Engine performance parameters

Engine Performance/emission parameters (output)	**Engine inputs** **Fuel properties**	**Engine Design parameters**	**Engine operating Conditions**
Power based: a). Ip*, Bp, m, Fp, BMEP, Imep, Fmep, P. b). Efficiency: Sfc, Bte, Ite, AF, airflow Emission: CO_2, CO, NO_x, NO, S, SO_2.	Fuel characteristic: a). Physical: ϑ, ρ, Bp, Mp, Fp, Pp b). Chemical: Cv, Id Composition: C, N, H, Fuel Blends: Mixture of biodiesel and diesel	Fixed: Piston shape, Bore stroke ratio, l, d, V_d, V_s, V_{cyl}. Ignition angle and Compression ratio	Engine speed Engine load Equivalent Brake power (Bp) or Equal energy delivery Environment factors: Pressure, Temperature

Key: *P= Torque, Bp=Brake power, BMEP = Brake means effective pressure and AF=Air fuel ratio*

Optimizing biodiesel blend levels is crucial for achieving a balance in engine performance and emissions. The Pareto-based NSGA-II method is ideal for addressing complex, multi-objective optimization problems due to its capability to handle non-linear relationships. In contrast, the Grey Taguchi method is better suited for single-objective optimization and is particularly effective in scenarios with uncertainty.

CHAPTER THREE

MATERIALS AND METHODS

The experiments were carried out at the Thermo-Fluids Laboratory, Department of Mechanical Engineering, Jomo Kenyatta University of Agriculture and Technology (JKUAT), situated in Juja, Thika, central Kenya, approximately 36km from Nairobi. JKUAT's geographical coordinates are 1.110°S latitude and 37.0370°E longitude, with an altitude of approximately 1662 meters above sea level. The research was conducted between September and December 2022, with temperatures of between 20°C to 24°C. Map of the experimental site is illustrated appendix 3.

3.1 Materials and equipment

3.1.1 Fuels used for the experiments

The waste vegetable oil (WVO), Oleander, canola, sunflower, Coconut biodiesels, and diesel used in the experiments were purchased from a petroleum outlet in Thika town, Kiambu County, Kenya. Selection of the biodiesels was based on their varied properties and compliance with recommended limits specified in EN14214 and ASTM D975 standards, as documented by Aybek *et al*. (2011), Palani *et al*. (2022), and Binhweel *et al*. (2021). The biodiesels were mixed with diesel at different ratios. The volumes were measured using a beaker and burette and their blend ratios were as detailed in table below.

Table 3.1: Biodiesel blend ratios and volumes used

Blend Name	Blend ratio (biodiesel: diesel)	Volume of Biodiesel (ml)	Volume of Diesel (ml)
B10	10:90	10	90
B15	15:85	15	85
B20	20:80	20	80
B25	25:75	25	75
B30	30:70	30	70
B100	100:0	100	0

After blending, the mixture was stirred using an electric blender for 3 minutes, allowed to settle for 2 hours before carrying out the fuel analysis.

3.1.2 Equipment for the experiments

a) Weighing scale

Plate 3.1: Electronic weighing scale

The electric weighing scale used in this research is shown in the plate above had the main features and their specifications as detailed in the table below.

Table 3.2: Specifications of weighing scale

Factor	Specification
Model	LWS-3C
Display	16.5mm digital high LCD display
Capacity	3000g
Readability	0.002g
Pan size	Diameter 120 mm
Keyboard	7membrane keys
Housing	ABS plastic
Attachment	Wind shield
Operating temperature	5^0C ~ +40^0C
Power	AC adapter(12V/500mA), Rechargeable battery (6V)
Gross weight	2 Kg

b) Redwood viscometer

The plate 3.2 was the Redwood Viscometer No. 1 was used to determine kinematic viscosity.

Plate 3.2: Redwood viscometer No. 1

The viscometer consists of vertical cylindrical oil cup having a hook pointing upward serve as a guide mark for filling the oil. The cylindrical cup has an orifice its base center, closed using a metal ball (valve). The cylindrical cup measures are 47.625mm in diameter and 88.90mm deep, while the orifice diameter is 1.70mm. The cylindrical cup surrounded by a water bath, whose temperature was raised using an immersed electric heater and maintained uniformly by continuous stirring. A beaker is used to collect the oil drained from the cup, whose time to drain is recorded using a stopwatch. The cylindrical oil cup was cleaned, to ensure that the orifice was free from any dirt, and orifice was closed using the metal ball bearing. The oil cup was then filled with oil up-to half point mark of the hook. The water bath was then, half fill with water, whose temperature was raised and maintained uniformly at 40^0C using an electric heater and continuous stirring. The oil was then allowed to flow freely into a 50ml beaby lifting the ball bearing and efflux. Water was used for calibration. The viscometer is suitable highly viscous oils.

c) Bomb calorimeter

Plate 3.3 below shows the bomb calorimeter (Model 1013-B), adiabatic Nenken type supplied by Anamet Inc., USA, used to determine the lower heating value of fuels.

Plate 3.3: Bomb calorimeter (Model 1013-B)

The main features were of the calorimeter were; stainless Combustion Vessel (Bomb), stainless steel calorimeter bucket, thermocouples, digital display and control unit. Its adiabatic design: ensures minimal heat exchange and temperature regulation with the surroundings, allowing for more accurate measurement of the sample's heat of combustion. The Nenken type, refers to a design optimized for specific types of samples or conditions, enhancing the precision and reliability of the measurements. The calorimeter was built with high-quality materials to withstand high pressures and temperatures generated during the combustion process. It is equipped with user-friendly controls and displays that make it easy to set up experiments, monitor progress, and record results. It had high accuracy in determining the calorific value of the sample, typically within ±0.1%.

d) Engine test rig

The research was conducted using the Apex 240PE engine test rig supplied by "Apex Innovation Pvt. Ltd.", India, installed at the thermos-fluids lab, department of mechanical engineering (map of location shown in appendices 3), Jomo Kenyatta University of Agriculture and Technology (JKUAT). The test rig used is shown in the photograph below

Plate 3.4: Test-rig engine used in the research

i. Engine

The engine used to carry out the experiments had specifications described in the table below.

Table 3.3: Engine specifications

Model/ Manufacturer/year	Apex 240PE / Sangi, India/1998
Maximum rated power	3.5 Kw @ 1500 rpm
Cooling system/Air intake	Water cooled/ Natural aspiration
Mode of injection	Direct injection
Number of cylinders/strokes	One/Four
Compression ratio (VCR)	Variable between 12.1 to 18.1
Loading device	Saj Eddy current electric dynamometer
Lubrication system	Fully forced closed lubrication system
Fueling	multi-fuel (diesel and ECU petrol), variable

ii. Dynamometer

The eddy current dynamometer used for the experiments had the following specifications;

Table 3.4: Dynamometer specification

Parameter	feature
type	Dynalec control ECB-15 kW
Capacity	60 Nm @500-1500 RPM/15Kw
Max. excitation current	6 amp DC
Coil resistance	12-15 ohms
Coil dynamometer	500 M ohms
Overall size	Width 510 mm and height 660mm center of the shaft

e) Horiba gas analyzer

The Horiba gas analyzer VA5000 is shown in the plate below with

Plate 3.5: Horiba gas analyzer model VA5000 series

The Horiba gas analyzer had gas sensors for; CO, CO_2, O_2, NO_x, SO_2 and HC. Its main features were the digital flow meter display, dual range sensors, self-leak check, flue gas, ambient and temperature sensor, averaging test for emissions. USB Interface, Bluetooth link, on-board printer, 15ft sample line, CO Purge pump to prevent oversaturation, Peltier cooler sample conditioner, peristaltic pump for automatic moisture removal, heated sensor block. 100-240 V AC (±10%, maximum voltage 250 VAC), 50/60 Hz (±1.0%), Consumption: 100 to 350 VA.

f) MATLAB Program

MATLAB 9.4 (R2018a) was used It has graphics card supporting OpenGL 3.3 of 1GB

3.2 Determination of the effects of biodiesel blending on fuel properties

The fuel properties determined were; density, kinematic viscosity, and lower heating value; were for the biodiesel blends. The biodiesel sources used were waste vegetable oil (WVO), Oleander, canola, sunflower, and Coconut, blends; B10, B15, B20, B25, and B30. Rigorous standard test procedures were adopted to ensure reliable and accurate property measurements within quantified uncertainty limits. This provides a robust baseline dataset for developing the model's performance and emissions. The uncertainty in the experimental measurements was determined by considering errors from repeatability and standard deviation of multiple measurements at 95% confidence level using standard methods (Figliola & Beasley, 2014). ASTM standard test methods were used to measure the fuel properties as described in the subsequent sub-sections below;

3.2.1 Determination of the density of the fuels.

The densities of the fuels (diesel and biodiesel blends) were determined using a 250 mm measuring cylinder, a pipette and a digital weighing scale described in section 3.1.2-a, above. An empty measuring cylinder was weighed, using a weigh balance, and its mass, was recorded in grams. Then, 25 ml of fuel was put into measuring cylinder using a pipette, while checking the level mark on the cylinder before weighing on the balance. The data of the measured mass and volume were recorded. This procedure was repeated by adding 25 ml of fuel into the cylinder each time while recording its new volume and total mass until the measuring cylinder was full.

The densities of the fuel at room temperature which averaged of 23^{o}C, were given as the gradient of the 'best fit' straight line plots of the mass of liquid (y-axis) against volume (x-axis). The procedure was used also to determine densities for the biodiesels and blends of WVO, Oleander, canola, sunflower, and Coconut. This method provided an accurate and standardized method for determination of density (Tesfa *et al.*, 2010).

3.2.2 Determination of the kinematic viscosity of the fuels.

The kinematic viscosity of the fuels (diesel, biodiesel and their biodiesel blends) were determined using a redwood viscometer as specified in test method ASTM D445-18 (Yang *et al.*, 2016), describe in section 3.1.2-b above. This method was selected since it measured viscosities accurately within the fuels range, industry acceptability, and its ability to handle high-viscosity samples (Paula *et al.*, 2019). The viscometer was calibrated using standard viscosity oils. The fuel samples were filled in the viscometer, and the time taken to fill the beaker recorded using a stopwatch (redwood

seconds) (efflux time) was measured, at 40°C. Three repetitions were carried out for a sample and the average time calculated for each treatment as shown in table below

Table 3.5: Calculations of kinematic viscosity

Exp. No.	Temperature of oil, ºC	Time (s), to fill the 50ml beaker	Density of the oil kg/m^3	Calculated Kinematic Viscosity
WVO	40	30.9	836.8 @ 24.5ºC	2.73
		31.7		
		32.0		
	Average	31.5		

Kinematic viscosity of the oil at 40^{0}C was calculated using the viscometer constant and average recorded redwood seconds of replications illustrated in table 3.4, using the equation 3.1 (ASTM, 2018c);

$$\upsilon = 0.26t - \frac{172}{t} \quad \text{..... (3.1)}$$

Where; υ- Kinematic viscosity, centistoke (mm^2/s), t - redwood seconds.

3.2.3 Determination of the lower heating value.

The lower heating values (CV) of the test fuels were determined using a Nenken-type adiabatic bomb calorimeter, Model 1013-B (Plate 3.5), following the ASTM D2015-18 standard test method (Yang *et al.*, 2016) describe in section 3.1.2-c. above. This procedure involved burning of a fuel with pure oxygen inside the calorimeter chamber and measuring the resulting temperature rise. An ignition wire (100mm) was threaded through the bomb cap electrodes and positioned above the sample, avoiding contact with the cup sides. The inner cylinder was loaded with 2,100 ml of water before being placed on the outer cylinder frame, also, filled with water.

The calorimeter was then assembled, ensuring proper placement of thermometers and stirrer. Approximately 0.8 - 1 gram of weighed fuel sample was placed in a cleaned calorimeter bomb cup, then charged with oxygen to approximately 30 bars, checked for leaks, dried, and connected to the electric supply. The fuel sample was ignited via external electrodes and the temperature rise of the calorimeter water measured accurately using the high-sensitivity Beckmann thermometer. Temperature stability was checked every minute for 5 minutes before initiating combustion by pressing the capacitor ignition unit. Temperature readings from the Beckmann thermometer were recorded every minute for 10 minutes and then every 5 minutes until three successive readings were consistent,

indicating the maximum temperature. When the maximum temperature was achieved, the calorimeter, water heater, and cold-water supply were then turned off. The Cv was computed from the temperature rise, fuel mass, and instrument constant as per ASTM D2015-18 (Alpgiray, 2006) using the average of the three replications for each blend, as shown in equation 3.2;

$$\mathrm{Cv} = \frac{W_e \times \Delta T - c}{m_f} \qquad (3.2)$$

Where;

w_e- water equivalent (cal/°C)

m_f- mass of the fuel used (g)

c- calory correction for ignition nickel wire Cv 775 cal/g

ΔT- temperature change

Note: The calorimeter was calibrated using a pellet of benzoic acid, as the standard fuel. It was chosen due to its proven accuracy and precision, its applicability to various fuel types, compatibility with the standard, safety considerations, and historical acceptance in the scientific community (Liptak,2003).

3.3 Determination of engine performance and emissions fueled by biodiesel blends

The research investigated engine performance and emissions using the IC Apex 240PE engine test rig (plate 3.4) and Horiba VA5000 gas analyzer (plate 3.5) as shown set-up figure 3.1.

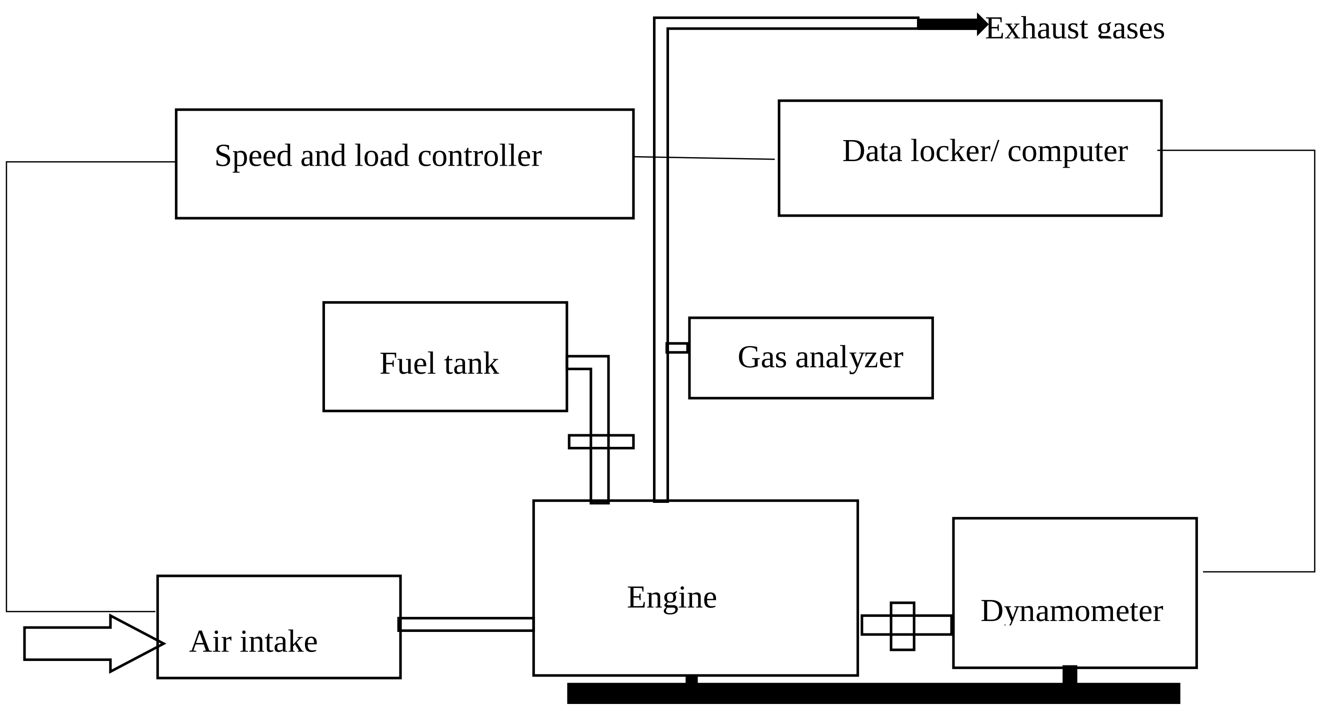

Figure 3.1: Engine tests experimental set-up

In addition, the set-up in figure 3.1, had a stand-alone panel box consisting of an air box, a fuel tanks, a manometer, a fuel measuring unit, transmitters for air and fuel flow measurements, a dashboard

load/speed knob, hardware/software interface switch, rotameters, and engine dashboard indicator. The engine speed or load was adjusted using the speed or load knob on the dashboard controlled by the eddy current dynamometer. Rotameter measured the water flow for the cooling engine and calorimeter. The indicators fitted in the control panel were used to capture the speed and load reading through signals from the engine sensors. The indicators, together with the panel box transmitters, were connected to the COM port of the computer. The computer, through its installed LabVIEW-based engine performance analysis software package "Engine soft" version 2.4, interfaced the signals to read, display, and store data. The gas analyzer used to capture emissions was mounted on the exhaust pipe.

Before starting the engine, all the nuts and bolts for the mounting of the dynamometer, propeller shaft, and base frame were tightened. In addition, the engine oil level, fuel level, and water supply connections to the calorimeter and dynamometer calibration checked. Also, electrical supply and computer connections were ascertained. When all checks were cleared, the electrical and water supply was switched 'ON,' then the engine was started and run with diesel fuel at the rated speed of 1500 rpm with 0kg (no load) for 10 minutes to attain steady state conditions. During this period, the computer was switched ON, and the "enginesoft" icon was selected to "configure" the fuel type.

The engine was fueled with diesel and before conducting any test, the engine was warm-up period at the speed and load were set at 1500 rpm or 0 kg using the dashboard. After the engine was stabilized, the data "capture" switch was turned ON while "engine mode" in the computer menu opened, and the RUN option was selected to give continuous display, processing, and all the measurement data were logged for one minute. At the end of the minute, the log-off key menu of "engine mode" was selected to stop data logging and store the record as a word document on the computer. The engine was then loaded gradually from 0 kg (no load) at intervals of 3kg to 12kg (full load). For each of the tests conducted, the data was stored as a set of five different load conditions: 0, 3, 6, 9, and 12 Kg at constant speed of 1500 rpm. In each of these test runs, exhaust gas analysis data was captured using the Horiba gas analyzer.

The previous steps experimental steps were then repeated for the engine running on the different biodiesel; WVO, oleander, sunflower, canola, and Coconut; and their blends of; 10% (B10), 15% (B15), 20% (B20), 25% (B25), 30% (B30), and 100% (B100). Software (enginesoft) was used to log in engine performance (brake thermal efficiency, specific fuel consumption) data. In contrast, the Horiba gas analyzer printout used emissions (carbon monoxide and nitrogen oxides) data. The error

for measured values was ± 10%. Tests were conducted guided by the ECE R49 engine test cycle (Abed) shown in table below.

Table 3.6: Test modes for the experiments

Input Parameters	**Input Range**				
Sources of Biodiesel	**WVO**	**Coconut**	**Sunflower**	**Oleander**	**Coconut**
Biodiesel blends (Bi), %	10	15	20	25	30
Load (W), kg (Equivalent brake power (Bp), kW)	0 (0)	3(0.86)	6(1.72)	9(2.58)	12(3.44)

The variables loads were converted to equivalent brake power (Bp) or equal energy delivery using equation 3.3. Equivalent Brake power was equal energy delivery means supplying an equal amount of energy to the engine by the fuel calculated using engine loads and speed as outline below.

$$Bp = \frac{2\pi gNWl}{60,000} \quad \ldots\ldots\ldots\ldots\ldots\ldots\ldots\ldots\ldots\ldots\ldots\ldots\ldots\ldots\ldots \text{(3.3)}$$

Where; g- gravitational force , kW, W- engine load, kg N- engine speed, rpmand l- arm length, mm

Equivalent brake power (Bp) was the most ideal for studying the performance characteristics {Brake thermal efficiency and Specific fuel consumption} and emissions {Nitrogen oxides and Carbon monoxides} of the fuel since it best identified the specific consumption efficiency. The experimental were carried out using the factorial design-of-experiments (DoE) technique as shown in table below.

Table 3.7: Experimental design for biodiesel blends

Biodiesel	**Blend**	**Loads**
WVO	B10	0(0)
Coconut	B15	0.86(3)
Canola	B20	1.72(6)
Sunflower	B25	2.56(9)
Oleander	B30	3.44 (12)

Diesel (B0) and biodiesels (B100) were used as controls

3.4 Modelling of engine performance fueled by biodiesel blends

The mathematical model for predicting engine performance (brake thermal efficiency (Bte), specific fuel consumption (Sfc)) and emission (carbon monoxide (CO), and nitrogen oxides (NOx)) as a function of equivalent brake power (Bp), fuel characteristics (density, kinematic viscosity, low heat value) and blend levels (B) for the given fuels were developed using the Buckingham's theory analytical methods. The assumptions of the model were;

i. The biodiesel-diesel mixture remained homogeneous within the scope of the analysis.
ii. The engine operated under lean conditions, with constant compression ratio (CR) and ignition angle (ɯ), thus air-fuel (AF) ratio had no influence on its performance and emission. Environmental conditions were constant throughout the engine test runs.
iii. The low heat value, kinematic viscosity, and density fuel parameters significantly affected engine performance and emission.
iv. The engine operating conditions setting remained constant through data acquisition.

The figure below gives the analysis of the engine process during combustion

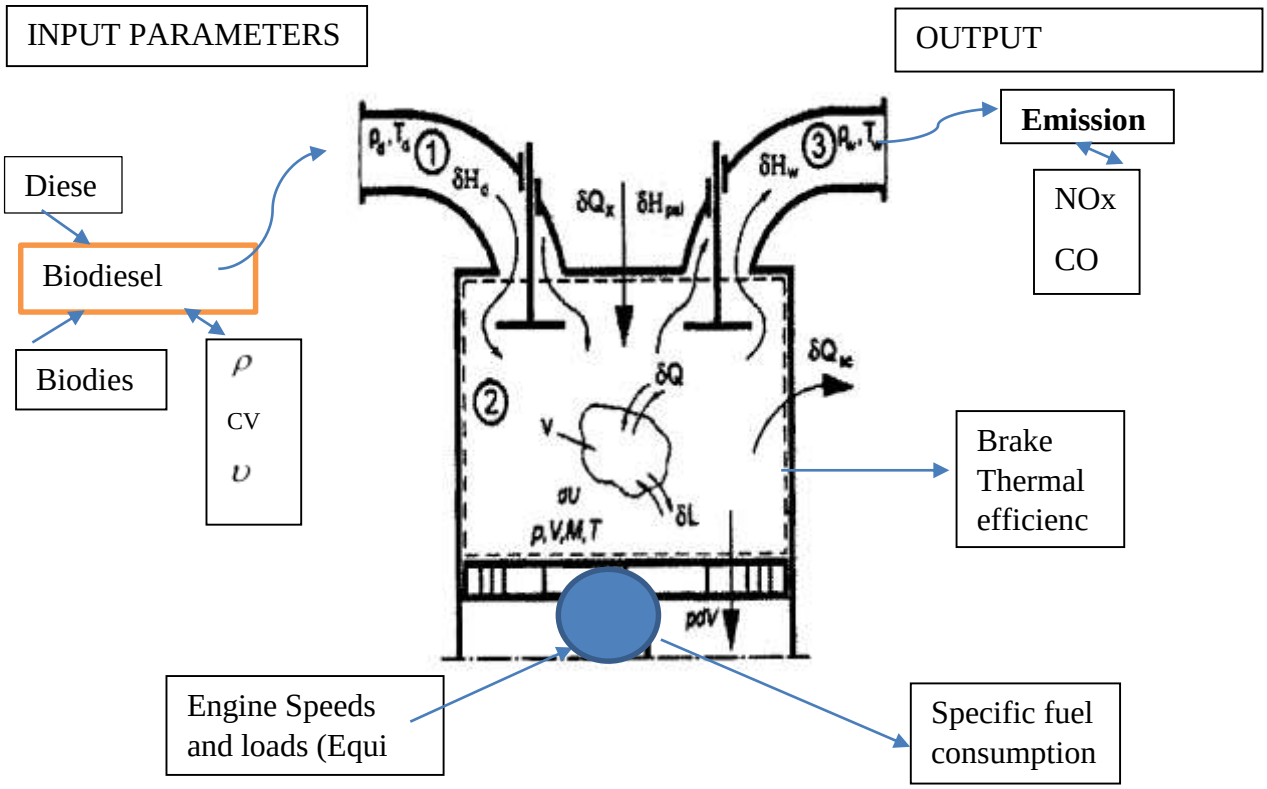

Figure 2.1: Engine performance and emissions analysis

Table 2.4, section 2.8 were used to develop analytical models discussed in sub-sections below;

3.4.1 Brake thermal efficiency analytical models

Table 3.8 below presents a concise overview of the parameters alongside their respective dimensions deployed in the development of the brake thermal efficiency (Bte) mathematical model.

Table 3.8: Parameters used to determine brake thermal efficiency model

Variable	Parameter	Symbol	Dimension
1.**Dependent (Output)**	Brake thermal efficiency	Bte	$M^0L^0T^0$
Independent (Inputs)			
2.	Blend Ratio	B	$M^0L^{-2}T^{-2}$
3.	Lower heat value	Cv	L^2T^{-2}
4.	Density	ρ P	M^1L^{-3}
5.	Kinematic viscosity	v N	L^2T^{-1}
6.	Equivalent Brake power	Bp	$M^1L^2T^{-3}$

The standard form Bte equation derived from the Table above are as given below;

$$\{Bte, B, Bp, Cv, \rho, v\} = 0 \quad \ldots\ldots\ldots\ldots\ldots\ldots\ldots\ldots\ldots\ldots\ldots\ldots\ldots\ldots\ldots\ldots\ldots\ldots\ldots\ldots\ldots\ldots \quad (3.4)$$

The Buckingham *pie* theorem used 3 π terms {No. of variables (n=6)-fundamental variables (m=3)} and selected as repeating variables (n= 3) Lower heat value (Cv), density (ρ), kinematic viscosity (ν) were, since the fuel parameters were constant for a fuel, to develop Bte models as;

The three (3) *pie (π) terms* for Bte equation;

$$\pi_1 = BCv^{a1}\rho^{b1}v^{c1}, \quad \pi_2 = BpCv^{a2}\rho^{b2}v^{c2} \quad \text{and} \quad \pi_3 = (Bte)Cv^{a3}\rho^{b3}v^{c3} \quad \ldots. (3.5)$$

Where; a_1, b_1, c_1, a_2, b_2, c_2 and a_3, b_3, c_3 were constants for the π_1, π_2 and π_2 for *pie (π) term*, determined by comparing coefficients of Mass (M), Length (L) and Time (T) of equation 3.5. Thus;

π_1= B Cv^{a1} ρ^{b1} ν^{c1}; $\quad [M^0L^0T^0] = [M^0L^0T^0]^1\,[M^0L^2T^{-2}]^{a1}\,[M^1L^{-3}T^0]^{b1}\,[M^0L^2T^{-1}]^{c1}$

π_2= Bp Cv^{a2} ρ^{b2} ν^{c2}; $\quad [M^0L^0T^0] = [M^1L^2T^{-3}]^1\,[M^0L^2T^{-2}]^{a2}\,[M^1L^{-3}T^0]^{b2}\,[M^0L^2T^{-1}]^{c2}$

$\pi_3 = (Bte)Cv^{a3}\rho^{b3}v^{c3}$ $\quad [M^0L^0T^0] = [M^0L^0T^0]^1\,[M^0L^2T^{-2}]^{a3}\,[M^1L^{-3}T^0]^{b3}\,[M^0L^2T^{-1}]^{c3`}$

The constants were determined using comparison method of the basic units as follows;

π_1; M: 0 = $-c_1$; L: 0 = $2a_1-3b_1-2c_1$; T: 0 = $2a_1-c_1$; thus; $a_1=0$, $b_1=0$ and $c_1=0$,

Therefore; Independent *pie term* $\pi_1 = B$ ……..……. (3.6)

π_2; M: 0 = $1+b_2$; L: 0 = $2+2a_2-3b_2+2c_2$; T: 0= $-3-2a_2-c_2$; then; $a_2= -½$, $b_2= -1$, $c_1= -2$; Then

Thus; Independent *pie term* $\pi_2 = \frac{Bp}{\rho Cv^{1/2}v^2}$ ……..… (3.7)

π_3 : M: 0 = b_3; L: 0 = $2a_3-3b_3+2c_3$; T: 0 = $-2a_3-c_3$, thus, $a_3 = 0$, $b_3 = 0$, $c_3 =0$;

Resulted into the Bte dependent *pie term* as; π_3 = Bte ……..…… (3.8)

Hence from equations 3.6, 3.7, and 3.8, the Brake thermal efficiency (Bte) relationship is given as;

$f\left\{Bte, \mathrm{B}, \frac{Bp}{\rho Cv^{1/2}v^2}\right\} = 0$; Thus,

$$Bte = k_1 \mathrm{B}^{p1}\left(\frac{Bp}{\rho Cv^{1/2}v^2}\right)^{q1} \quad \text{……... (3.9)}$$

Where; k_1, p_1, q_1 were constants for brake thermal efficiency (Bte),

The constants k_1, p_1, and $q_1$were determined using experimental data of brake thermal efficiency.

3.4.2. Specific fuel consumption analytical model

The table 3.9 presents the parameters along with their respective dimensions, which were deployed in development of the specific fuel consumption model (Sfc).

Table 3.9: Parameters used to determine specific fuel consumption model

Dependent (Output)	Parameter	Symbol	Dimension
1	Specific fuel consumption	Sfc	$M^0L^2T^{-2}$
Independent (Inputs)			
2.	Blend Ratio	B	$M^0L^{-2}T^{-2}$
3	Lower heat value	Cv	L^2T^{-2}
4	Density	P	M^1L^{-3}
5	Kinematic viscosity	N	L^2T^{-1}
6.	Equivalent Brake power	Bp	$M^1L^2T^{-3}$

The standard form of the equations for specific fuel consumption (Sfc);

f {Sfc, B, Bp, Cv, ρ, ν,} = 0 ……... (3.10)

From equation 3.6 and 3.7, the independent variables *pie terms* given as;

$\pi_1 = B$; And $\pi_2 = \frac{Bp}{\rho C v^{1/2} \nu^2}$;

Then dependent variable *pie term* for specific fuel consumption (Sfc) was evaluated as follows;

$\pi_4 = sfc\ Cv^{a4}\ \rho^{b4}\ \nu^{c4}$ …….....…….. (3.11)

a_4, b_4 and c_4 determined by comparing coefficients of Mass (M), Length (L), Time (T) equation 3.11

$[M^0L^0T^0] = [M^0L^{-2}T^2]^1\ [M^0L^2T^{-2}]^{a4}\ [M^1L^{-3}T^0]^{b4}\ [M^0L^2T^{-1}]^{c4}$; Thus, M: $0 = b_4$; L: $0 = -2+2a_4-3b_4+2c_4$; T: $0 = 2-2a_4-c_4$, thus, $a_4 = 1$, $b_4 = 0$, $c_4 = 0$ gave;

$\pi_4 = sfc(Cv)$ ……... (3.12)

Hence from equations 3.6, 3.7, and 3.12, the mass flow rate (m) relationship is given as;

$f\left\{ sfc(Cv), B, \frac{Bp}{\rho C v^{-1/2} \nu^{-2}} \right\} = 0$; Thus,

$sfc = k_2 Cv^{-1}\ B^{p2} \left(\frac{Bp}{\rho C v^{1/2} \nu^2}\right)^{q2}$ ……..……..... (3.13)

Where; k_2, p_2 and q_2 constants were determined using experimental results for Sfc in section 4.3.

3.4.3 Carbon monoxide emissions analytical model

Table 3.11 provides a concise overview of the utilized parameters and their respective dimensions, integral to the construction of the carbon monoxide (CO) mathematical model.

Table 3.10: Parameters used to determine carbon monoxides model

	Parameter	**Symbol**	**Dimension**
Dependent (Output)			
1	Carbon monoxide	CO	$M^0L^0T^0$
Independent (Inputs)			
2.	Blend Ratio	B	$M^0L^{-2}T^{-2}$
3	Lower heat value	Cv	L^2T^{-2}
4	Density	P	M^1L^{-3}
5	Kinematic viscosity	N	L^2T^{-1}
6.	Equivalent Brake power	Bp	$M^1L^2T^{-3}$

The standard form of the equations for Carbon monoxide (CO)

f ([CO_2], B, Cv, ρ, ν) = 0……..... (3.14)

Then dependent variable *pie term* for [CO] was evaluated as follows;

$\pi_6 = [CO]\ C_v^{a6}\ \rho^{b6}\ \nu^{c6}$ ……..... (3.15)

Where; a_6, b_6 and c_6 are constants, determined by equating the powers of M, L and T thus CO equation;

$$\pi_5 = [\mathrm{CO}] \quad \text{..... (3.16)}$$

Hence from equations 3.6, 3.7, and 3.20, the carbon monoxide [CO] relationship is given as;

$$f\left\{[\mathrm{CO}], \mathrm{B}, \frac{Bp}{\rho C v^{-1/2} \nu^{-2}}\right\} = 0; \text{ Thus,}$$

$$[\mathrm{CO}] = k_4 \mathrm{B}^{p4} \left(\frac{Bp}{\rho C v^{1/2} \nu^2}\right)^{q4} \quad \text{..... (3.17)}$$

k_4, p_4 and q_4 were constants determined from experimental results for CO emission in section 4.3.

3.4.4. Nitrogen oxides emissions analytical model

Parameters and dimensions for development of Nitrogen Oxides (NOx) model are shown in the table.

Table 3.11: Parameters used to determine nitrogen oxide model

	Parameter	Symbol	Dimension
1.Dependent (Output);	Nitrogen Oxide	NOx	$M^0L^0T^0$
2. Independent (Inputs);	Blend Ratio	B	$M^0L^{-2}T^{-2}$
	Lower heat value	Cv	L^2T^{-2}
	Density	P	M^1L^{-3}
	Kinematic viscosity	N	L^2T^{-1}
	Equivalent Brake power	Bp	$M^1L^2T^{-3}$

The standard form of the equations for Nitrogen Oxides (NOx)

$$f([NO_X], B, Bp, Cv, \rho, \nu) = 0 \quad \text{..... (3.18)}$$

Then dependent variable *pie term* for [NOx] was evaluated as follows;

$$\pi_5 = [\mathrm{NOx}]\, Cv^{a5}\, \rho^{b5}\, \nu^{c5} \quad \text{..... (3.19)}$$

Where the dependent variable constants a_5, b_5 and c_5 were determined, Thus, the NOx equation;

$$\pi_5 = [\mathrm{NOx}] \quad \text{..... (3.20)}$$

Hence from equations 3.6, 3.7 and 3.19, the nitrogen oxide [NOx] relationship is given as;

$$f\left\{[\mathrm{NOx}], \mathrm{B}, \frac{Bp}{\rho C v^{1/2} \nu^2}\right\} = 0; \quad \text{Thus,}$$

$$[\mathrm{NOx}] = k_3 \mathrm{B}^{p3} \left(\frac{Bp}{\rho C v^{1/2} \nu^2}\right)^{q3} \quad \text{..... (3.21)}$$

Where; k_2, p_2 and q_2 were constants determined from experimental data of nitrogen oxides.

3.4.5: Determination of the model constants

In this study, analytical equations 3.9, 3.13, 3.17 and 3.21 in section 3.3, were used to develop the mathematical models to predict brake thermal efficiency (Bte), specific fuel consumption (Sfc), carbon monoxide (CO), and nitrogen oxides (NOx) based on blending level (B), fuel parameters; density (ρ); kinematic viscosity (ϑ) and low heating value (Cv), together with the equivalent brake power (Bp) using engine test results from section 4.3. It is important to note that; B, Bp, ρ, ν an C_v were common to the output parameters (Bte, Sfc, NOx and CO) outlined equations 3.6 and 3.7. Below is an analysis of the usefulness of the *pie terms* used as outlined in the table below;

Table 3.12: The pie terms and their usefulness

Pie Term	Physical Meaning
$\boldsymbol{\pi_1}$= B	Biodiesel blend ratio, B, measures the amount of biodiesel added to the diesel
$\boldsymbol{\pi_2} = \frac{\boldsymbol{Bp}}{\boldsymbol{\rho C v^{1/2} \nu^2}}$	Measures the ability of an engine to convert the fuel energy into useful power

Thus, equations 3.9, 3.13, 3.17 and 3.21 were generalized in the format below for easy entry;

$$\text{output parameters} \; = k_i \, \pi 1^{\,p_i} (\pi 2)^{q_i} \qquad (3.22)$$

The equations logarithms of format (equation 4.1) done as follows;

$$\log(output\ parameters) \; = log k_i + p_i log \pi_1 + q_i log \pi_2 \qquad (3.23)$$

The constants k_i, p_i, q_i for the equation from section 3.3 were determined using experimental data in section 4.3, converted using equation 4.2 and MATLAB 2018 *script* for non-linear curve-fitting method, given below;

```
ydata (output parameters) = data (:20);

[xfitted (log (π1), log( π2)), errorfitted] = lsqcurvefit (fitfcn, p0, data, ydata);

Plot (x, ydata, '*', x, fitfcn (xfitted, yi, data),'g');

< stopping criteria details>

X fitted for (output parameters) = {Ki, pi, qi};
```

3.5 Determination of the optimal blend levels

Non-Dominated Sorting Genetic Algorithm-II (NSGA-II) was for optimization. NSGA-II was chosen for its ability to handle multi-objective problems of maximizing performance while minimizing emissions effectively. The methodology in the figure 3.2 below provided a systematic approach to explore engine performance while adhering to the emission regulatory requirements.

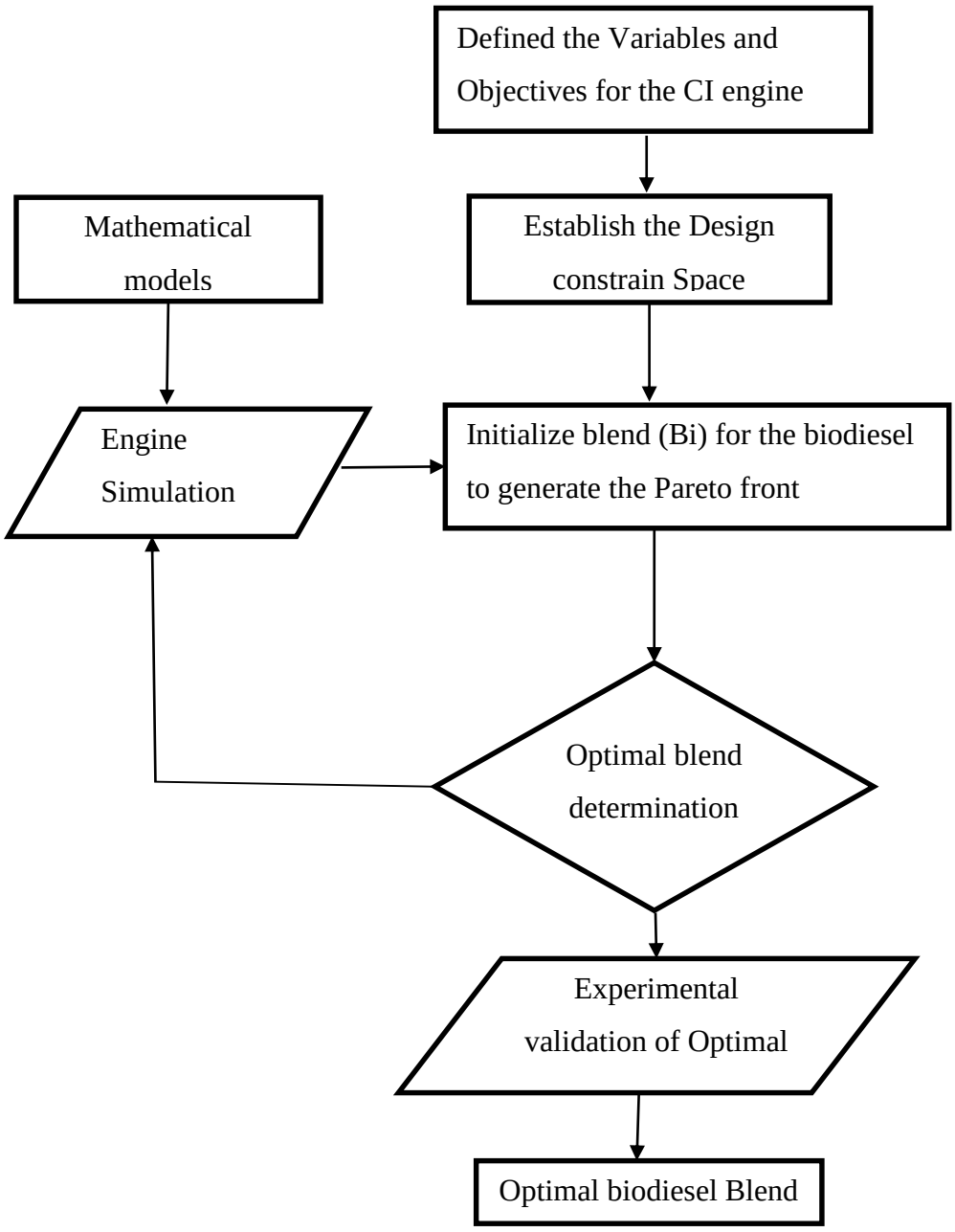

Figure 3.2: Flowchart for the optimization of the biodiesel blend level

3.5.1 Procedure for the Non-Dominated Sorting Genetic Algorithm-II optimization

Below was the description of the procedure of NSGA-II in the flow chart outline in figure 3.2;

i. The optimization process identified key objective functions for maximization of brake thermal efficiency (Bte) and minimization of nitrogen oxide (NOx) emissions, based on the mathematical models obtained from section 3.4 and their input parameters being; biodiesel blend ratio, fuel properties, and engine operating conditions.

ii. The design space was established on the basis of limitations of; biodiesel blend level, engine operating condition and the carbon monoxide acceptable level.

iii. Thereafter, an initial random population of blend ratio and engine operating conditions were generated within the design space and evaluated by the models to determine fitness values with respect to the objectives.

iv. Identification of the Pareto-optimal solution for population

v. Iterations based on the engine simulations were carried out to obtain set of Pareto-optimal solutions.

vi. The Pareto fronts of the selected optimal blends were validated using engine experimentation, ensuring alignment with model predictions.

vii. Finally, the validated set of the Pareto fronts were classified using the Pareto ranking method and the biodiesel blend optimal selected

The NSGA-II algorithm utilized MATLAB's capabilities for non-linear constraint handling and efficiently explored the solution space. The resulting optimal blend levels demonstrated a trade-off between Bte and NOx emissions, balancing engine performance objectives under specified constraints.

3.5.2 Optimization procedure code

The MATLAB 9.4 (R2018a) code was developed as described below;

I. **Objective Functions code** (`*fitnesSfcn*` *function*) is a multi-objective optimization, aimed to determine the best solutions for a problem with two objectives.

II. **Decision Variables***:* The optimization is performed over two decision variables subject to constraints defined by the problem, represented by the vector x. The first column of vector blend and the second column is dependent on blend.

III. **Constraints***:* The nonlinear constraints on the decision variables are handled by the function `my Constraint`, which is assigned to `*nonlcon*`. The constraint function is defined as follows:

- *'my Constraint function''* is supposed to give back equality and inequality nonlinear constraints as return values of the function.
- upper and lower bounds for blends were 0.1 and 0.3

IV. **Optimization Method***:* The multi-objective optimization was performed using the `*gamultiobj*` function (better solver as compared to Pareto search). This function employed genetic algorithm to explore the solution space and find a set of solutions that represent trade-off of the objectives.

V. **Results***:* The optimization results, stored in the variable (x, represent a set of Pareto-optimal solutions. These solutions are not dominated by other solutions, providing a range of trade-offs between the objectives.

VI. **Visualization***:* The Pareto-optimal solutions are plotted using a scatter plot, where each point represents a solution. The x-axis corresponds to the first decision variable x(1) which is blend, and the y-axis corresponds to the second decision variable x(2) dependent on Bp.

The script of MATLAB 9.4 (R2018a) code below was used to obtain optimal biodiesel blend.

```
fitnesSfcn = @(x)[-1.2 * x(1)^(-0.42) * x(2)^(0.68), 24000 * x(1)^(0.6) * x(2)^1.3];
nonlcon = @myConstraint;
nvars = 2;
ub = [0.3, 433.36];
lb = [0.1, 104.36];
rng default % for reproducibility
x = gamultiobj(fitnesSfcn,nvars,[],[],[],[],lb,ub,nonlcon)
plot(x(:,1),x(:,2),'ko')
xx = linspace(0.100, 0.108);
yy = myConstraint(xx);
hold on plot (xx, yy,'b--')
```

objective functions

```
function [c, ceq] = myConstraint(x)
c = 0.03 * x (1) ^ (-0.12) * x(2)^0.35 - 1500; ceq=[]; end
```

Sensitivity analysis was performed to obtain the impact of input parameter variations on Pareto front.

CHAPTER FOUR

RESULTS AND DISCUSSION

4.1 General observations

The experiments conducted on the engine test rig at Jomo Kenyatta university of agriculture and technology (JKUAT) whose altitude of approximately 1662 meters above sea level with temperature ranged between 20 to 24^{o}C. The engine performance results observed, were primarily attributed the biodiesel properties and blending metrics rather than environmental factors, since atmospheric temperature changes significant to induce variations in the tests. Thus, the results gave a clear understanding how biodiesel source and blending impacted on the fuel properties and engine performance, critical to successfully adoption as replacement to diesel. The output results were obtained using IC enginesoft given in appendices D.2 a.

4.2 Effects of biodiesels blends on its fuel properties

The selected biodiesel properties: density, kinematic viscosity and lower heating value were determined using ASTM D1298, ASTM D445-18 and ASTM D2015-18 procedures respectively, describe in section 3.2. The densities were determined as a gradient of the plots of measured weights versus volume, kinematic viscosity was measured using redwood viscometer and lower heating value data capture by adiabatic bomb calorimeter. All the measurements were replicated three times for each fuel property as shown in appendices 4.1; density (A1.1-A1.7); kinematic viscosity (A2.1-2.7) and heat value (3.1-3.5) analyzed using ANOVA and presented in table below.

Table 4.1: Determined properties of the selected biodiesels

Selected fuel Properties	**Diesel**	**Selected Biodiesels**					
		WVO	**Coconut**	**Canola**	**Sunflower**	**Oleander**	**SEM**
Density (kg/m3@23 ^{o}C)	820.0^{f}	876.6^{d}	872.3^{e}	891.6^{b}	882.9^{c}	925.1^{a}	7
Kinematic viscosity (mm^2/s@40 ^{o}C)	3.2^{f}	4.2^{e}	4.4^{d}	4.7^{c}	5.2^{b}	5.5^{a}	0.2
Heat value (kJ/kg)	43906^{a}	39421^{b}	38736^{c}	37572^{e}	37818^{d}	36206^{f}	430

The means in the same row followed by the same letter are not significantly different at alpha= 0.05 and p <0.0001

4.2.1: Effects of biodiesels blends on density

Table 4.1 above and figure 4.1 below shows the of densities determined by the procedure in section 3.2.1 for the five different biodiesels oleander, canola, sunflower, Coconut, WVO and diesel.

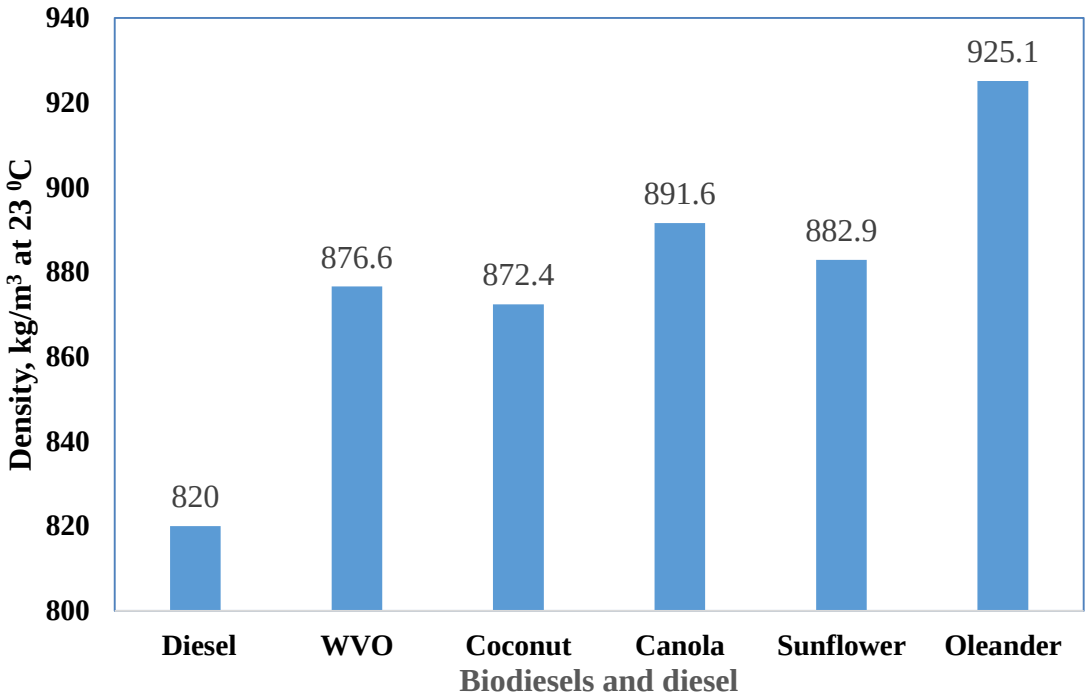

Figure 3.1: Densities for the selected biodiesels and diesel

Figure 4.1 shows clearly that biodiesels had higher densities compared to diesel (820 kg/m^3), though different, depending on the source of their feedstock. The results also showed that the density of oleander (925.1^a) was the highest amongst the biodiesels tested. Canola Biodiesel (891.6^b) had the second-highest density, followed by sunflower (882.9^c), coconut (872.3^e) with WVO (876.6^d) recording the lowest. Results were aligned with the findings from Lapuerta *et al*. (2008), Binhweel *et al*. (2021), and El-Shafay *et al*. (2023 The higher densities of biodiesels are attributed to the long chains of fatty acid methyl esters, agreeing with the finding of Ramírez-Verduzco *et al*. (2012), Binhweel *et al*. (2021), Giakoumis (2013). Similarly, differences in the densities were associated to feedstock by Atabani *et al*. (2014). The more saturated biodiesels such as oleander and canola exhibited higher densities, while the less saturated biodiesels such WVO and coconut showed lower densities, as illustrated in Figure 4.1. ANOVA findings on small SEM of 0.170 and $p < 0.0001$ indicated significant differences of the biodiesel density and the Tukey ranking across blends are consistent with findings of Yuan *et al*. (2022).

The biodiesel blends densities were presented in appendices 4.1-a (A1.1-1.7) were analyzed using ANOVA (SAS) and their data presented in the table below.

Table 2: Density for the biodiesels' blends

% Blend	WVO	Coconut	Canola	Sunflower	Oleander
30	840.0[a]	837.8[a]	846.0[a]	842.8[a]	852.9[a]
25	836.6[b]	835.2[b]	841.6[b]	838.9[b]	847.7[b]
20	833.6[c]	832.5[c]	837.6[c]	835.2[c]	842.4[c]
15	830.7[d]	830.0[d]	833.4[d]	831.5[d]	837.2[d]
10	827.9[e]	827.4[e]	829.3[e]	828.4[e]	831.9[e]
SEM	0.0802	0.0333	0.0314	0.0299	0.0333
P-values	<.0001	<.0001	<.0001	<.0001	<.0001

From Table 4.2, it is evident that the density of the blends increased as percent of biodiesel increased from 10% to 30%. The ANOVA test confirmed significant differences in density among the biodiesels since at the 95% confidence level, $p< 0.0001$. At a 10% blend, oleander biodiesel exhibited the highest density at 831.9 kg/m³, followed by canola, sunflower, coconut, and WVO in descending order. The density ranking of the biodiesels remained consistent across all blend levels.

As the percentage of biodiesel in the blend rose, the overall density of the fuel increased in an approximately linear relationship Singh *et. al.* (2007). Although this density increase is typically small but measurable, a B20 blend (20% biodiesel, 80% diesel) can have a density about 1-2% higher than diesel (Brown, 2021), which impact engine performance. The exact change in density depends on factors such as the specific biodiesel feedstock used and their properties (Wang *et al*., 2020). Although density increased for higher biodiesel in the blend, implying more fuel, the engine power reduced, since biodiesel had lower energy density compared to diesel (Taylor, 2019). ANOVA analysis quantifies these inherent chemical factors as key determinants of biodiesel properties.

4.2.2: Effect of biodiesel blends on kinematic viscosity

Table 4.1 above and figure 4.2 below illustrated that coconut biodiesel exhibited the lowest viscosity at 4.4 mm²/s, followed by WVO at 4.2 mm²/s, canola at 4.7 mm²/s, sunflower at 5.2 mm²/s, and oleander at 5.5 mm²/s. Diesel, kinematic viscosity of 3.2 mm²/s, is lower than the biodiesels.

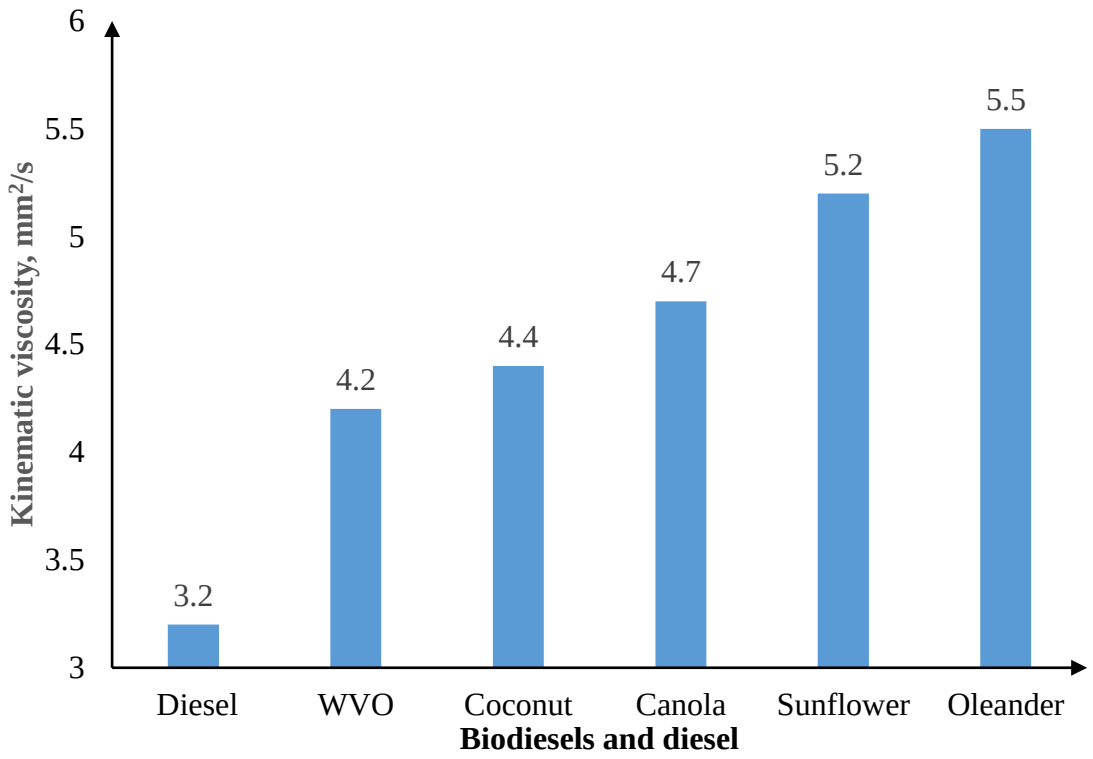

Figure 4.2: Kinematic viscosity for the selected biodiesels and diesel

Tukey pairwise comparison was employed to test differences in kinematic viscosity among various biodiesel fuels. Diesel (superscript 'f'), followed WVO (superscript 'e'), coconut (superscript 'd') Canola (superscript 'c'), sunflower (superscript 'b') and oleander (superscript 'a'). ANOVA (SAS) gave the SEM of 0.033 and p<.0001 values (95% confidence level) indicating significant difference for the biodiesels kinematic viscosities. These differences can be attributed to the chemical composition and saturation level of the biodiesels, as reported by studies of Binhweel *et al*. (2021), Lapuerta (2008), and Refaat (2009). Results indicated also differences in the viscosity of biodiesel compared to Diesel. Furthermore, the high viscosities of coconut and oleander were primarily due to their longer chain length and degree of unsaturation. Studies of Knothe and Steidley (2005) explained that higher kinematic viscosities of biodiesel are due to high saturation leading to stronger intermolecular bonds. Notably, oleander biodiesel exhibited the highest viscosity due to its chemical structure, while WVO biodiesel demonstrated the lowest viscosity among the tested biodiesels.

The effects of different biodiesel blending on kinematic viscosity were presented in appendices 4.1-b (tables A2.1-2.7) and the analysis summarized in the table below.

Table 4.3: Kinematic viscosity for biodiesels' blends

	Kinematic viscosity (ϑ), mm^2/s				
% Blend (Bi)	**WVO**	**coconut**	**Canola**	**Sunflower**	**Oleander**
30	3.65[a]	3.71[a]	3.79[a]	3.95a	4.06[a]
25	3.57[b]	3.61[b]	3.69[b]	3.82[b]	3.91[b]
20	3.5 [b]	3.53 [c]	3.59 [c]	3.7 [c]	3.76 [c]
15	3.42 [c]	3.45 [d]	3.49 [d]	3.56 [d]	3.61 [d]
10	3.33 [d]	3.35 [e]	3.38 [e]	3.42 [e]	3.44 [e]
SEM	0.0352	0.0359	0.0324	0.0399	0.0533
P-values	<.0001	<.0001	<.0001	<.0001	<.0001

As illustrated in the table, kinematic viscosity significantly decreased as the blend percentage reduced from B30 to B10 for all the biodiesels, since they inherently possess higher viscosity compared to diesel. Consequently, the differential in viscosity was consistently maintained across all blend levels, for instance, at B30 blend level, coconut biodiesel exhibited the highest viscosity at 4.06 mm^2/s, whereas WVO biodiesel had the lowest viscosity at 3.65 mm^2/s. This observed trend aligns with findings by Tat *et al*. (2014), who reported that viscosity deviation from diesel fuel diminishes as the blend percentage reduces from B100 to B20, corroborating the trends seen in Table 4.3. The higher viscosity of Coconut biodiesel compared to other feedstock's is also consistent with Lapuerta *et al*. (2008), which attributes the increased viscosity of saturated biodiesels to stronger intermolecular interactions. According to Mohamad *et al*. (2014), the higher viscosity of biodiesels can impair fuel atomization and lead to incomplete combustion, while reduction in viscosity is beneficial as it enhanced fuel atomization, combustion efficiency to improve overall engine performance.

Table 4.3 ANOVA results showed that the variations in kinematic viscosity between the different biodiesels are were statistically significant, with a p-value <0.0001. These differences can be attributed to the distinct physiochemical properties of the biodiesels. The higher degree of unsaturation and larger molecular weight of coconut biodiesel, resulting to higher viscosities.

However, this adverse effect significantly diminishes for blends above B20, aligning with the rapid viscosity decrease observed from B30 to B10 blends. Based on the potential negative impact of high viscosity on engine performance, thus, limiting biodiesel blends to below 30%.

4.2.3: Effects of biodiesel blends on lower heating value

Table 4.1 above and figure 4.4 below presented lower heating values (Cv) of the biodiesels used in the experiments were measured and found to range between 36.206 MJ/kg and 39.421 MJ/kg, compared to diesel's Cv of 43.906 MJ/kg.

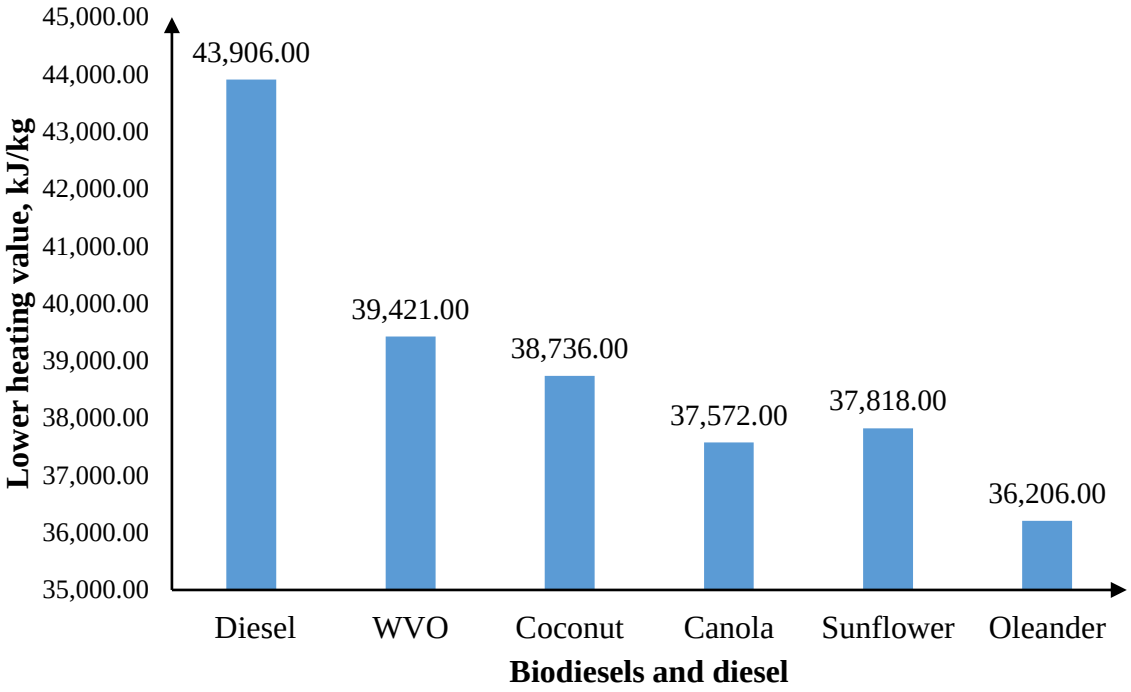

Figure 4.3: Lower heating value for the selected biodiesels and diesel

The lower heating value (Cv) serves as a crucial indicator of fuel power, measuring the heat released during combustion, t hereby, higher Cvs indicate greater energy content per unit of fuel. The lower heating value (Cv) serves as a crucial indicator of low fuel power during combustion. Consequently, higher Cv indicate greater energy content for a fuel. Tukey pairwise comparison tested differences in lower heating values (CVs) among various biodiesel fuels in comparison to diesel. Diesel had the highest Cv at 43,906 kJ/kg, (distinct subgroup denoted by 'a,') indicating its significant difference from all other biodiesels. WVO followed with the second-highest Cv at 39,421 kJ/kg, designated 'b,' indicating a significant difference from diesel and the other biodiesels. Coconut biodiesel ranked third with an Cv of 38,736 kJ/kg ('c'), followed by Sunflower had the fourth-highest Cv at 37,818 kJ/kg ('d'), then canola with an Cv of 37,572 kJ/kg ('e'). Oleander, had the lowest Cv at 36,206 kJ/kg ('f'), significantly different from all other biodiesels and Diesel. These findings revealed distinct differences in the energy content of biodiesel with Diesel. The low C_V for biodiesels was

attributed to the presence of chemically bound oxygen in its structure and also, the carbon chain length and degree of saturation play significant roles in determining heating values, with longer and more saturated chains releasing more energy during combustion ((Hoekman *et al*., 2012. The small SEM of 0.043 and p <0.0001, strongly supports the conclusion that there are significant differences in lower heating values among the biodiesel types and diesel fuels tested.

The effect of blending on lower heating values (Cv) was assessed using data in appendices 4.1 (Tables A3.1-3.5) for the biodiesel blends were analyzed and summarized in the table below.

Table 4.4: Lower heating value for biodiesels' blends

Percent Blend, Bi	WVO	Coconut	Canola	Sunflower	Oleander
30	42.202[a]	42.056[a]	41.853[a]	41.922[a]	41.576[a]
25	42.461[b]	42.321[b]	42.170[b]	42.228[b]	41.942[c]
20	42.719[c]	42.616[c]	42.486[c]	42.532[c]	42.306[d]
15	42.977[d]	42.891[d]	42.803[d]	42.836[d]	42.671[e]
10	43.236[e]	43.168[e]	43.119[e]	43.140[e]	43.056[f]
SEM	0.0015	0.0006	0.0004	0.0017	0.0016
P-value	<.0001	<.0001	<.0001	<.0001	<.0001

Table 4.4 shows that as the proportion of biodiesel increased in blends, the Cv decreased consistently. their). The findings of this study align with prior researches, showing an increase in Cv's by approximately 8-9% in B30 dependent on the feedstock composition blends (Demirbas, 2009. The ANOVA results showed that the variations in low heat value (Cv) between the different biodiesels are were statistically significant, with a p-value <0.0001 across biodiesel types and blend percentages. As the biodiesel content increased in blends, CVs decreased due to biodiesel's chemical composition. However, this adverse effect significantly diminishes for blends levels were below B20, for example, B10 WVO biodiesel closely resembled diesel in terms of heating value, while B10 oleander biodiesel showed the greatest increase in its Cv.

These findings in section 4.3, 4.4 and 4.5 below, underscored the importance of considering biodiesel feedstock sources and blend ratios when optimizing engine performance and emissions.

4.3 Effects of biodiesel blending on engine performance and emission

This study employed a factorial experimental design in table 3.7 (section 3.3) to investigate the effects of the different biodiesels (Waste Vegetable Oil (WVO), Oleander, Canola, Sunflower, and Coconut) and their blends; B10, B15, B20, B25, and B30 (mix ratio's on section 3.2 –table 3.1) on engine performance and emissions across a range of operating conditions from equivalent brake power (Bp) of 0.83 kW to 3.43 kW. The research utilized analyzed the results using one-way analysis of variance (ANOVA) – SAS 2019 and excel 2015 t-distribution statistical methods. Data points at Bp of 0 kW were amorphous, thus not used, since they inconsistent, as noted by Heywood (1988), due to fluctuations in the set load and speeds. The averaged Bp values were used for similar engine setting on operating conditions across fuels. The subsequent sections discussed the test results on the effects of blending on the engine performance and emission charcteristics;

4.3.1 Brake thermal efficiency

a) Brake thermal efficiency of the biodiesels

The results presented in Table 4.5 and figure 4.4 were obtained from an experimental study of engine brake thermal efficiency described in section 3.3.

Table 4.5: Brake thermal efficiency of the biodiesels

Equivalent Bp	Percent brake thermal efficiency, (% Bte) for the biodiesels						
(kW)	WVO	Coconut	Canola	Sunflower	Oleander	SEM	P-value
0.83	3.64^{ab}	3.78^{a}	3.48^{b}	2.63^{c}	1.51^{d}	0.0501	<.0001
1.17	5.64^{a}	5.69^{a}	4.64^{b}	4.24^{b}	2.68^{c}	0.0726	<.0001
1.48	8.04^{a}	7.4^{b}	6.02^{c}	5.2^{d}	4.09^{e}	0.0997	<.0001
1.74	9.5^{a}	8.38^{b}	7.15^{c}	5.91^{d}	4.46^{e}	0.1785	<.0001
1.79	9.48^{a}	8.43^{b}	7.37^{c}	6.26^{d}	4.47^{e}	0.0057	<.0001
2.13	10.49^{a}	9.61^{b}	7.97^{c}	7.62^{d}	5.83^{e}	0.0115	<.0001
2.25	10.98^{a}	10.05^{b}	8.09^{c}	7.66^{d}	5.62^{e}	0.0171	<.0001
2.53	11.66^{a}	10.6^{b}	9.22^{c}	8.34^{d}	6.71^{e}	0.01155	<.0001
2.82	12.44^{a}	11.52^{b}	9.69^{c}	9^{d}	6.89^{e}	0.01154	<.0001
3.43	13.5^{a}	12.06^{b}	10.38^{c}	9.4^{d}	7.64^{e}	0.0115	<.0001

The data was analyzed using ANOVA, for the different biodiesel (WVO, coconut, canola, sunflower, and oleander). The engine was operated at equivalent brake power (Bp) range from 0.83 to 3.43 kW.

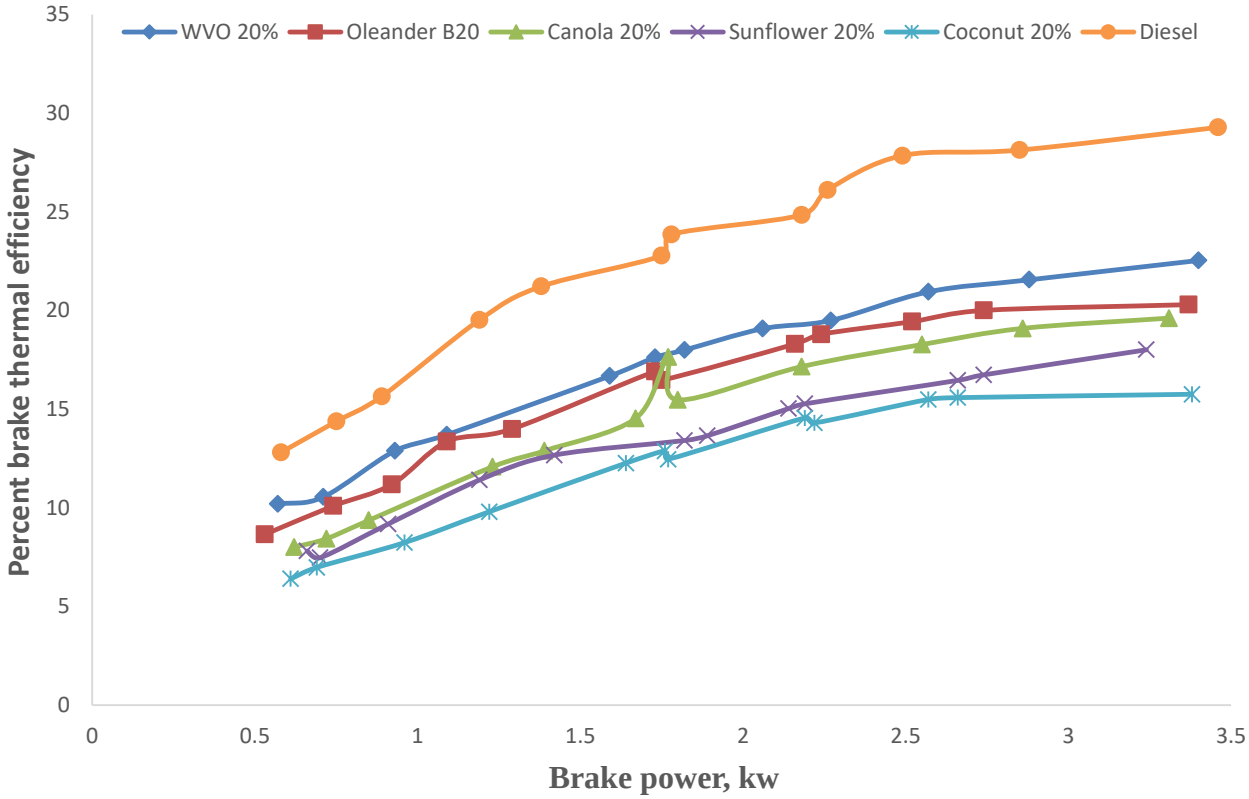

Figure 4.4: Brake thermal efficiency of the selected biodiesels and diesel

Table 4.5 and figure 4.4 illustrate that at the lowest brake power (Bp) setting of 0.83 kW, coconut biodiesel exhibited the lowest brake thermal efficiency (Bte), compared to other biodiesels. WVO biodiesel had the highest Bte at Bp= 3.4 kW, significantly similar to oleander at 3.5 kW. As Bp increased, the differences of Bte between biodiesels became more pronounced. At the highest Bp of 3.43 kW, WVO remained having the highest Bte while oleander the lowest. Generally, WVO biodiesel consistently demonstrated the highest Bte across all Bp levels, followed by coconut, canola, sunflower, and oleander, which ranked the lowest. These efficiency variations can be attributed to differences in density, kinematic viscosity and heating value properties among the biodiesels, since they directly affect combustion characteristics (Baskar *et al*., 2016). Biodiesels had higher densities and lower viscosities when used to an engine, exhibiting higher Bte. However, the rate of increase in efficiency was lower for lower quality biodiesels like oleander, suggesting that engine power output is constrained by fuel quality, particularly under higher loads.

Additionally, also, the data revealed that Bte generally increased at higher Bp for all the biodiesels, because heavy loads typically lead to improved combustion efficiency in diesel engines. At lower Bp values, the engine experienced poor fuel-air mixing, resulting in inefficient combustion lead to reduced overall Bte. Moreover, lower Bp conditions are associated with increased friction due to mechanical and pumping losses, as found out by other researchers (Kamil *et al*., 2014).

The ANOVA test results indicated highly statistically significant differences (low SEM, $p < 0.0001$) in Bte among the different biodiesels, underscoring the impact of the sources on engine performance and emissions. In summary, the combination of experimental engine testing and ANOVA analysis offers valuable insights into how biodiesel sources impact brake Bte across Bp.

b) Effects of biodiesels' blends on brake thermal efficiency

Biodiesel typically has a lower energy content compared to diesel. Table 4.6 and figure 4.5 showed the effects of biodiesel blend level on brake thermal efficiency (Bte).

Table 36: Brake thermal efficiency for the biodiesels' blends

Biodiesel	**Percent brake thermal efficiency (% Bte) for the biodiesel blends**				
	B10	**B15**	**B20**	**B25**	**B30**
WVO	26.8[a]	24.39[a]	22.54 [a]	19.91[a]	18.15[a]
Coconut	25.87[b]	23.7[b]	20.3 [b]	17.29[b]	16.75[b]
Canola	23.75[c]	21.63[c]	19.61 [c]	16.27[c]	15.12[c]
Sunflower	22.31[d]	20.94[d]	18.01 [d]	15.17[d]	14.19[d]
Oleander	21.23[e]	20.01[e]	15.75 [e]	14.34[e]	12.8[e]
SEM	0.0033	0.0152	0.0033	0.0032	0.0042
P-values	<.0001	<.0001	<.0001	<.0001	<.0001

The ANOVA analysis revealed highly significant differences ($p < 0.0001$) in Bte across the biodiesels at each blend level. At B10, WVO exhibited the highest Bte of 26.8%, while oleander showed the lowest at 21.23%. As the blend level increased, WVO consistently maintained the highest efficiency, whereas oleander continued to ranked the lowest. Specifically, at a Bp of 3.43 kW, diesel recorded the highest Bte of 29.28%, followed by B10 (23.75%), B15 (21.63%), B20 (19.61%), B25 (16.27%), and B30 (15.12%). The ANOVA results confirmed decline in Bte when biodiesel in the blends increased. Reduced Bte was attributed to poor properties of the blends compared to diesel. Also,

research work of Rakopoulos (2016) provided insight into the performance of biodiesels, showing that long-chain fatty acids formed larger droplets during injection, thus evaporating and combusting more slowly, thereby leading to reduced Bte.

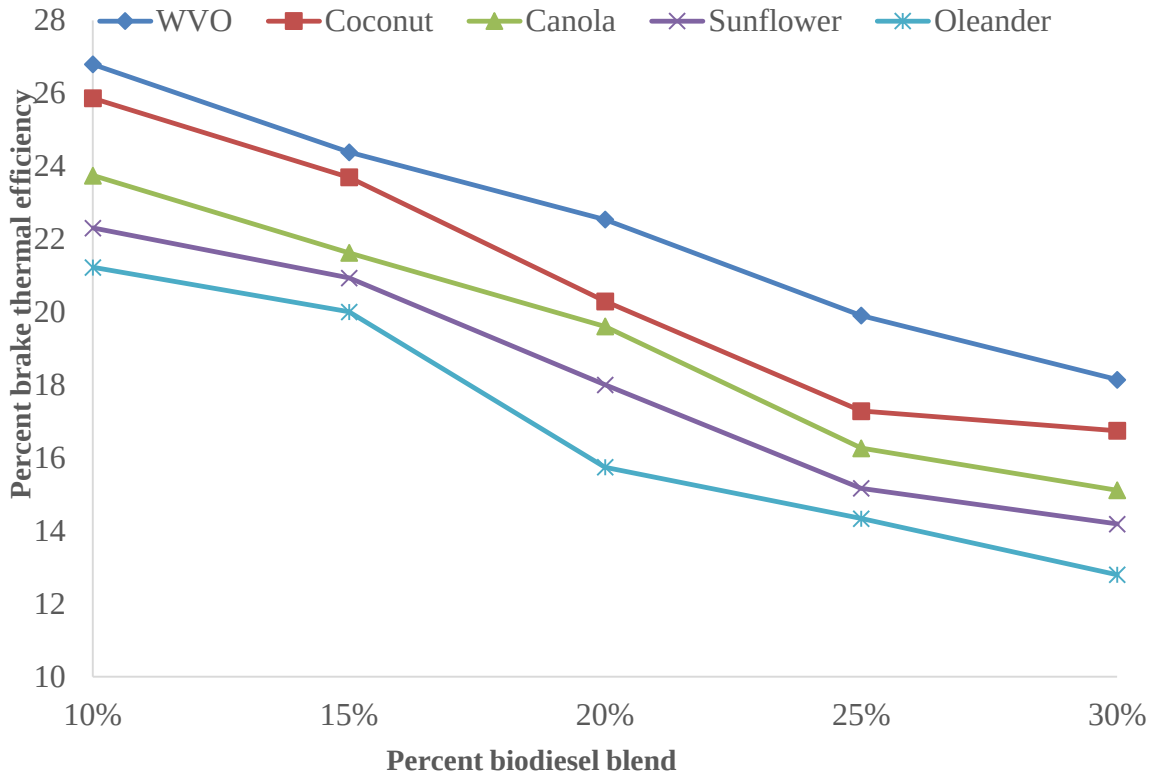

Figure 4.5: Effect of the biodiesels' blends on brake thermal efficiency

Figure 4.5 further demonstrated that the biodiesel properties different sources are key to Bte. Overall, the ANOVA results provided a robust statistical evidence that biodiesel source significantly influences brake thermal efficiency at various blend levels, with increasing biodiesel blend percentages generally leading to decreased efficiency for each fuel source. These findings are consistent with previous research (Xue *et al*., 2011), which highlighted the impact of biodiesel's lower energy content on Bte.

4.3.2 Specific fuel consumption

a) Specific fuel consumption of biodiesels

specific fuel consumption (Sfc) was used measured the amount of the fuel per hour to generate one kilowatt of power. Table 4.7 and figure 4.6 between the different biodiesels and diesel at the different levels of equivalent brake power (Bp).

Table 4.7: Specific fuel consumption for biodiesels and diesel

Brake power, kW	WVO	Coconut	Canola	Sunflower	Oleander	Diesel	SEM	P-value
0.83	2.97^{d}	2.89^{e}	3.28^{c}	4.63^{b}	7.42^{a}	0.51^{f}	0.0033	<.0001
1.17	1.80^{d}	1.82^{d}	2.35^{c}	2.59^{b}	3.96^{a}	0.46^{e}	0.0139	<.0001
1.48	1.22^{e}	1.36^{d}	1.76^{c}	2.06^{b}	2.54^{a}	0.38^{f}	0.0032	<.0001
1.74	1.02^{e}	1.19^{d}	1.46^{c}	1.78^{b}	2.32^{a}	0.35^{f}	0.0033	<.0001
1.79	1.02^{e}	1.18^{d}	1.41^{c}	1.67^{b}	2.31^{a}	0.37^{f}	0.0034	<.0001
2.13	0.92^{e}	1.03^{d}	1.29^{c}	1.34^{b}	1.76^{a}	0.33^{f}	0.0032	<.0001
2.25	0.88^{e}	0.98^{d}	1.27^{c}	1.35^{b}	1.82^{a}	0.31^{f}	0.0031	<.0001
2.53	0.82^{e}	0.93^{d}	1.11^{c}	1.23^{b}	1.52^{a}	0.33^{f}	0.0033	<.0001
2.82	0.77^{e}	0.85^{d}	1.05^{c}	1.13^{b}	1.48^{a}	0.29^{f}	0.0031	<.0001
3.43	0.71^{e}	0.81^{d}	0.98^{c}	1.08^{b}	1.33^{a}	0.28^{f}	.0040	<.0001

The tabulated data in the table 4.7 above, shows Sfc for various biodiesel blends and diesel at different Bp levels ranging from 0.83 kW to 3.43 kW. Further the results indicated that Bp and Sfc relationship are not linear due to variations in engine operating characteristics. From the results, oleander biodiesel recorded highest Sfc over the entire Bp range, while diesel had the lowest, while WVO had the second-lowest specific fuel consumption across all power levels. This was attributed inherent fuel properties of the biodiesels, for example the lower heating value (Cv), meant more fuel was injected to produce an equivalent Bp. Also, the higher viscosity and density lead to poor atomization and vaporization, thereby reducing combustion efficiency. The data also revealed that Sfc for all biodiesels converged as at low brake power (Bp). For instance, when Bp was 0.83 kW, the difference between WVO and oleander biodiesel 4.42 kg/kWh, while at 3.43 kW, this difference dropped to around 0.43 kg/kWh. On the other hand, the reduced Sfc gap at higher Bp was due to the higher cylinder temperatures and turbulence at higher loads improve fuel vaporization and mixing, thereby reducing differences. Further, as Bp increased, Sfc decreased sharply upto Bp=1.5 kW before gently dropping to a minimum at Bp = 3.5 kW. This is explained by the slower vaporization of biodiesels.

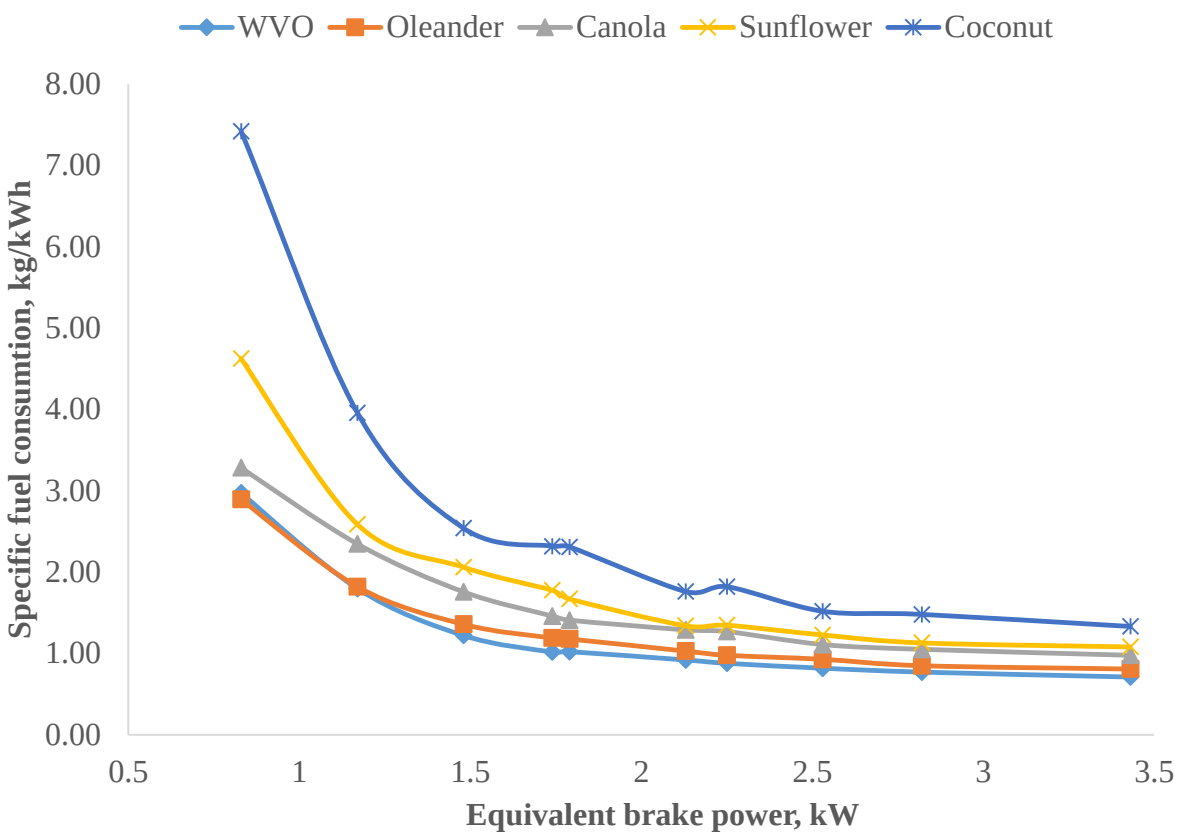

Figure 4.6: Specific fuel consumption of the selected biodiesels

The trend in the data was because as Bp increased, Sfc decreased due to improved combustion efficiency and energy conversion, thus the engine typically consumes less fuel, which aligned with results of research by Lapuerta *et al*. (2008). Also, research work done by Puhan *et al*. (2005) reported that at low Bp the engine may operate less efficiently, resulting in higher Sfc and at higher Bp, the engine approaches its optimal operating point, leading to low Sfc.

Table 4.7 illustrated the Tukey analysis and ANOVA. The Tukey analysis (superscript letters) showed biodiesels ranking and remained consistent, regardless of the level of Bp. For example, Oleander biodiesel blends (superscript "a") consistently exhibited the highest Sfc across all blending ratios, followed by sunflower (superscript "b"), canola (superscript "c"), (superscript "d"), and WVO (superscript "e"), in descending order.

ANOVA was conducted to determine significant differences of the biodiesels. The results showed that Sfc for fuels were significantly different ($p<0.0001$, and low SEM), throughout the Bp range, agreeing with the study of Sarin *et al*. (2009).

b) Effects of biodiesel blending on specific fuel consumption

The results in Table 4.8 shows the specific fuel consumption (Sfc) for the biodiesel blends from five different biodiesel sources: WVO, Oleander, Canola, Sunflower, and Coconut. These biodiesels were blended with regular diesel at five blending ratios: B10, B15, B20, B25, and B30. Also ANOVA was conducted to determine if there were statistically significant differences in specific fuel consumption between the different biodiesel sources and blending ratios.

Table 48: Specific fuel consumption for the selected biodiesel blends

	Biodiesel blends level				
Biodiesel	**B10**	**B15**	**B20**	**B25**	**B30**
WVO	0.31^{c}	0.34^{c}	0.37^{d}	0.4^{e}	0.47^{e}
Coconut	0.32^{c}	0.35^{c}	0.41^{c}	0.49^{d}	0.51^{d}
Canola	0.35^{b}	0.39^{b}	0.43^{c}	0.52^{c}	0.56^{c}
Sunflower	0.37^{ab}	0.4^{ab}	0.47^{b}	0.56^{b}	0.6^{b}
Oleander	0.39^{a}	0.42^{a}	0.54^{a}	0.6^{a}	0.68^{a}
SEM	0.00568	0.00689	0.00577	0.00598	0.00591
P-value	<.0001	<.0001	<.0001	<.0001	<.0001

Note: The analysis (at $\alpha = 0.05$) were done along the column and ranked using superscript letters.

The data revealed that Sfc increased with higher biodiesel blend levels across various biodiesel types. Sfc systematically increased as the percent of biodiesel in the blend rose for all biodiesel sources. The low Sfc of WVO biodiesel was consistent with results shown by Puhan *et al*. (2005), which demonstrated that high calorific value and kinematic viscosity lead to less complete combustion due to slower droplet vaporization. WVO and Coconut blends maintained the closest specific fuel consumption at all Bp levels. The increase is likely attributed to the lower energy density of biodiesel compared to diesel. Variations between biodiesel sources may be ascribed to differing properties such as viscosity, density, and kinematic viscosity, which influence combustion efficiency. Similar trends were also noted by Singh *et. al.* (2018).

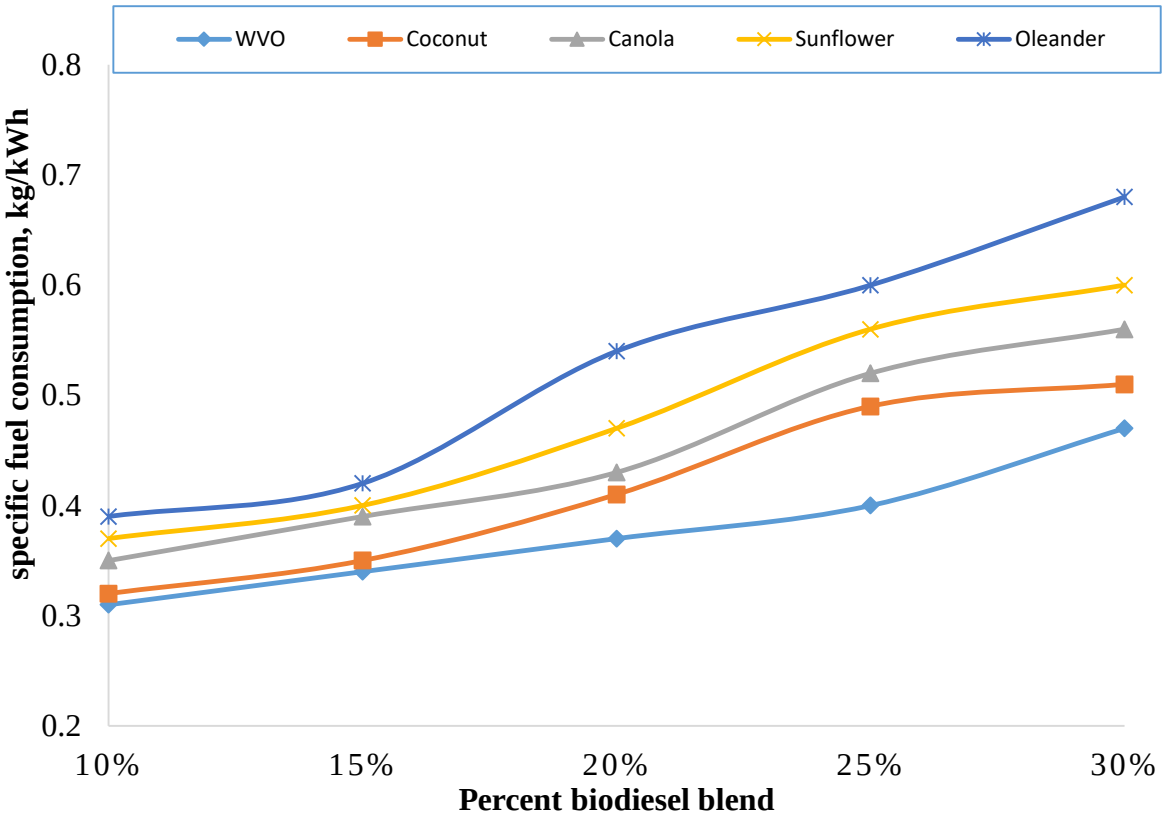

Figure 4.7: Effect of the biodiesels' blends on specific fuel consumption

The factors contributing to these differences in Sfc were; chemical composition, viscosity, density, and oxidative stability (Antolin *et al*., 2002. The results align with research by Lapuerta *et al*. (2008), which identified the degree of biodiesel saturation as the primary factor influencing efficiency across fuel types The observed trends align with previous studies; for instance, Singh *et. al.* (2018) noted a 3-5% increase in Sfc with B20 blends and Lee (2017) reported a 7% rise in Sfc for B40 blends compared to diesel.

Biodiesel source and blending ratio significantly impact specific fuel consumption evidenced by the ($p<0.0001$). This indicates differences in Sfc between biodiesel sources and among different blending ratios. At a constant brake power of 3.43 kW, clear disparities in consumption were evident among biodiesel types. Coconut biodiesel blends exhibited the highest fuel consumption rates, whereas WVO biodiesel blends demonstrated the lowest. Fuel consumption consistently rose across all biodiesel types as the blend percent increased. the ANOVA findings substantiate measurable distinctions in Sfc among different biodiesel sources and blending ratios.

4.3.3 Carbon monoxide emissions

a. Carbon monoxide emissions for the biodiesels

Table 4.9 and figure 4.8 gives ANOVA results, clearly demonstrated by that biodiesels type had effect on carbon monoxide (CO) emissions from the diesel engine.

Table 4.9: Carbon monoxide emissions for the selected biodiesels and diesel

Brake power, (kW)	Carbon monoxide emissions, ppm							
	WVO	Coconut	Canola	Sunflower	Oleander	Diesel	SEM	P-value
0.83	1247^{f}	1359^{e}	1411^{d}	1553^{b}	1516^{c}	2128^{a}	0.5774	<.0001
1.17	1208^{f}	1310^{e}	1379^{d}	1461^{b}	1434^{c}	2123^{a}	0.5783	<.0001
1.48	1058^{f}	1209^{e}	1270^{d}	1361^{b}	1320^{c}	2009^{a}	0.5771	<.0001
1.74	1046^{f}	1148^{e}	1248^{d}	1351^{b}	1214^{c}	1940^{a}	0.5783	<.0001
1.79	1007^{f}	1128^{e}	1149^{d}	1270^{b}	1265^{c}	1862^{a}	0.5763	<.0001
2.13	895^{f}	1008^{e}	1029^{d}	1181^{b}	1013^{c}	1796^{a}	0.5775	<.0001
2.25	865^{f}	978^{e}	1049^{d}	1170^{b}	1204^{c}	1822^{a}	0.5764	<.0001
2.53	835^{f}	937^{e}	988^{d}	1069^{b}	1032^{c}	1765^{a}	0.5784	<.0001
2.82	673^{f}	846^{e}	916^{d}	959^{b}	969^{c}	1554^{a}	0.5779	<.0001
3.43	672^{f}	784^{e}	836^{d}	908^{b}	909^{c}	1554^{a}	0.5784	<.0001

The results indicate a statistically significant difference in CO emissions among the various fuels at each brake power level (P-value <0.0001). The low standard error of the mean (SEM) of 0.5774 also suggests high precision and repeatability in the results. SEM reflects the expected random variation between test repetitions, and the small SEM here indicates minimal variability between runs, thereby enhancing confidence in the observed differences across fuels and brake power levels. The trend reveals that CO emissions decreased for all fuel types as brake power increased from 0.83 to 3.43 kW. This pattern was also observed by Xue *et al*. (2011) and Ozsezen *et al*. (2009), which indicates that higher engine loads lead to more efficient combustion, resulting in more complete oxidation of fuel and reduced production of partial combustion products like CO. Xue *et al*. (2011) noted up to a 30% reduction in CO emissions at peak torque compared to no-load conditions for various biodiesels.

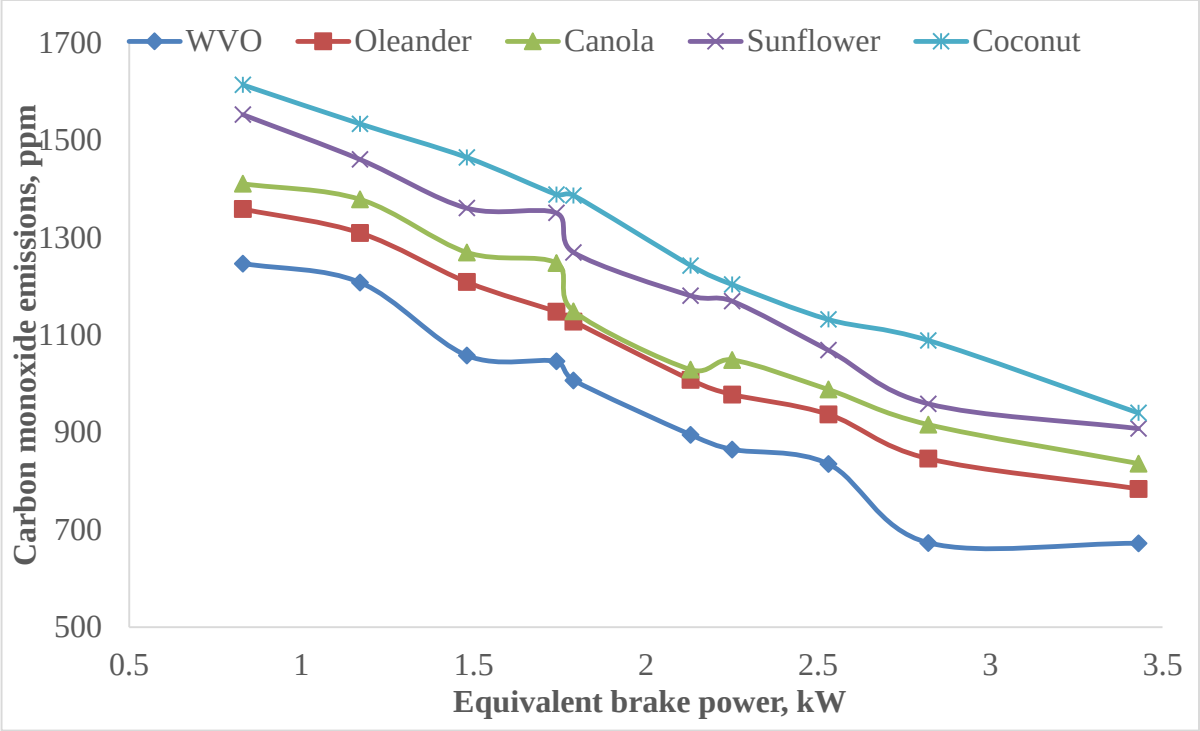

Figure 4.8: Carbon monoxide emission for the selected biodiesels and diesel

From figure 4.8 diesel consistently exhibited the highest CO emissions across all loads, Coconut, produced the highest CO emissions among biodiesels, while WVO had the lowest. The oxygenated nature of biodiesels promotes more complete combustion which lowered the CO production compared to hydrocarbon-only diesel (Lapuerta *et al*., 2008). Additionally, the chemical structure of biodiesel fuels, with WVO containing more saturated fatty acid methyl esters, enhances combustion efficiency, as noted by Ozsezen *et al*. (2009). CO emissions tend to increase with higher fuel density and viscosity, and decrease with higher heating value, although this effect is relatively minor. Higher density of biodiesel compared to diesel results in a slightly higher mass injected into the engine per unit volume, potentially causing longer ignition delays and slower combustion, which contribute to incomplete combustion and higher CO emissions. Higher kinematic viscosity reduces fuel atomization and air-fuel mixing, also leading to incomplete combustion and higher CO.

The differences in CO emissions between biodiesel fuels diminished at higher Bp levels. For instance, CO emissions from WVO and sunflower biodiesels differed by approximately 100 ppm at 3.43 kW, compared to around 300 ppm at 0.83 kW. This suggests that engine combustion efficiency improves at higher Bp, reducing the influence of specific fuel characteristics, nonetheless, all biodiesels consistently exhibited significantly lower CO than diesel across the range of Bp tested.

Fuels with higher lower heating values release more energy during combustion, resulting in increased brake power. Higher brake power levels generally lead to higher combustion temperatures, which facilitate the conversion of CO to carbon dioxide (CO2), a less harmful greenhouse gas. Moreover, higher lower heating values may enable engines to operate with leaner air-fuel mixtures, further promoting CO2 formation over CO (Ozsezen *et al*., 2009). Fuels with higher densities provide more fuel mass per unit time, contributing to higher brake power. Like higher lower heating values, higher brake power levels can result in increased combustion temperatures, typically reducing CO emissions by enhancing the conversion of CO to CO_2. Additionally, dense fuels may require higher injection pressures and improved fuel atomization, thereby promoting more complete combustion and lower CO emissions. While higher brake power levels generally enhance combustion efficiency and CO_2 conversion, excessively high brake powers can lead to elevated temperatures and increased heat losses, potentially elevating CO emissions. The ANOVA results corroborated these findings with a low P-value (<0.0001), indicating significant differences in CO emissions among tested fuels.

b. Effect of biodiesels' blends on carbon monoxide

The Table 4.10 and figure 16 below presents carbon monoxide emissions for 5 different biodiesel feedstock's (WVO, Coconut, canola, sunflower, Oleander) at blend levels from B10 to B30. measured at a constant brake power of 3.43 kW.

Table 4.10: Carbon monoxide emission biodiesels' blends

Biodiesels	**Biodiesel blend level**				
	B10	**B15**	**B20**	**B25**	**B30**
WVO	2211[a]	2123[a]	2075[a]	2037[a]	1914[a]
Oleander	2175[b]	2103[b]	2036[b]	1854[b]	1863[b]
Canola	2088[c]	2004[c]	1952[c]	1832[c]	1762[c]
Sunflower	2036[d]	1994[d]	1874[d]	1820[d]	1710[d]
Coconut	2001[e]	1949[e]	1789[e]	1709[e]	1628[e]
SEM	0.5774	0.5794	0.5788	0.5789	0.5799
P-value	<.0001	<.0001	<.0001	<.0001	<.0001

The results from the highlighting a significant decrease in carbon monoxide (CO) emissions as biodiesel blend percentage increased. Specifically, at 3.43 kW brake power, CO emissions exhibited a clear downward trend with increased biodiesel content in the blend. For instance, WVO-B10 emitted

2211ppm, decreasing to 1914 ppm, while coconut-B10 was 2001 ppm, reduced to 1628 at B30. The study also, observed a consistent decrease in CO emissions across all brake powers (Bp) when increasing biodiesel blend percentages in diesel fuel. Reduction in CO emissions was primarily attributed to biodiesel's higher oxygen content compared to diesel, enhancing combustion efficiency and promoting more complete oxidation of carbon yield CO_2, rather than partially oxidized CO. Reductions in CO emissions were not perfectly linear across the blends WVO-B10 showed higher CO emissions than B30, as such the reduction from B10 to B15 (88 ppm) was greater than from B15 to B20 (48 ppm). This was an indication likely due to complex chemical kinetics involving biodiesel components and engine combustion processes.

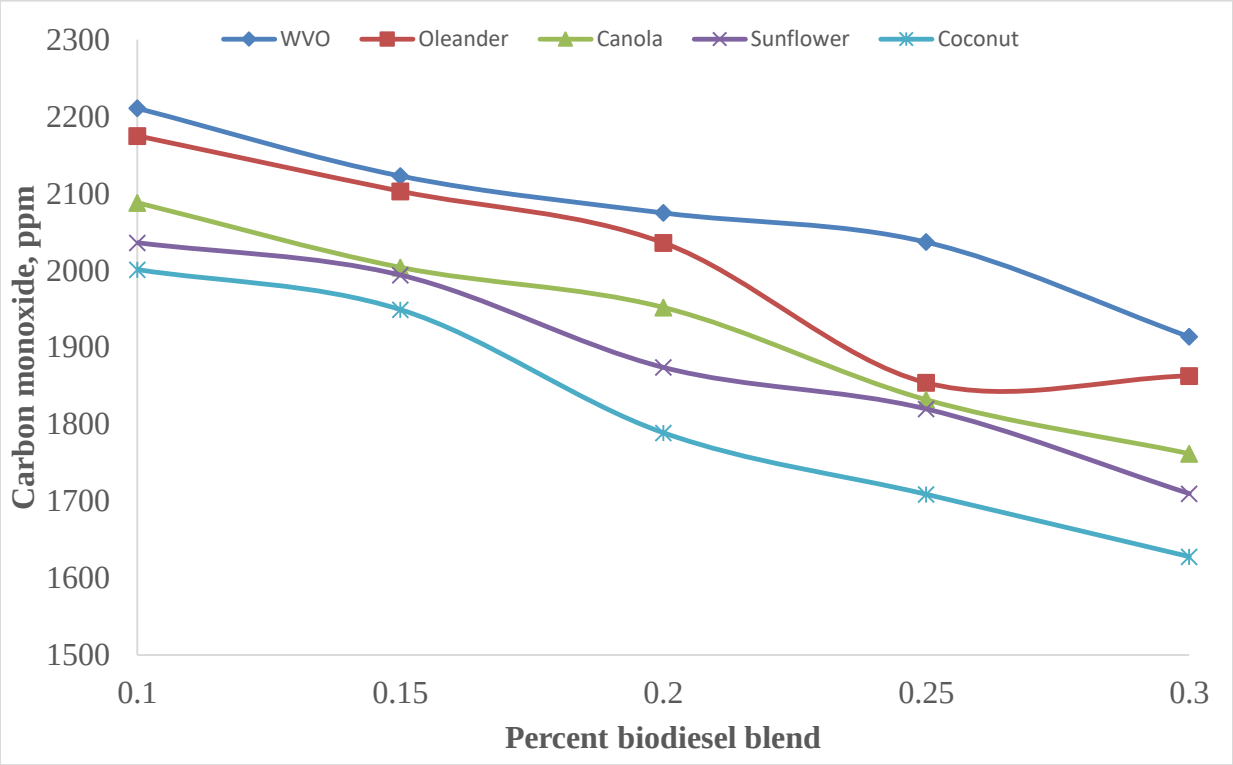

Figure 4.9: Effects of biodiesels blends on carbon monoxide emissions

Research has consistently demonstrated that increasing percent of biodiesel blend is an effective strategy for reducing CO from diesel engines at tested Bp. Studies by Lapuerta *et al*. (2008) and Shojaee *et al*. (2013) have similarly reported reductions in CO with biodiesel blends, affirming this as an effective approach in mitigating emissions. ANOVA result underscored highly significant differences ($P < 0.0001$) in CO emissions among different biodiesels across all blends.

4.3.4 Nitrogen oxide emissions

a) Nitrogen oxide emissions of the biodiesels

The figure 4.11 presents the nitrogen oxides (NOx) emissions for the different biodiesel fuels; (waste vegetable oil (WVO), Oleander, canola, sunflower, Coconut) and diesel, ran at 10 different engine brake power (Bp) levels from 0.83 kW to 3.43 kW. A one-way ANOVA was conducted to determine if there were significant differences in NOx emissions between the different biodiesel fuels at each Bp level, as shown Table 4.11.

Table 4.11: Nitrogen oxides for biodiesels and diesel

	Biodiesels					**Diesel**		
Brake power, kW	**WVO**	**Oleander**	**Canola**	**Sunflower**	**Coconut**		**SEM**	**P-value**
0.83	79^{a}	77^{a}	65^{c}	72^{b}	57^{d}	22^{e}	0.5793	<.0001
1.17	102^{a}	94^{b}	77^{d}	85^{c}	65^{e}	28^{f}	0.6871	<.0001
1.48	121^{a}	112^{b}	91^{d}	94^{c}	82^{e}	37^{f}	0.5774	<.0001
1.74	129^{a}	122^{b}	102^{d}	106^{c}	84^{e}	46^{f}	0.5778	<.0001
1.79	140^{a}	130^{b}	109^{d}	115^{c}	90^{e}	50^{f}	0.4774	<.0001
2.13	153^{a}	144^{b}	122^{d}	135^{c}	113^{e}	61^{f}	0.5722	<.0001
2.25	160^{a}	157^{b}	134^{d}	143^{c}	120^{e}	64^{f}	0.5783	<.0001
2.53	180^{a}	174^{b}	146^{d}	152^{c}	138^{e}	75^{f}	0.5774	<.0001
2.82	210^{a}	198^{b}	169^{d}	174^{c}	151^{e}	89^{f}	0.5761	<.0001
3.43	249^{a}	241^{b}	210^{d}	220^{c}	194^{e}	109^{f}	0.5984	<.0001

The findings reveal significant differences in NOx emissions among biodiesel fuels at all tested brake power (Bp) levels, with p-values consistently below 0.0001. WVO biodiesel consistently exhibited the highest NOx emissions across all power levels, followed by Oleander, sunflower, canola, Coconut, and diesel, which showed the lowest emissions. For instance, at 2.25 kW power level, WVO emitted 160 ppm NOx, Oleander 157 ppm, sunflower 143 ppm, canola 134 ppm, Coconut 120 ppm, and diesel only 64 ppm. This hierarchy of NOx emissions—WVO > Oleander > sunflower > canola > Coconut > diesel—remained consistent throughout all tested Bp levels.

Lower heat value of biodiesel, influencing the energy content, can also contribute to higher NOx emissions by prolonging combustion duration and elevating peak temperatures. The impact of biodiesel properties on NOx emissions is intertwined and dependent on operational conditions and combustion characteristics. Higher biodiesel density can contribute to increased NOx emissions due to longer ignition delays, allowing more time for nitrogen oxide formation during combustion. Additionally, higher kinematic viscosity in biodiesel combustion temperature, leading more NOx.

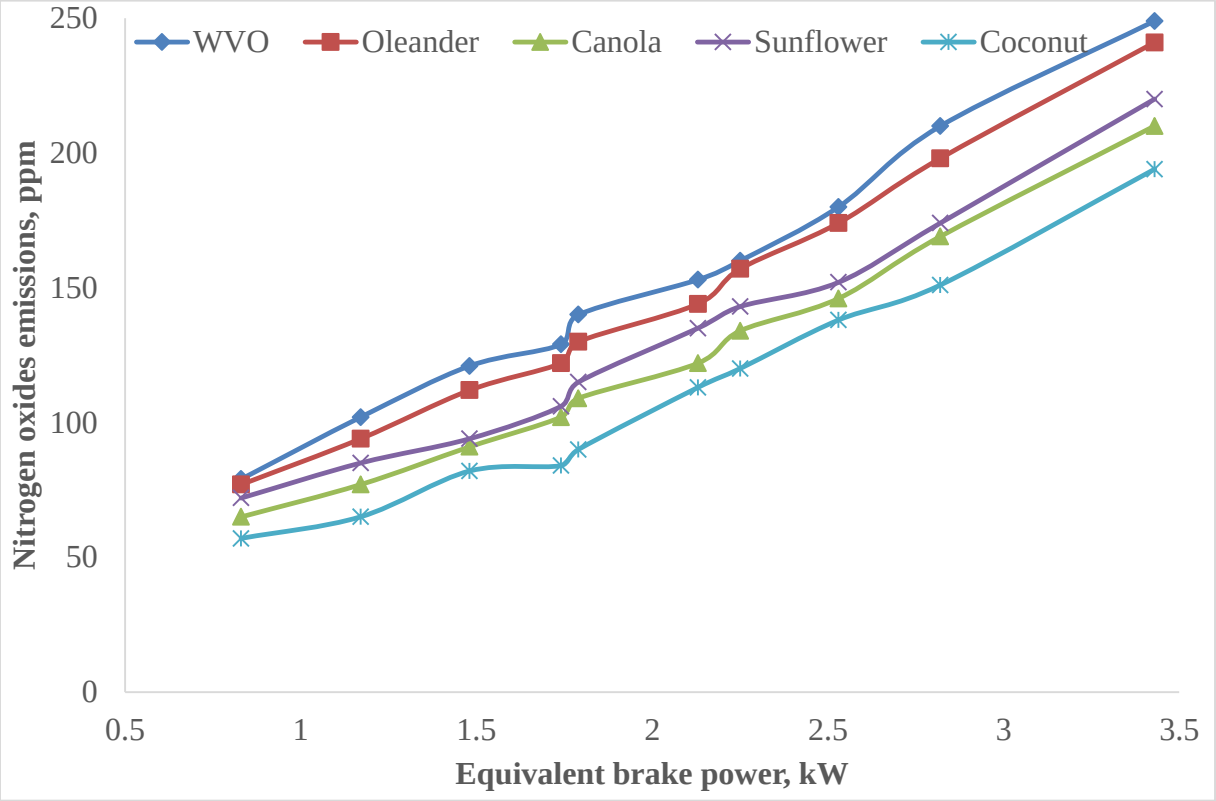

Figure 4.10: Nitrogen oxide emissions for the selected biodiesels and diesel

Biodiesels with higher unsaturation, such as WVO and Oleander, tend to promote NOx formation, while more saturated biodiesels like Coconut exhibit lower NOx emissions. Engine operating conditions, as indicated by Bp levels, also influence NOx emissions, typically increasing with higher Bp due to elevated combustion temperatures. ANOVA results emphasize that both biodiesel type and engine Bp play crucial roles in NOx emissions, underscoring need for careful selection of biodiesel and engine operating parameters to mitigate harmful emissions.

Biodiesel blends with higher lower heat values release more energy during combustion, potentially increasing brake power (Bp). Also, the blends, have higher densities provide more fuel

mass per unit time, potentially increasing Bp. Higher Bp elevate engine temperatures, leading to increased NOx (Xue *et al*. (2011). Conversely, higher viscosity fuels typically promote better combustion efficiency increasing engine temperatures, leading to higher NOx emissions. ANOVA confirm that different biodiesels ($p<0.0001$) significantly influences NOx emission from engines.

b) Effect of biodiesels' blends on nitrogen oxides

The results reported in Table 4.12 and figure 4.11 the ANOVA results conducted showed to significant differences in NOx emissions between the different biodiesel blends derived from various feedstock's, at equivalent brake power of 3.44 kW.

Table 4.12: Nitrogen oxide emissions for the biodiesels' blends

Biodiesels	B10	B15	B20	B25	B30
WVO	124[a]	131[a]	152[a]	178[a]	204[a]
Oleander	119[b]	128[b]	138[b]	152[b]	189[b]
Canola	87[d]	99[d]	106[e]	135[d]	168[d]
Sunflower	91[c]	104[c]	120[c]	146[c]	171[c]
Coconut	86[d]	96[e]	114[d]	123[e]	147[e]
SEMs	0.5774	0.5873	0.5991	0.5446	0.5431
P-value	<.0001	<.0001	<.0001	<.0001	<.0001

The ANOVA results clearly demonstrate that both biodiesel feedstock and increasing blend levels significantly impact engine-out NOx emissions ($p < 0.0001$) across all five blend levels tested, as shown in Table 4.12. Tukey's test comparisons indicate that waste vegetable oil (WVO) biodiesel consistently exhibits significantly higher NOx emissions compared to other biodiesels, with Oleander following as the second highest, then sunflower, canola, and Coconut biodiesel showing the lowest NOx emissions. The ANOVA results from Table 4.6a further confirm a significant effect of brake power (Bp) on NOx emissions across all tested biodiesel blends (B10, B15, B20, B25, B30), with all p-values < 0.0001, indicating strong evidence against the null hypothesis of no difference in NOx emissions across blend levels. Additionally, NOx emissions increase progressively as the blend level increases from B10 to B30 for all biodiesels. The elevated NOx emissions observed for WVO and Oleander biodiesels can be attributed to their higher nitrogen and aromatic content. In contrast, the saturated hydrocarbon structure of Coconut biodiesel contributes to its lower NOx emissions.

Consistent with prior research, NOx emissions typically rise with increasing brake power for all blend types. Studies by Lapuerta *et al*. (2008) and Agarwal *et al*. (2013) have noted similar trends, attributing higher NOx emissions to increased cylinder temperatures resulting from higher brake power, which enhances thermal NOx formation. The higher oxygen content in biodiesel compared to diesel also contributes to increased NOx emissions.

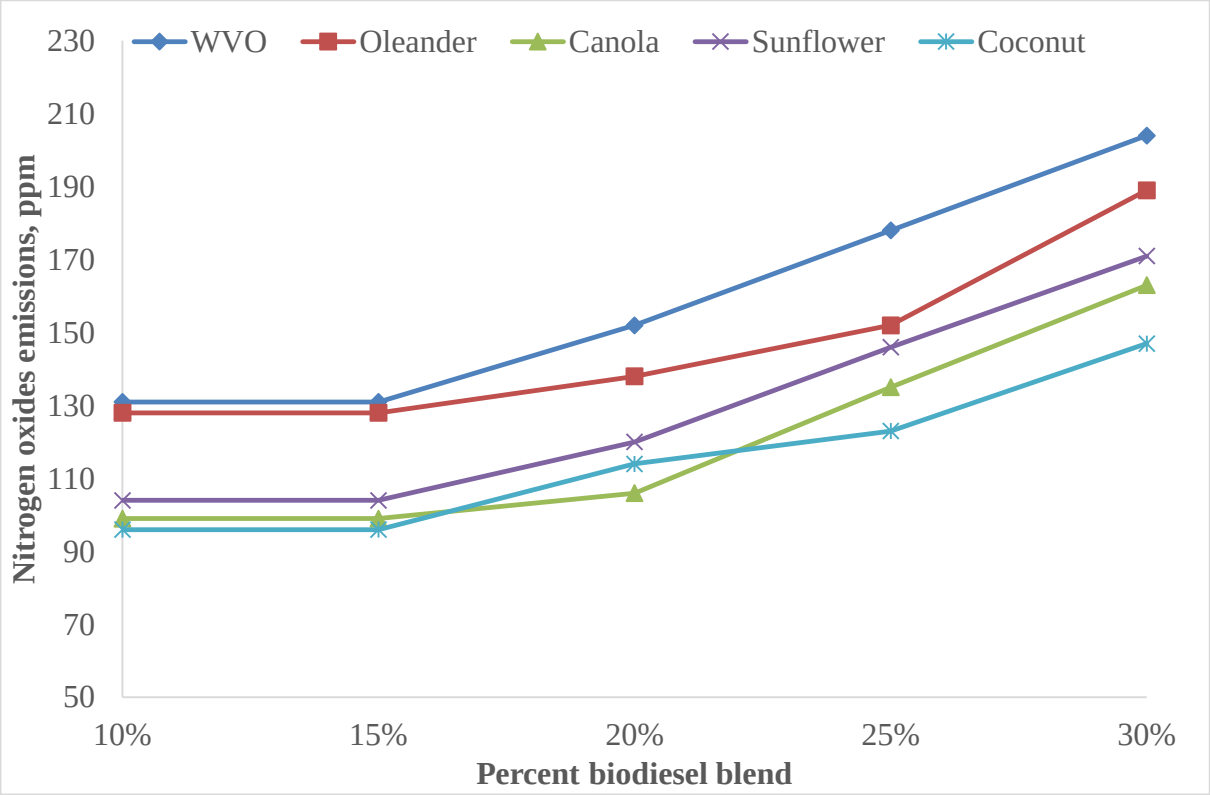

Figure 4.11: Effects of biodiesels' blends on nitrogen oxides emissions

The results further show that among the biodiesels' blends, B30 consistently exhibits the highest NOx emissions across the range of brake powers tested, while B10 generally shows the lowest emissions. This aligns with literature suggesting that higher biodiesel content correlates with heightened NOx production (Agarwal *et al*., 2013; Lapuerta *et al*., 2008).

In summary, the ANOVA provides robust statistical evidence that NOx emissions increase significantly with brake power for biodiesel blends, and higher biodiesel content amplifies NOx emissions. Initially, as Bp increases from lower values, since there was moderate increase of combustion temperatures, promoting NOx emission formation during combustion.

4.4 Mathematical models

To validate the models, a series of experiments were conducted using three biodiesels (soybean, linseed, and jatropha) at three different blend levels (B10, B20, and B30). Validation data were kept independent from the data used for model development was representative of various selection of the biodiesel's blends to ensure a rigorous test on the model's performance. Statistical analysis was used to ensure models reliability and applicability over variety of engine operating conditions. Validation made efforts to minimize model's bias that could affect outcomes of the biodiesels' blends by ensuring the accuracy, robustness, and generalizability of the models were effectively achieved. The validation procedures for the engine performance and emissions parameters are provided in the subsequent sections below;

4.4.1 Brake thermal efficiency model

(a) Model

The Brake thermal efficiency (Bte) semi-empirical model was developed using the analytical model in section 3.4.1, equation 3.9 and results from engine tests run of different biodiesel (WVO, Oleander, canola, sunflower, and Coconut) blended at 10% (B10), 15% (B15), 20% (B20), 25% (B25) and 30% (B30) given in section 4.3.1-b (table 4.6) converted using equation 4.1 above. MATLAB 9.4 (R2018a) was used to determine the constants in the equation 3.9, using regression analysis and curve fitting methods on the experimental data. Thus the mathematical model developed for Bte was given in equation 4.2;

$$Bte = 1.2B^{-0.42}\left(\frac{Bp}{\rho\vartheta^2 {C_v}^{1/2}}\right)^{0.68} \quad \text{..... (4.1)}$$

Where:

Bte = bake thermal efficiency; B = blend percentage of biodiesel

Bp = equivalent brake power; ϑ = kinematic viscosity of the biodiesel

ρ = density of the biodiesel *Cv*= lower heating value

The equation shows Bte is dependent on brake power (Bp), biodiesel properties (kinematic viscosity (ϑ), Lower heat value and density (ρ)) and their blend level (B). Equation 4.1 above, clearly shows Bte decreased that as the biodiesel blend level rose, while, Bte increased with an increase in the ratio of Bp to fuel property. The constants values showed high dependability of Bte on the input variables. To ensure the accuracy and reliability of the results, Ochoa *et al.* (2020) recommended the

predictions be tested with actual engine. Experimental presented in tables 4.13, were done for the validation and found to be consistent with engine test results.

(b) Brake Thermal Efficiency Model Validation

ANOVA was used to provide a statistical validation of the model by comparing predicted Pred.) and experimental (exp.) Bte data, showing no significant difference between them as shown in Figure 4.13 plotted by the Matlab software for the analyzes

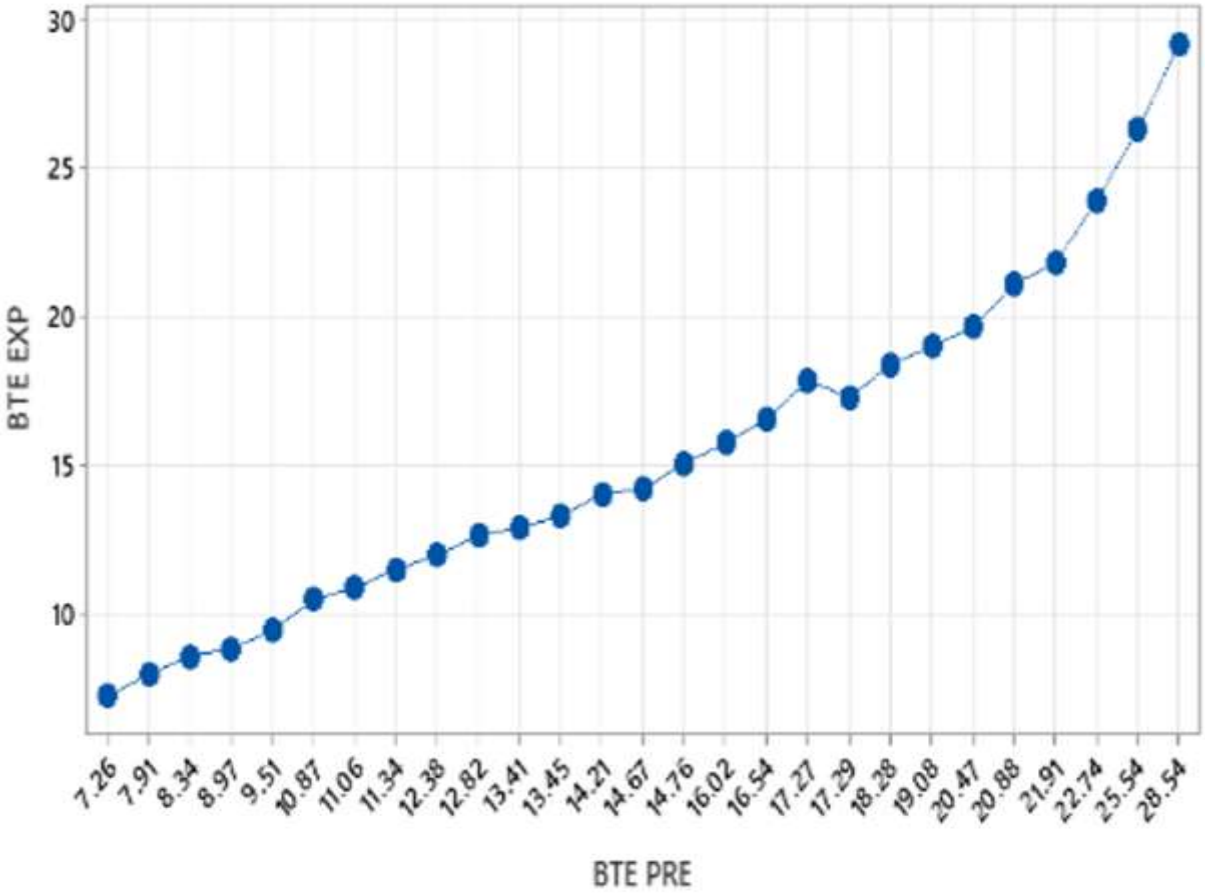

Figure 4.12: Brake thermal efficiency of experimental against predicted

Figure 4.12 above illustrates ANOVA results in table 4.14 below quantify the discrepancies between predicted and experimental Bte across the tests range, highlighting areas where the model requires refinement. The comparison of the predicted Bte were approximately 2.29% lower than the experimental results as shown in table below.

Table 4.13: Validation of brake thermal efficiency

Experiment	Fuels	N	W	Bp	Exp. Bte	Pred. Bte
1	Linseed B10	958	5.96	1.17	14.21	14.05
2		1253	8.61	2.13	20.88	21.11
3		1481	12.02	3.43	28.54	29.19
4	Linseed B20	1095	5.86	1.17	10.87	10.50
5		1278	9.03	2.13	16.02	15.78
6		1506	11.98	3.43	21.91	21.82
7	Linseed B30	1009	5.66	1.17	8.97	8.86
8		1250	8.54	2.13	13.45	13.31
9		1502	12.16	3.43	18.28	18.40
10	Soybean B10	1001	5.7	1.17	12.82	12.65
11		1250	9.05	2.13	19.08	19.02
12		1519	11.61	3.43	25.54	26.30
13	Soybean B20	1024	5.68	1.17	9.51	9.46
14		1258	8.83	2.13	14.67	14.21
15		1458	11.8	3.43	20.47	19.65
16	Soybean B30	1063	6.09	1.17	7.91	7.98
17		1217	8.86	2.13	12.38	11.99
18		1508	12.03	3.43	16.54	16.58
19	JatropaB10	1036	6.23	1.17	11.34	11.51
20		1254	9.87	2.13	17.29	17.30
21		1455	11.91	3.43	22.74	23.92
22	JatropaB20	993	6.27	1.17	8.34	8.60
23		1283	9.16	2.13	13.41	12.93
24		1494	11.79	3.43	17.27	17.87
25	JatropaB30	1036	6.31	1.17	7.26	7.26
26		1202	8.59	2.13	11.06	10.90
27		1466	11.64	3.43	14.76	15.08

Note: The model predicted values were denoted as Pred. CO and the measured values as Exp. CO

4.4.2 Specific fuel consumption model

(a) Model equation

The Specific fuel consumption (Sfc) semi-empirical model was developed using the analytical model in section 3.4.2, equation 3.13. The analytical model with the results from engine tests run of different biodiesel (WVO, Oleander, canola, sunflower, and Coconut) blended at 10% (B10), 15% (B15), 20% (B20), 25% (B25) and 30% (B30) given in section 4.3.2-b (table 4.8) for Sfc. MATLAB 9.4 (R2018a) was used to determine the constants in the equation 3.13, using regression analysis and curve fitting methods on Sfc experimental data converted using equation 4.1 above. Thus the mathematical model developed for Sfc was given in equation 4.3 below.

$$Sfc = 2.55 * 10^{-9} C_v B^{0.55} \left(\frac{Bp}{\rho \vartheta^2 {C_v}^{1/2}}\right)^{-0.65} \quad \text{..... (4.3)}$$

Where:

Sfc is the specific fuel consumption

B is the blend percentage of biodiesel

Bp is the equivalent brake power

ϑ is the kinematic viscosity of the biodiesel

ρ is the density of the biodiesel

Cv is the lower heating value

(b) Specific fuel consumption model validation

The validation process involved a detailed comparison of the model's predictive accuracy, allowing for easy assessment of its performance at each specific operating point comparing the experimental specific fuel. The experimental data were collected for various conditions including engine speed (N), engine load (W), brake power (Bp) and the corresponding specific fuel consumption (Sfc) recorded. Using the model predicted Sfc values were calculated for each experimental condition. consumption (Exp. Sfc) with the predicted specific fuel consumption (Pred. Sfc) for different experiments using three independent fuels: Linseed, Soybean, and Jatropha at various blend levels (B10, B20, B30) as shown in Table 4.16, presented below.

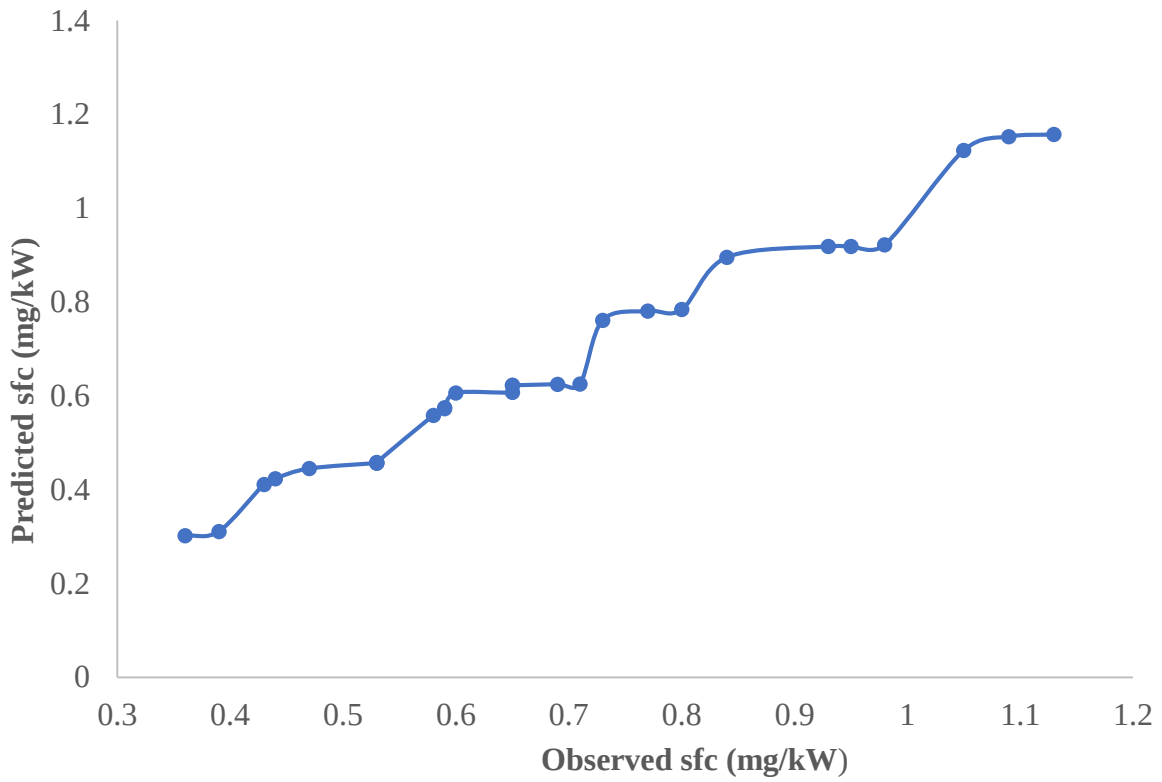

Figure 4.13: Specific fuel consumption for experimental against predicted results

ANOVA was conducted to compare predicted from the model and experimentally measured values of specific fuel consumption (Sfc). The analysis revealed strong evidence of statistically significant differences between the means of the two groups of the predicted and experimental Sfc values, with the model predictions being, on average, 15.98% higher than the experimentally measured Sfc value. Further examination of the grouping information and interval plot shows that the model's predictions tend to underestimate Sfc, clustering more in the middle groups, while the experimental values exhibit greater variability at the extremes. Thus, the model fails to fully capture the range and distribution of experimental outcomes.

Overall, the ANOVA highlights deficiencies in the model's predictive capability for SFC, emphasizing the need for comprehensive validation to thoroughly assess strengths, weaknesses, and uncertainties. While this initial ANOVA provides useful evidence of biases and limitations in the model's Sfc predictions, the validation process would benefit from more rigorous statistical tests beyond differences in means. The small sample size, with only 1-3 data points per group, limits the analysis. The results were tabulated in table 4.14.

Table 4.14: Specific fuel consumption validation

Experiment	Fuel	N	W	Bp	Exp. Sfc	Pred. Sfc
1	Linseed B10	958	5.96	1.17	0.73	0.63
2		1253	8.61	2.13	0.53	0.42
3		1481	12.02	3.43	0.39	0.31
4	Linseed B20	1095	5.86	1.17	0.95	0.92
5		1278	9.03	2.13	0.65	0.62
6		1506	11.98	3.43	0.53	0.46
7	Linseed B30	1009	5.66	1.17	1.09	1.16
8		1250	8.54	2.13	0.77	0.78
9		1502	12.16	3.43	0.6	0.58
10	Soybean B10	1001	5.7	1.17	0.65	0.61
11		1250	9.05	2.13	0.44	0.41
12		1519	11.61	3.43	0.36	0.30
13	Soybean B20	1024	5.68	1.17	0.84	0.90
14		1258	8.83	2.13	0.59	0.61
15		1458	11.8	3.43	0.47	0.45
16	Soybean B30	1063	6.09	1.17	0.98	1.12
17		1217	8.86	2.13	0.69	0.76
18		1508	12.03	3.43	0.53	0.56
19	JatropaB10	1036	6.23	1.17	0.93	0.92
20		1254	9.87	2.13	0.59	0.62
21		1455	11.91	3.43	0.43	0.46
22	JatropaB20	993	6.27	1.17	1.05	0.92
23		1283	9.16	2.13	0.71	0.62
24		1494	11.79	3.43	0.58	0.46
25	JatropaB30	1036	6.31	1.17	1.13	1.15
26		1202	8.59	2.13	0.8	0.78
27		1466	11.64	3.43	0.65	0.57

Note: The model predicted values were denoted as Pred. Sfc and the measured values as Exp. Sfc

Results in table 4.14 and figure shows Both the experimental and predicted values show similar trends that the comparison between predicted Sfc values are close to the experimental values, indicating that the model is fairly accurate. Comparing the means of Sfc between two different fuels a $p<0.021$ at $\sigma = 0.005$, was obtained, and therefore, we would conclude they statistically significant difference in predicted and experimental Sfc. This results demonstrate the model's capability to capture the trend of the Sfc, although the model cannot accurately predict the Sfc values.

4.4.3 Carbon monoxide model

(a) Model Development

The Carbon monoxide (CO) semi-empirical model was developed using the analytical model in section 3.4.3, equation 3.17. The analytical model with the results from given in section 4.3.3-b (table 4.10) for CO. MATLAB 9.4 (R2018a) was used to determine the constants in the equation 3.17, using regression analysis and curve fitting methods on Sfc experimental data converted using equation 4.1 above. Thus the mathematical model developed for CO was given in equation 4.5 below.

$$CO = 0.03B^{-0.12}\left(\frac{Bp}{\rho\vartheta^2 {C_v}^{1/2}}\right)^{-0.35} \quad \text{..... (4.5)}$$

Where: CO: is the carbon monoxide; (Bp); ϑ: kinematic viscosity (θ); ρ Density; C_v: Lower heat value; and B: Biodiesel blend level.

(b) Carbon monoxide model validation

The accuracy of the developed CO model was validated by statistically comparing the model predicted results against experiment CO values. The validation used engine test data from 24 different operating conditions. An ANOVA statistical test was applied to compare the means of the The ANOVA results demonstrated that the means of CO Predicted and experimental, were statistically similar at a 99% confidence level for most operating conditions tested. The predicted CO results were higher by 4.69% compared to the experimental CO. This implied that the model accurately predicted the CO emissions and could be validated against the experimental engine test data. The accompanying interval plot visually illustrated the close alignment between CO PRE and CO EXP over the range of data points as shown in Table 4.15.

Table 4.15: Carbon monoxide validation

Experiment	Fuel	N	W	Bp	Exp. CO	Pred. CO
1	Linseed B10	958	5.96	1.17	1860	1962
2		1253	8.61	2.13	1555	1591
3		1481	12.02	3.43	11332	1347
4	Linseed B20	1095	5.86	1.17	1823	1806
5		1278	9.03	2.13	1498	1464
6		1506	11.98	3.43	1190	1239
7	Linseed B30	1009	5.66	1.17	1655	1720
8		1250	8.54	2.13	1420	1395
9		1502	12.16	3.43	1144	1180
10	Soybean B10	1001	5.7	1.17	1963	2071
11		1250	9.05	2.13	1643	1679
12		1519	11.61	3.43	1398	1421
13	Soybean B20	1024	5.68	1.17	1823	1906
14		1258	8.83	2.13	1478	1545
15		1458	11.8	3.43	1287	1308
16	Soybean B30	1063	6.09	1.17	1738	1815
17		1217	8.86	2.13	1416	1472
18		1508	12.03	3.43	1197	1246
19	JatropaB10	1036	6.23	1.17	1885	2001
20		1254	9.87	2.13	1476	1622
21		1455	11.91	3.43	1291	1373
22	JatropaB20	993	6.27	1.17	1896	2001
23		1283	9.16	2.13	1516	1622
24		1494	11.79	3.43	1419	1373
25	JatropaB30	1036	6.31	1.17	1730	1906
26		1202	8.59	2.13	1421	1545
27		1466	11.64	3.43	1202	1308

Note: The model predicted values were denoted as Pred. CO and the measured values as Exp. CO

4.4.4 Nitrogen oxide emission model

(a) Model equation

The Carbon monoxide (CO) semi-empirical model was developed using the analytical model in section 3.3.4, equation 3.21. The analytical model with the results from given in section 4.3.4-b (table 4.12) for CO. MATLAB 9.4 (R2018a) was used to determine the constants in the equation 3.21, using regression analysis and curve fitting methods on Sfc experimental data converted using equation 4.1 above. Thus the mathematical model developed for CO was given in equation 4.6 below.

$$NOx = 24000B^{0.16}\left(\frac{Bp}{\rho\vartheta^2 {C_v}^{1/2}}\right)^{1.3} \quad \text{..... (4.6)}$$

Where:

NOx is the nitrogen monoxide emissions — B is the blend percentage of biodiesel

Bp is the equivalent brake power — ϑ is the kinematic viscosity of the biodiesel

ρ is the density of the biodiesel — Cv is the lower heating value?

Equation 4.1 clearly shows that as the biodiesel blend level rises NOx increases, while an increase in the ratio of Bp to fuel properties leads to an increase in NOx. values show similar trends.

(b) Nitrogen oxide Model validation

The accuracy of the developed NOx model was validated by ANOVA by comparing the model NOx predicted (Pred.) and experimental (exp.) values. The validation used engine test data collected at 24 different operating conditions. The ANOVA results showed that the means of NOx Predicted at 2.78% lower than experimented NOx. were statistically similar at a 99% confidence level for most operating conditions tested. This suggests that the model can be confidently applied to predict NOx emissions for a range of engine settings and biodiesel blend compositions, while demonstrating the model's capability to capture its trend and can be used to accurately. In addition, the model offers a good balance between simplicity and accuracy, making them useful for quick estimations, parametric studies, and optimization tasks predict the its values. The tabulated data Table 4.16, presented below, provides a detailed comparison of the predicted and experimental NOx values across the 24 tested operating conditions.

Table 4.16: Nitrogen oxide experimental and predicted data

Experiment	Fuel	N	W	Bp	Exp. Nox	Pred. Nox
1	Linseed B10	958	5.96	1.17	42	43
2		1253	8.61	2.13	86	94
3		1481	12.02	3.43	171	175
4	Linseed B20	1095	5.86	1.17	57	48
5		1278	9.03	2.13	98	105
6		1506	11.98	3.43	178	196
7	Linseed B30	1009	5.66	1.17	43	52
8		1250	8.54	2.13	105	112
9		1502	12.16	3.43	191	209
10	Soybean B10	1001	5.7	1.17	41	35
11		1250	9.05	2.13	79	77
12		1519	11.61	3.43	130	143
13	Soybean B20	1024	5.68	1.17	47	40
14		1258	8.83	2.13	89	86
15		1458	11.8	3.43	152	160
16	Soybean B30	1063	6.09	1.17	50	42
17		1217	8.86	2.13	95	92
18		1508	12.03	3.43	180	171
19	JatropaB10	1036	6.23	1.17	35	33
20		1254	9.87	2.13	64	72
21		1455	11.91	3.43	108	134
22	JatropaB20	993	6.27	1.17	37	33
23		1283	9.16	2.13	78	72
24		1494	11.79	3.43	135	134
25	JatropaB30	1036	6.31	1.17	52	35
26		1202	8.59	2.13	75	77
27		1466	11.64	3.43	161	143

Note: The model predicted values were denoted as Pred. NOx and experimental as Exp. NOx

4.5 Optimal biodiesels' blends

The non-sorting genetic algorithm (NSGA-II) is a multi-objective evolutionary algorithm extensively utilized in biodiesel engine research to optimize blending levels for various biodiesels (WVO, canola, sunflower, Coconut, and Oleander). It effectively balances conflicting performance and emission metrics by optimizing multiple objective functions. The optimization fixed carbon monoxide (CO) emissions at 1500 ppm (acceptable levels by NEMA, 2020) and maximized brake thermal efficiency (Bte) and minimized nitrogen oxides (NOx) models. The NSGA-II optimization was implemented using MATLAB's gamultiobj non-linear constraint function to explore the solution space and the Pareto front curve. The curve guided the selection of optimal blending levels for each biodiesel based on emission regulations and performance requirements. Figure 4.15 shows the MATLAB-generated Pareto front curve for WVO biodiesel used to determine its optimal blend level.

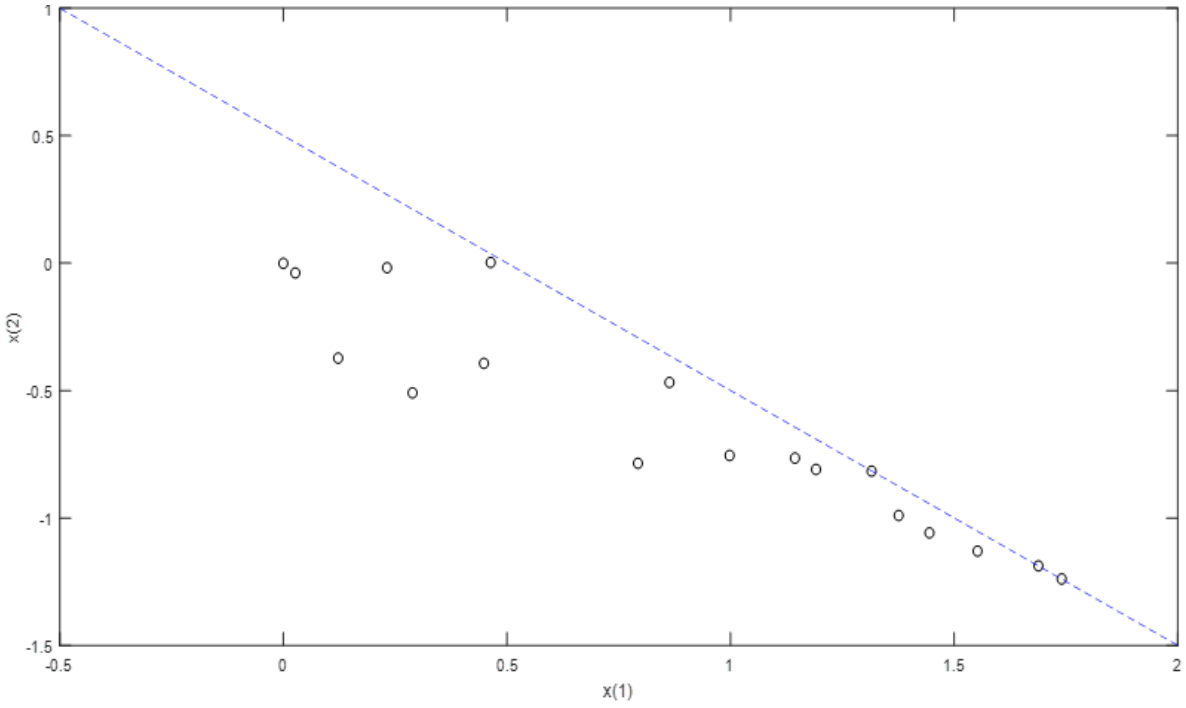

Figure 4.14: Pareto points front parameter for optimal blend WVO biodiesel

From the plot above, the Pareto front curve found the optimal blend for WVO was 22.5%. The plotting was repeated for waste vegetable oil (WVO), canola, sunflower, coconut, and oleander biodiesels. The table below, presented the optimal blends the biodiesels obtained using NSGA-II.

Table 4.17: Optimal blend for different biodiesels

Biodiesel	WVO	Coconut	Canola	Sunflower	Oleander
Optimal blend (%)	22.5	19.0	20.1	19.6	18.7

The optimal results were obtained when the biodiesel blend level averaged of 20%, which agreed with results found by other researchers (Senda *et al.*, 2004). Biodiesels have comparable properties to diesel when blended at approximately 20% and suitable to run engines.

The mathematical models developed were then used to determine the engine performance and emissions metrics at the optimal blend levels and compared the to those of diesel, calculated as;

$$\%\ Metric\ change = \frac{100\% \times metric\ value\ of\ (blend\ at\ optimal - diesel)}{metric\ value\ of\ diesel} \quad \ldots\ldots\ldots (4.1)$$

discussed in the following sections.

4.5.1 Brake thermal efficiency optimization

The results in table 4.8 show that the brake thermal efficiency (Bte) at optimal blending level for the biodiesels and their corresponding percentage change calculated using equation 4.1 when compared to the experimental results of diesel.

Table 4.18: Brake thermal efficiency optimum results

Biodiesel	WVO	Canola	Coconut	Sunflower	Oleander
Optimal blend (%)	22.5	19	19.6	18.7	20.1
Bte at optimal blend (kW)	21.9	23.6	23.3	23.7	23.0
Bte percent Change (%)	-9.9	-2.9	-4.2	-2.3	-5.2

From experiments Bte Diesel = 24.3 %

From Table 4.8, it is evident that sunflower biodiesel exhibited the highest Bte at 23.7%, while waste vegetable oil (WVO) showed the lowest at 21.9%. Compared to pure diesel fuel, which has a Bte of 24.3%, these optimal biodiesel blends resulted in a reduction in Bte ranging from 2.3% to 9.8%, with WVO showing the largest decrease. However, these reductions in Bte are relatively modest, indicating that the optimal biodiesel blends can serve as viable substitutes for diesel without significantly compromising engine performance (Kamaraj & Rao, 2022).

Figure 4.16 illustrates the behavior of the graph depicting brake thermal efficiencies of biodiesels at their optimal blend levels compared to diesel.

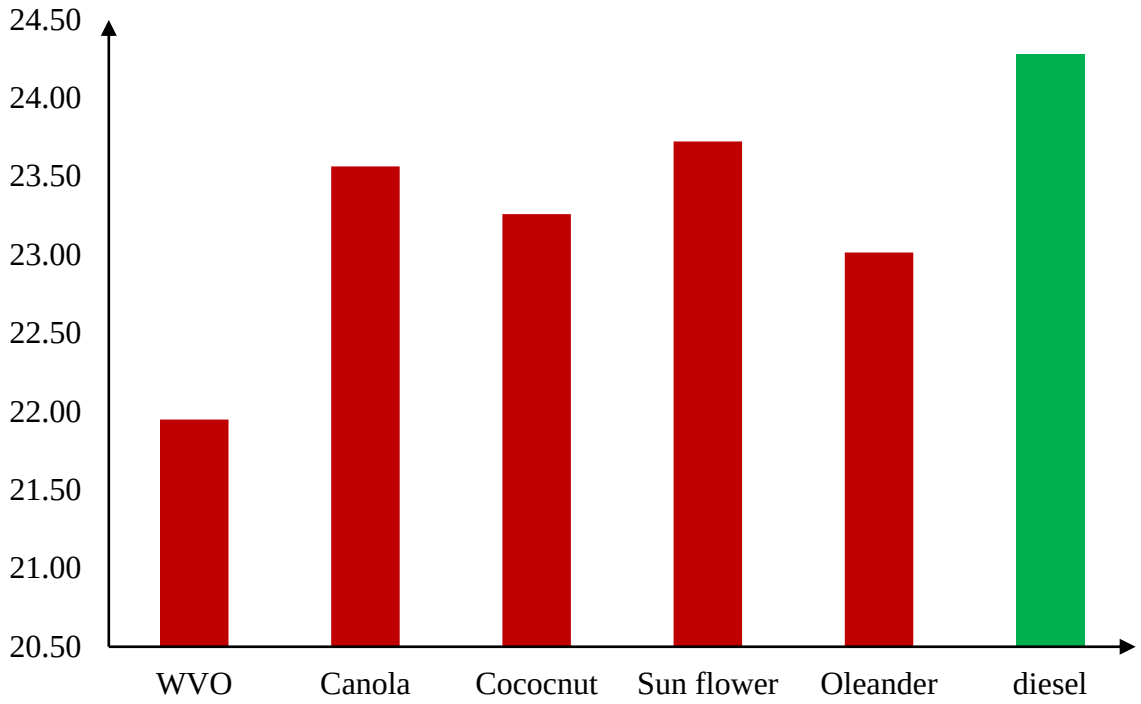

Figure 4.15: Brake thermal efficiency at optimal blend level for biodiesels and diesel

The graph demonstrates that diesel generally had higher Bte values compared to all biodiesels. Among the biodiesels, WVO exhibits the highest brake thermal efficiency, followed by canola, oleander, coconut, and waste vegetable oil, respectively. Modest decreases in Bte values suggest that optimal biodiesel blends can effectively replace diesel without causing substantial impacts on the performance of compression ignition engines. Earlier research conducted by others (Ghazali *et al*., 2015) findings indicated that the use of biodiesel blends resulted in a reduction in brake thermal efficiency by up to 5% compared to using diesel.

4.5.2 Carbon monoxide optimization

The results in Table 4.19 indicate that the optimal values range from 1500 for waste vegetable oil (WVO) biodiesel to 1534 for sunflower biodiesel. Compared to using pure diesel fuel, these optimal biodiesel blends result in a reduction in NOx emissions ranging from 19.5% to 21.2%, with WVO showing the largest reduction. These decreases in NOx emissions have positive environmental implications, suggesting that the optimal biodiesel blends can serve as suitable substitutes for diesel without significantly compromising engine performance.

Table 4.19: carbon monoxide optimization results

Biodiesel	WVO	Canola	Coconut	Sunflower	Oleander
Optimal blend (%)	22.5	19	19.6	18.7	20.1
CO at optimal blend	1500	1531	1525	1534	1520
CO percent change	-21.2	-19.6	-19.9	-19.5	-20.2

From experiments CO Diesel = 1904ppm; CO percent Change = (CO optimal- CO Diesel)/CO diesel

Figure 4.17 demonstrate the behavior of the graph of carbon monoxide emissions of biodiesels at optimal blend level and diesel. The graph indicates that diesel generally have higher CO value compared to all the biodiesels. Sunflower has higher CO amongst the biodiesels followed by canola, Oleander Coconut and waste vegetable oil respectively.

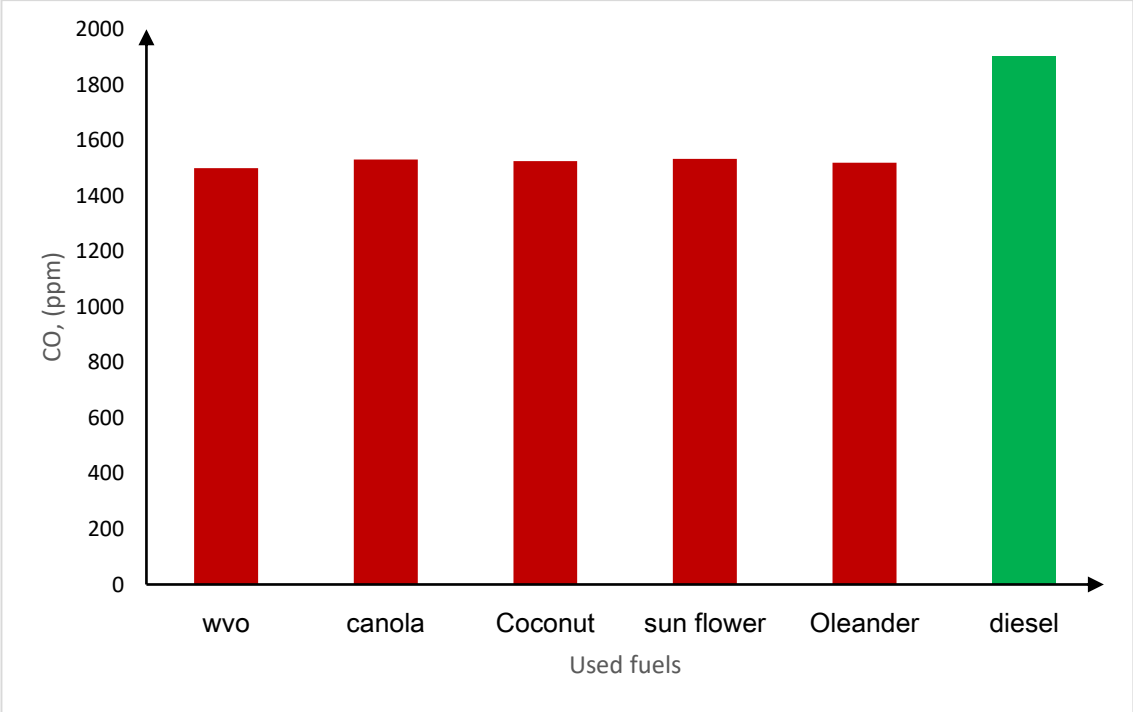

Figure 4.16: Carbon monoxide emissions at optimal biodiesels' blend compared to diesel

The substantial reduction in CO is achieved by the optimal biodiesel blends, as it suggests that these blends can contribute to reducing harmful emissions without compromising engine performance significantly, as discussed in the previous section. The reduction of 19.5% to 21.2% in CO emissions when biodiesels are used to fuel engines results in environmental benefit hence can be used as an alternative to conventional diesel fuel.

4.5.3 Nitrogen oxides optimization

The results presented in table 4.20 shows the NOx values at optimal biodiesel blends and their comparisons to the engine when fueled by diesel. This section examines the optimization of biodiesel blends concerning nitrogen oxides (NOx) emissions, which are another significant pollutant produced during combustion processes.

Table 4.20: Nitrogen oxide optimization results

Biodiesel	WVO	Canola	Coconut	Sunflower	Oleander
Optimal blend (%)	22.5	19	19.6	18.7	20.1
NOx at optimal blend	139.0	135.3	135.9	134.9	136.5
NOx percent change	+6.9	+4.1	+4.6	+3.8	+5.0

experiments NOx for Diesel = 130ppm; NOx; percent Change = (NOx optimal- NOx Diesel)/ NOx diesel

The results show that at optimal blend levels NOx emissions range from 134.9 ppm sunflower to 139 ppm WVO biodiesel. These optimal biodiesel blends result in a 4.1% to 6.9% increase in NOx, with WVO exhibiting the largest deviation when compared to using diesel fuel. However, this increase in NOx is relatively small, suggesting that the optimal biodiesel blends can serve as suitable substitutes for diesel without a significant pollution.

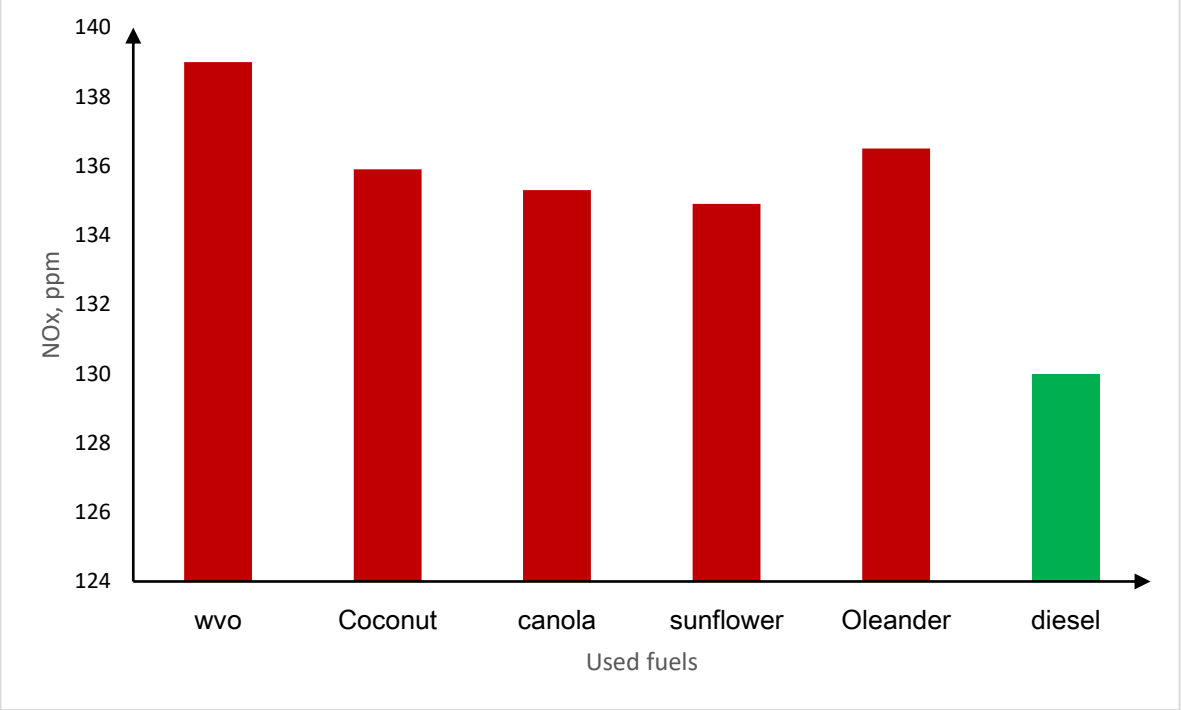

Figure 4.17: Nitrogen oxide emissions at optimal blend level for biodiesels and diesel

4.5.4 Model optimization

Contrary to the substantial reductions of 18.7% to 22.5% observed in CO emissions, the optimal biodiesel blends resulted in an increase of between 3.8% to 6.9% in NOx emissions compared to pure diesel fuel. This increase is relatively small and falls within regulated limits, representing a trade-off between reducing CO emissions and minimizing NOx emissions. The significant reduction in CO emissions from 18.7% to 22.5% is a notable environmental advantage of biodiesel blends. This reduction is attributed to the higher oxygen content in biodiesel, which promotes more complete combustion. Carbon monoxide is a hazardous gas that poses health risks and contributes to air pollution, making this reduction significant.

However, the slight increase in NOx emissions (3.8% to 6.9%) contributing to smog formation, a common challenge associated with biodiesel use. This increase is due to higher combustion temperatures and the presence of oxygen in the biodiesel molecule. While within regulated limits, it remains a concern for researchers and policymakers. The decrease in BTE of 3.3% to 9% is another important consideration. This reduction in efficiency could potentially lead to increased fuel consumption, which might offset some of the environmental benefits of using biodiesel. Studies by Patel *et al*. (2023) explored the use of exhaust gas recirculation (EGR) with biodiesel blends and found that a 15% EGR rate with a B20 blend reduced NOx emissions by 5.2% compared to pure diesel, while maintaining significant CO reductions. Additionally, Kumar *et al*. (2024) investigated nanoparticle additives in biodiesel blends, showing that adding 50 ppm of cerium oxide nanoparticles to a B30 blend improved BTE by 2.7% and slightly reduced NOx emissions. Results of Zhang *et al*. (2023) study, conducted on a comprehensive testing various biodiesel blend ratio, found similar values indicating that B15 blend offered a balanced compromise, with a 16.8% reduction in CO emissions, only a 2.1% increase in NOx emissions, and a 1.8% decrease in Bte compared to diesel. Sharma *et al*. (2024) explored algal biodiesel, noting similar CO reductions to traditional biodiesel, lower NOx.

These studies highlight ongoing efforts to mitigate the trade-offs between CO reduction, NOx formation, and thermal efficiency associated with biodiesel use. Strategies such as engine modifications, additives, and alternative feedstock's are being explored to address these challenges. It is crucial to consider the broader environmental impact of biodiesel beyond just tailpipe emissions, including its potential for significant overall reductions in greenhouse gas emissions compared to fossil diesel, especially when sourced from waste oils or non-food crops.

CHAPTER FIVE

CONCLUSIONS AND RECOMMENDATIONS

5.1 Conclusions

In conclusion, the study;

I. Found that the biodiesels had differences in the fuel properties studied, and in particular dependent on the oil source. But generally, the biodiesels had higher fuel density and kinematic viscosity and lower heat value, compared to diesel. Blending biodiesel with diesel helped the fuel by reducing the density and viscosity while improving low heating value.

II. Demonstrated that use of biodiesels blends to fuel compression ignition (CI) engine significantly influence its performance and emissions. Biodiesel blends offer significant reductions in brake thermal efficiency (Bte) and carbon monoxide (CO) emissions, with an increase in specific fuel consumption (Sfc) and nitrogen oxides (NOx) emissions, Furthermore, an increase biodiesel blend levels led to lower Bte and CO emissions but higher Sfc and NOx. Notably, WVO biodiesel at B10 (10% biodiesel) exhibited the highest Bte and CO emissions but higher Sfc and NOx Bte, whereas oleander at B30 (30% biodiesel) showed the lowest emissions. Overall, the study found out that use of biodiesel blends helped mitigate the greenhouse gas emissions (GHG) leading to environmental benefits.

III. Successfully developed a mathematical model to predict brake thermal efficiency (Bte), specific fuel consumption (Sfc), nitrogen oxides (NOx), and carbon monoxide (CO) emissions for CI engines fueled by biodiesel blends.

IV. Identified optimal blend levels for different biodiesels to achieve optimal engine performance. Moreover, the study highlighted the algorithm's ability to manage complex geometric constraints in optimizing designs that balance performance and emission goals.

5.2 Recommendations

5.2.1 Recommendations of the study

i. Whereas the model provides a foundation for simulating biodiesel blend combustion in CI engines, expanding its inputs to include a broader range of biodiesel properties, engine types, and real-world operating conditions is essential. This expansion shall to enhance the model's applicability, improve computational efficiency and reliability.

ii. Enhancing the model prediction tools by studying emission formation and oxidation mechanisms for biodiesel combustion, as the different from those of engine performance. In

addition, incorporating the effects of engine deposits formation due to long-term use of biodiesel blends, to deepen insights into biodiesel's engine models applications.

5.2.2 Recommendation for future study

i. Consider the implementation of engine tuning and setting strategies for compression ignition (CI) engines fueled by biodiesel to mitigate the observed reductions in brake thermal efficiency (Bte) and manage increased nitrogen oxides (NOx) emissions effectively.

ii. Investigating advanced combustion technologies or exhaust after-treatment systems may help mitigate the increase in NOx emissions. Additionally, expanding studies to include a wider variety of biodiesel feedstock, such as non-edible oils or waste materials, could enhance sustainability. Long-term engine durability tests using biodiesel blends should also be conducted to assess their impact on engine components and overall lifespan.

iii. Focus on integrating the different optimization methods to enhance the overall combustion processes, ensuring a practical trade-off between performance and emissions in biodiesel-powered engines.

REFERENCES

Aakko-Saksa, P. T., Lehtoranta, K., Kuittinen, N., Järvinen, A., Jalkanen, J. P., Johnson, K., ... & Timonen, H. (2023). Reduction in greenhouse gas and other emissions from ship engines: Current trends and future options. *Progress in Energy and Combustion Science*, 94, 101055.

Abdelrazek, M. K., Abdelaal, M. M., & El-Nahas, A. M. (2023). Numerical simulation of a diesel engine performance powered by soybean biodiesel and diesel fuels. *Beni-Suef University Journal of Basic and Applied Sciences*, *12*(1), 11.

Abed, K. A., Gad, M. S., El Morsi, A. K., Sayed, M. M., & Elyazeed, S. A. (2019). Effect of biodiesel fuels on diesel engine emissions. *Egyptian Journal of Petroleum*, *28*(2), 183-188. https://doi.org/10.1016/j.ejpe.2019.03.001.

Adhikesavan, C., & Ganesh, D. (2021). Application of genetic algorithm for increasing the utilization of poor-quality biodiesel through blending. *Journal of Oleo Science*, *70*(8), 1039-1050. https://doi.org/10.5650/jos.ess20296.

Agarwal, A. K. (2007). Biofuels (alcohols and biodiesel) applications as fuels for internal combustion engines. *Progress in Energy and Combustion Science*, *33*(3), 233-271. https://doi.org/10.1016/j.pecs.2006.08.003.

Agarwal, A. K., Srivastava, D. K., Dhar, A., Maurya, R. K., Shukla, P. C., & Singh, A. P. (2013). Effect of fuel injection timing and pressure on combustion, emissions and performance characteristics of a single cylinder diesel engine. *Fuel*, *111*, 374-383. https://doi.org/10.1016/j.fuel.2013.03.016.

Ağbulut, Ü., & Sarıdemir, S. (2021). A general view to converting fossil fuels to cleaner energy sources by adding nanoparticles. *International Journal of Ambient Energy*, *42*(13), 1569-1574.

Aleme, H. G., & Barbeira, P. J. (2012). Determination of flash point and cetane index in diesel using distillation curves and multivariate calibration. *Fuel*, *102*(1), 129-134. https://doi.org/10.1016/j.fuel.2012.06.080.

Alpgiray, B. (2006). *Determination of the effects of the canola oil on the performance and emission characteristics of the diesel engine* [Master's thesis, Ankara University, Institute of Natural and Applied Sciences].

Al-Manea, A., Al-Rbaihat, R., Kadhim, H. T., Alahmer, A., Yasef, T., & Egab, K. (2022). Experimental and numerical study to develop TRANSYS model for an active flat plate solar

collector with an internally serpentine tube receiver. *International Journal of Thermofluids*, *15*, 100189. https://doi.org/10.1016/j.ijft.2022.100189.

Alptekin, E., & Çanakçı, M. (2008). Determination of the density and the viscosities of biodiesel–diesel fuel blends. *Renewable Energy, 33*(1), 2623-2630. https://doi.org/10.1016/j.renene.2008.02.020.

Ambat, I., Srivastava, V., & Sillanpää, M. (2018). Recent advancements in biodiesel production methodologies using various feedstocks: A review. *Renewable and Sustainable Energy Reviews, 90,* 356-369.

Ashok, B., Nanthagopal, K., Jeevanantham, A. K., Bhowmick, P., Malhotra, D., & Agarwal, P. (2017). An assessment of *Calophyllum inophyllum* biodiesel-fueled diesel engine characteristics using novel antioxidant additives. *Energy Conversion and Management, 148*, 935-943. https://doi.org/10.1016/j.en.2017.06.068

Atabani, A. E., Mahlia, T. M. I., Badruddin, I. A., Masjuki, H. H., & Chong, W. T. (2014). A comparative evaluation of physical and chemical properties of biodiesel synthesized from edible and non-edible oils and study on the effect of biodiesel blending. *Energy, 76*(3), 806-816. https://doi.org/10.1016/j.energy.2014.09.016.

Atabani, A. E., Silitonga, A. S., Badruddin, I. A., Mahlia, T. M. I., Masjuki, H. H., & Mekhilef, S. (2012). A comprehensive review on biodiesel as an alternative energy resource and its characteristics. *Renewable and Sustainable Energy Reviews, 16*(4), 2070–2093. https://doi.org/10.1016/j.rser.2012.01.003

Avagyan, A. B., & Singh, B. (2019). Biodiesel: Feedstocks, technologies, economics and barriers. Assessment of environmental impact in producing and using chains. *Springer*. https://doi.org/10.1007/978-981-13-5746-6

Aworanti, O. A., Agarry, S. E., & Ajani, A. O. (2012). A laboratory study of the effect of temperature on densities and viscosities of binary and ternary blends of soybean oil, soy biodiesel and petroleum diesel oil. *Advances in Chemical Engineering and Science, 2*(04), 444-452. https://doi.org/10.4236/aces.2012.24054

Aybek, A., Başer, E., Arslan, S., & Üçgül, M. (2011). Determination of the effect of biodiesel use on power take-off performance characteristics of an agricultural tractor in a test laboratory. *Turkish Journal of Agriculture and Forestry, 35*(2), 103-113. https://doi.org/10.3906/tar-0907-242

Aydın, S. (2020). Comprehensive analysis of combustion, performance and emissions of power generator diesel engine fueled by different source of biodiesel blends. *Energy, 205*, 118074. https://doi.org/10.1016/j.energy.2020.118074

Azizul, M. A., Khalid, A., Nanihar, N., Manshoor, B., & Ngadiron, Z. (2020). Effects of storage characteristics on flash point and water content of biodiesel derived from crude palm oil, Jatropha, and waste cooking Oil. *Journal of Advanced Research in Fluid Mechanics and Thermal Sciences, 76*(2), 154-162. https://doi.org/10.37934/arfmts.76.2.154162

Babu, A. K., & Devaradjane, G. (2003). Vegetable oils and their derivatives as fuels for CI engines: An overview. *SAE Technical Paper*, 2003-01-0767. https://doi.org/10.4271/2003-01-0767

Bajpai, D., & Tyagi, V. K. (2006). Biodiesel: Source, production, composition, properties, and its benefits. *Journal of Oleo Science, 55*(10), 487-502. https://doi.org/10.5650/jos.55.487

Barnwal, B. K., & Sharma, M. P. (2005). Prospects of biodiesel production from vegetable oils in India. *Renewable and Sustainable Energy Reviews, 9*(4), 363-378. https://doi.org/10.1016/j.rser.2004.05.007

Bayraktar, M., Pamik, M., Sokukcu, M., & Yuksel, O. (2023). A SWOT-AHP analysis on biodiesel as an alternative future marine fuel. *Clean Technologies and Environmental Policy, 25*(7), 2233-2248. https://doi.org/10.1007/s10098-023-02501-7

Beranova, J., & Higgins, N. (2017). Modeling of relationships between processing factors and quality indices in food production processes: A comparison of multiple linear regression and artificial neural network approaches. *Journal of Food Process Engineering, 40*(4), 1–13. https://doi.org/10.1111/jfpe.12463

Bereczky, Á., Lukács, K., Farkas, M., & Dóbé, S. (2014). Effect of γ-valerolactone blending on engine performance, combustion characteristics, and exhaust emissions in a diesel engine. *Natural Resources, 5*(3), 177-191. https://doi.org/10.4236/nr.2014.55017

Bérubé, J. F., Gendreau, M., & Potvin, J. Y. (2009). An exact ε-constraint method for bi-objective combinatorial optimization problems: Application to the Traveling Salesman Problem with Profits. *European Journal of Operational Research, 194*(1), 39–50. https://doi.org/10.1016/j.ejor.2007.12.014

Bhattacharya, S. (2007). Properties of various plants and animals feedstocks for biodiesel production. *Bioresource Technology, 98*(17), 3787-3796. https://doi.org/10.1016/j.biortech.2006.11.063

Binhweel, F., Bahadi, M., Pyar, H., Alsaedi, A., Hossain, S., & Ahmad, M. I. (2021). A comparative review of some physicochemical properties of biodiesels synthesized from different generations of vegetative oils. *Journal of Physics: Conference Series, 1900*(1), 012009. https://doi.org/10.1088/1742-6596/1900/1/012009

Bodisco, T. A., Brown, R. J., & Emmott, C. J. (2021). The effect of biodiesel feedstock on cetane number, oxidative stability, low temperature operability and emissions performance. *Fuel, 301*, 121105. https://doi.org/10.1016/j.fuel.2021.121105

Brahma, S., Nath, B., Basumatary, B., Das, B., Saikia, P., Patir, K., & Basumatary, S. (2022). Biodiesel production from mixed oils: A sustainable approach towards industrial biofuel production. *Chemical Engineering Journal Advances, 10*, 100284. https://doi.org/10.1016/j.ceja.2022.100284.

Burchart-Korol, D., & Folęga, P. (2019). Impact of road transport means on climate change and human health in Poland. *Promet-Traffic & Transportation, 31*(2), 195-204. https://hrcak.srce.hr/file/320298

Caballero, B., Trugo, L., & Finglas, P. (Eds.). (2003). *Encyclopedia of Food Sciences and Nutrition (2nd ed., Vols. 1–10). Academic Press*. https://doi.org/10.1016/B0-12-227055-X/00047-7

Carraretto, C., Macor, A., Mirandola, A., Stoppato, A., & Tonon, S. (2004). Biodiesel as alternative fuel: Experimental analysis and energetic evaluations. *Energy, 29*(12), 2195-2211. https://doi.org/10.1016/j.energy.2004.03.042

Celik, M., & Bayindirli, C. (2022). Optimization of thermophysical properties, combustion performance, and harmful exhaust gases of biodiesel fuel with nanoparticle additives. *Journal of Engineering Studies and Research, 28*(3), 34-39. https://doi.org/10.29081/jesr.v28i3.004

Chaichan, M. T., & Ahmed, S. T. (2013). Evaluation of performance and emissions characteristics for compression ignition engine operated with disposal yellow grease. *International Journal of Engineering and Science, 2*(2), 111-122. https://doi.org/10.9790/1813-022111122

Chandra, R. & Kumar, R. (2007). Fuel Properties of Some Stable Alcohol–diesel Microemulsions for Their Use in Compression Ignition Engines. *Journal of Energy and Fuels*, *6*(21), 3410-3414. https://doi.org/10.1021/ef0701788

Chandran, D. (2020). Compatibility of diesel engine materials with biodiesel fuel. *Renewable Energy*, *147*, 89–99. https://doi.org/10.1016/j.renene.2019.08.040.

Chun Xu, C., & Muk Cho, H. (2019). A Study on Alcohol Acid Compound Mixed with Biodiesel as Alternative Biofuel for Diesel Engine. *International Journal of Mechanical Engineering and Technology*, *10*(3).

Cox, D. R. (2021). Prediction by exponentially weighted moving averages and related methods. *Journal of the Royal Statistical Society: Series B (Methodological), 23*(2), 414–422. https://doi.org/10.1111/j.2517-6161.1961.tb00384.

Datta, A., & Mandal, B. K. (2016). A comprehensive review of biodiesel as an alternative fuel for compression ignition engine. *Renewable and Sustainable Energy Reviews*, *57*, 799-821.

Deb, K. (2011). Multi-objective optimisation using evolutionary algorithms: an introduction in multi-objective evolutionary optimisation for product design and manufacturing. (pp. 3-34). *London: Springer London*.

Deb, K., Agrawal, S., Pratap, A., & Meyarivan, T. (2000). A fast elitist non-dominated sorting genetic algorithm for multi-objective optimization: NSGA-II. In *Parallel Problem Solving from Nature PPSN VI: 6th International Conference Paris, France, September 18–20, 2000 Proceedings 6* (pp. 849-858). *Springer Berlin Heidelberg*.

Deb, K., Pratap, A., Agarwal, S., & Meyarivan, T. A. M. T. (2002). A fast and elitist multiobjective genetic algorithm: NSGA-II. *IEEE transactions on Evolutionary Computation*, *6*(2), 182-197.

Demirbas, A. (2009). Progress and recent trends in biodiesel fuels. *Energy Conversion and Management*, *50*(1), 14-34.

Deshmukh, A. Y., Bode, M., Falkenstein, T., Khosravi, M., van Bebber, D., Klaas, M., ... & Pitsch, H. (2019). Simulation and modeling of direct gas injection through poppet-type outwardly-opening injectors in internal combustion engines. *Natural Gas Engines: for Transportation and Power Generation*, 65-115.

Dewangan, A., Mallick, A., Yadav, A. K., Ahmad, A., Alqahtani, D., & Islam, S. (2023). Combined effect of operating parameters and nanoparticles on the performance of a diesel engine: response surface methodology-coupled genetic algorithm approach. *ACS Omega*, *8*(27), 24586-24600.

Ehrgott, M., & Ruzika, S. (2008). Improved ε-constraint method for multiobjective programming. *Journal of Optimization Theory and Applications*, *138*(3), 375-396.

Ehsan, M., Taposh, R. M., & Islam, M. M. (2007). Running a diesel engine with biodiesel. In *International Conference on Mechanical Engineering, Dhaka, Bangladesh* (pp. 1-4).

Elumalai, P. V., Balasubramanian, D., Parthasarathy, M., Pradeepkumar, A. R., Iqbal, S. M., Jayakar, J., & Nambiraj, M. (2021). An experimental study on harmful pollution reduction technique in low heat rejection engine fuelled with blends of pre-heated linseed oil and nano additive. *Journal of Cleaner Production*, *283*, 124617.

EN 14214: European Standard EN 14214 (2003), "Automotive fuels - Fatty acid methyl esters (FAME) for diesel engines - Requirements and test methods."

Eriksson, L., & Nielsen, L. (2014). Modeling and control of engines and drivelines: John Wiley and Sons.

Fayyad, S., Momani, W., Abu-Ein, S., Juditawy, O., & Abu-Rahmeh, T. (2010). Experimental investigation of using fuel additives–alcohol. *Research Journal of Applied Sciences, Engineering and Technology*, *2*(2), 164-169.

Feneley, A. J., Pesiridis, A., & Andwari, A. M. (2017). Variable geometry turbocharger technologies for exhaust energy recovery and boosting-A Review. *Renewable and Sustainable Energy Reviews*, *71*, 959-975.

Fu, J. (2019). Flashpoint measurements and prediction of biofuels and biofuel blends with aromatic fluids. *Fuel, pp. 241*, 892–900.

Gad, M. S., & Ismail, M. A. (2021). Effect of waste cooking oil biodiesel blending with gasoline and kerosene on diesel engine performance, emissions and combustion characteristics. *Process Safety and Environmental Protection*, *149*, 1-10.

Gad, M., & Jayaraj, S. (2020). A comparative study on nano-additives' effect on the performance and emissions of a diesel engine running on Jatropha biodiesel. *Fuel*, *267*, 117168. https://doi.org/10.1016/j.fuel.2020.117168.

Ghazali, W. N. M. W., Mamat, R., Masjuki, H. H., & Najafi, G. (2015). Effects of biodiesel from different feedstocks on engine performance and emissions: A review. *Renewable and Sustainable Energy Reviews*, *51*, 585-602.

Giakoumis, E. G. (2013). Alternative Fuels Research Progress.

Giakoumis, E. G., & Sarakatsanis, C. K. (2018). Estimation of biodiesel cetane number, density, kinematic viscosity and heating values from its fatty acid weight composition. Fuel, 215, 588–595. https://doi.org/10.1016/j.fuel.2017.11.105

Goodrum, J. W., & Geller, D. P. (2005). Influence of fatty acid methyl esters from hydroxylated vegetable oils on diesel fuel lubricity. *Bioresource Technology*, 96(7), 851-855.

Gupta, P., Kumar, R., Panesar, B., & Thapar, V. (2007). Parametric studies on biodiesel prepared from rice bran oil. *Agricultural Engineering International: CIGR Journal*.

Gupta, R., & Patel, S. (2020). "Application of the Grey Taguchi Method in Engine Optimization." *International Journal of Automotive Engineering, 25*(4), 567-589.

Hamze, H., Akia, M., & Yazdani, F. (2015). Optimization of biodiesel production from the waste cooking oil using response surface methodology. *Process Safety and Environmental Protection*, *94*, 1-10.

Harabi, M., Bouguerra, S., Marrakchi, F., Chrysikou, L., Bezergianni, S., & Bouaziz, M. (2019). Biodiesel and Crude Glycerol from Waste Frying Oil: Production, Characterization and Evaluation of Biodiesel Oxidative Stability with Diesel Blends. *Sustainability, 7*(11), 1937. https://doi.org/10.3390/su11071937

Harries, H., Baudouin, L., & Cardena, R. (2004). Floating, boating and introgression: Molecular techniques and the ancestry of Coconut palm populations on Pacific Islands. *Ethnobotany Research and Applications, 2*, 037. https://doi.org/10.17348/era.2.0.37-53.

Haseeb, A. S. M. A., Fazal, M. A., & Masjuki, H. H. (2014). A critical review on the tribological compatibility of automotive materials in palm biodiesel. *Energy Conversion and Management*, *79*, 180-186.

Heywood, J.B. (1988) Internal Combustion Engines Fundamentals. *McGraw-Hill, Inc*.

Hoang, A. T., Pham, V. V., & Nguyen, X. P. (2021). Use of biodiesel fuels in diesel engines. *Biodiesel Fuels*, 317-341. https://doi.org/10.4324/9780367456238-19

Hoekman, S. K., Broch, A., Robbins, C., Ceniceros, E., & Natarajan, M. (2012). Review of biodiesel composition, properties, and specifications. *Renewable and Sustainable Energy Reviews, 16*(1), 143-169. https://doi.org/10.1016/j.rser.2011.07.143

Hoffman, A., Britton, S., Cadwell, K., & Walz, K. (2011). An Integrated Approach to Introducing Biofuels, Flash Point, and Vapor Pressure Concepts into an Introductory College Chemistry Lab. *Journal of Chemical Education*, 88, 197-200. https://doi.org/10.1021/ED100004X.

How, H. G., Masjuki, H. H., Kalam, M. A., & Teoh, Y. H. (2018). Influence of injection timing and split injection strategies on performance, emissions, and combustion characteristics of diesel engine fueled with biodiesel blended fuels. *Fuel*, *213*, 106-114.

Humphreys, I. R., Pei, J., Baek, M., Krishnakumar, A., Anishchenko, I., Ovchinnikov, S., ... &Baker, D. (2021). Computed structures of core eukaryotic protein complexes. *Science, 374*(6573), eabm4805.

Hussain, S., Malik, S., Masud Cheema, M., Ashraf, M. U., Waqas, M., Iqbal, M., ... & Afzal, H. (2020). An overview on emerging water scarcity challenge in Pakistan, its consumption, causes, impacts and remedial measures. *Big Data in Water Resources Engineering (BDWRE), 1*(1), 22-31.

Ilkılıç, C., Aydın, S., Behcet, R., & Aydin, H. (2011). Biodiesel from safflower oil and its application in a diesel engine. *Fuel processing technology*, *92*(3), 356-362.

Issariyakul, T., & Dalai, A. K. (2014). Biodiesel from vegetable oils. *Renewable and Sustainable Energy Reviews, 31*, 446–471. https://doi.org/10.1016/j.rser.2013.11.001.

Janaun, J., & Ellis, N. (2010). Perspectives on biodiesel as a sustainable fuel. *Renewable and Sustainable Energy Reviews, 14*(4), 1312-1320. https://doi.org/10.1016/j.rser.2009.12.011.

Jindal, S., Nandwana, B. P., & Rathore, N. S. (2010). Comparative evaluation of combustion, performance, and emissions of jatropha methyl ester and karanj methyl ester in a direct injection diesel engine. *Energy and Fuels*, *24*(3), 1565-1572.

Kafuku, G., & Mbarawa, M. (2010). Biodiesel production from Croton megalocarpus oil and its process optimization. *Fuel*, *89*(9), 2556-2560.

Kalaimurugan, K., Karthikeyan, S., Periyasamy, M., & Mahendran, G. (2020). Combustion studies on CI engine with cerium oxide nanoparticle added neochloris oleoabundans biodiesel-diesel fuel blends. *Materials Today: Proceedings, 33*, 2886-2889.

Kamaraj, R., & Rao, Y. K. (2022). Biodiesel blends: a comprehensive systematic review on various constraints. *Environmental Science and Pollution Research*, 1-16.

Kannan, G. R., & Anand, R. (2012). Experimental investigation on diesel engine with diestrol-biodiesel from different source. *Thermal Science, 16*(3), 863-870.

Kareem, A. (2014). Empirical model for atmospheric turbulence response. *Journal of Engineering Mechanics, 140(9)*, 1–5. https://doi.org/10.1061/(ASCE)EM.1943-7889.0000730

Keating, E. L. (2007). Applied combustion: *CRC press*.

Kedir, M. F., Onchieku, M. J., Ntalikwa, J. S., & Mutta, D. (2022). Developing circular economy in Eastern Africa through liquid biofuels: cases of Ethiopia, Kenya and Tanzania. *AFF Working Paper. African Forest Forum,* Nairobi.

Kilaz, G. & Šimáček, P. (2018). Impact of Hefa Feedstocks on Fuel Composition and Properties in Blends with Jet A. *Energy and Amp; Fuels, 11*(32), 11595-11606. https://doi.org/10.1021/acs.energyfuels.8b02787

Knothe, G. (2015). Dependence of biodiesel fuel properties on the structure of fatty acid alkyl esters. *Fuel processing technology, 86*(10), 1059-1070.Knothe, G., and Razon, L. F. (2017). Biodiesel fuels. Progress in Energy and Combustion Science, 58, 36-59. https://doi.org/10.1016/j.pecs.2016.08.001

Knothe, G., & Steidley, K. R. (2005). Lubricity of components of biodiesel and diesel. The origin of biodiesel lubricity. *Energy and fuels, 19*(3), 1192-1200.

Kohse-Höinghaus, K. (2021). Combustion in the Future: The Importance of Chemistry. *Proceedings of the Combustion Institute, 1*(38), 1-56. https://doi.org/10.1016/j.proci.2020.06.375

Küçükosman, R., Yontar, A. A., & Ocakoglu, K. (2022). Nanoparticle additive fuels: Atomization, combustion and fuel characteristics. *Journal of analytical and applied Pyrolysis, 165*, 105575.

Kumar, C., Babu, M. G., & Das, L. (2006). Experimental investigations on a karanja oil methyl ester fueled di diesel engine: *SAE Technical Paper*.

Kumar, M. V., Babu, A. V., & Kumar, P. R. (2018). The impacts on combustion, performance and emissions of biodiesel by using additives in direct injection diesel engine. *Alexandria Engineering Journal, 57*(1), 509-516. https://doi.org/10.1016/j.aej.2016.12.016.

Kumar, P., *et al*. (2019). "Optimization of Engine Parameters for Improved Fuel Efficiency and Emission Reduction Using Grey Relational Analysis." *Journal of Cleaner Production, 216*, 595-606.

Lakshminarayanan, P. A., Aghav, Y. V., & Shi, Y. (2010). *Modelling diesel combustion* (Vol. 53, p. 287). New York: Springer.

Lapuerta, M., Rodríguez-Fernández, J., & Agudelo, J. R. (2008). Diesel particulate emissions from used cooking oil biodiesel. *Bioresource Technology, 99*(4), 731-740.

Leach, F., Kalghatgi, G., Stone R., & Miles, P. (2020). The scope for improving the efficiency and environmental impact of internal combustion engines. *Transportation Engineering,1*, 10005.

Lee, C., Park, a., & Kwon, S. (2005). An Experimental Study On the Atomization and Combustion Characteristics of Biodiesel-blended Fuels. *Energy and Fuels, 5*(19), 2201-2208. https://doi.org/10.1021/ef050026h

Leung, D. Y. C., Wu, X., & Leung, M. K. H. (2010). A review on biodiesel production using catalyzed transesterification. *Applied Energy*, *87*(4), 1083–1095. https://doi.org/10.1016/j.apenergy.2009.10.006

Liaquat, A. M., Masjuki, H. H., Kalam, M. A., Fattah, I. R., Hazrat, M. A., Varman, M., ... & Shahabuddin, M. (2013). Effect of Oleander biodiesel blended fuels on engine performance and emission characteristics. *Procedia Engineering*, *56*, 583-590.

Lin, Y., *et al*. (2017). "Grey-Taguchi Method Based Multi-Objective Optimization of Engine Operating Parameters for Lowering Fuel Consumption and NOx Emission*." Energy*, *120*, 502-515.

Lindstad, E., Eskeland, G. S., Rialland, A., & Valland, A. (2020). Decarbonizing maritime transport: The importance of engine technology and regulations for LNG to serve as a transition fuel. *Sustainability*, *12*(21), 8793.

Liptak, B. G. (Ed.). (2003). *Instrument Engineers' Handbook, Volume One: Process Measurement and Analysis (Vol. 1)*. CRC press.

Liu, J., & Quek, S. T. (2013). An ultra-accurate hybrid smoothed finite element method for piezoelectric problem. *Engineering Analysis with Boundary Elements*, *50*, 188-197.

Mahmudul, H. M., Hagos, F. Y., Mamat, R., Adam, A. A., Ishak, W. F. W., & Alenezi, R. (2017). Production, characterization and performance of biodiesel as an alternative fuel in diesel engines–A review. *Renewable and Sustainable Energy Reviews*, *72*, 497-509.

Maithomklang, S., Wathakit, K., Sukjit, E., Sawatmongkhon, B., & Srisertpol, J. (2022). Utilizing Waste Plastic Bottle-based Pyrolysis Oil as an Alternative Fuel. *ACS Omega*, *24*(7), 20542-20555. https://doi.org/10.1021/acsomega.1c07345.

Mäki, E., Saastamoinen, H., Melin, K., Matschegg, D., & Pihkola, H. (2021). Drivers and barriers in retrofitting pulp and paper industry with bioenergy for more efficient production of liquid, solid and gaseous biofuels: A review. *Biomass and Bioenergy*, *148*, 106036.

Masime, J. O., Mbatia, B. N., Ogur, E. O., Aluoch, A. O., Lalah, J. O., & Otieno, G. (2022). Life Cycle Analysis of Yellow Oleander Biodiesel Production in Kenya. *Life*, *9*(6), 01-15.

Mat, A, N. S., Khoo, K. S., Chew, K. W., Show, P. L., Chen, W. H., & Nguyen, T. H. P. (2020). Sustainability of the four generations of biofuels–a review. *International Journal of Energy Research*, *44*(12), 9266-9282. https://doi.org/10.1002/er.5557.

Mavrotas, G., & Florios, K. (2013). An improved version of the augmented ε-constraint method (AUGMECON2) for finding the exact Pareto set in multi-objective integer programming problems. *Applied Mathematics and Computation*, *219*(18), 9652-9669.

McCarthy, P., Rasul, M. G., & Moazzem, S. (2011). Comparison of the performance and emissions of different biodiesel blends against petroleum diesel. *International Journal of Low-Carbon Technologies*, *6*(4), 255-260.

McCormick, R. L., Tennant, C. J., Hayes, R. R., Black, S., Ireland, J., McDaniel, T., Williams, A., Frailey, M., & Sharp, C. A. (2006). Regulated emissions from biodiesel fuels from on/off-road applications. *SAE Transactions,* 883-895. https://doi.org/10.4271/2006-01-3281

Medina, M. (2020). *Experimental Studies of High-pressure Gasoline Fuel Sprays for Advanced Internal Combustion Engines* (Doctoral dissertation).

Menga, L. (2022). Industrial revolution and the birth of modern architecture. *International Scientific Journal Vision*, *7*(1), 105-123.

Mishra, S., Anand, K., & Mehta, P. (2016). Predicting the Cetane Number of Biodiesel Fuels from Their Fatty Acid Methyl Ester Composition. *Energy and Fuels, 12*(30), 10425-10434. https://doi.org/10.1021/acs.energyfuels.6b01343

Mofijur, M., Masjuki, H. H., Kalam, M. A., Hazrat, M. A., Liaquat, A. M., Shahabuddin, M., & Varman, M. (2012). Prospects of biodiesel from Jatropha in Malaysia. *Renewable and sustainable energy reviews*, *16*(7), 5007-5020.

Mofijur, M., Masjuki, H. H., Kalam, M. A., Atabani, A. E., Fattah, I. R., & Mobarak, H. M. (2014). Comparative evaluation of performance and emission characteristics of Moringa oleifera and Palm oil based biodiesel in a diesel engine. *Industrial crops and products*, *53*, 78-84.

Mofijur, M., Masjuki, H.H., Kalam, M.A., Atabani, A.E., Fattah, I.M.R., & Mobarak, H. M., (2014). Comparative evaluation of performance and emission characteristics of Moringa oleifera and palm oil based biodiesel in a diesel engine. *Industrial Crops and Products, 53*, 78-84. https://doi.org/10.1016/j.indcrop.2013.12.011

Mofijur, M., Rasul, M., Hyde, J., & Bhuyia, M. (2015). Role of Biofuels On IC Engines Emission Reduction. *Energy Procedia, (75),* 886-892. https://doi.org/10.1016/j.egypro.2015.07.211.

Monirul, I., Masjuki, H., Kalam, M., Zulkifli, N., Rashedul, H., Rashed, M., … & Mosarof, M. (2015). A Comprehensive Review On Biodiesel Cold Flow Properties and Oxidation Stability Along

with Their Improvement Processes. *RSC Advances, 105*(5), 86631-86655. https://doi.org/10.1039/c5ra09555g.

Montgomery., D. C. & Lynch, C. M, (2017). Optimal experimental designs for hypothesis testing with multiple factors: maximising power for the biological sciences. *International Journal of Experimental Design and Process Optimisation*, *7*(2), 105-114.

Mosarof, M. H., Kalam, M. A., Masjuki, H. H., Ashraful, A. M., Rashed, M. M., Imdadul, H. K., & Monirul, I. M. (2015). Implementation of palm biodiesel based on economic aspects, performance, emission, and wear characteristics. *Energy conversion and Management*, *105*, 617-629.

Moser, B. R., & Vaughn, S. F. (2010). Evaluation of alkyl esters from Camelina sativa oil as biodiesel and as blend components in ultra-low-sulfur diesel fuel. *Bioresource technology*, *101*(2), 646-653.

Muanruksa, P., Dujjanutat, P., & Kaewkannetra, P. (2020). Entrapping Immobilisation of Lipase On Biocomposite Hydrogels Toward for Biodiesel Production from Waste Frying Acid Oil. *Catalysts, 8*(10), 834. https://doi.org/10.3390/catal10080834.

Mueller, C. J., Boehman, A. L., & Martin, G. C. (2009). An experimental investigation of the origin of increased NOx emissions when fueling a heavy-duty compression-ignition engine with soy biodiesel. *SAE International Journal of Fuels and Lubricants*, *2*(1), 789-816.

Murugesan, A., Umarani, C., Chinnusamy, T. R., Krishnan, M., Subramanian, R., & Neduzchezhain, N. (2009). Production and analysis of bio-diesel from non-edible oils—a review. *Renewable and Sustainable Energy Reviews*, *13*(4), 825-834.

Mustayen, A. G. M. B., Rasul, M. G., Wang, X., Bhuiya, M. M. K., Negnevitsky, M., & Hamilton, J. (2022). Theoretical and experimental analysis of engine performance and emissions fuelled with jojoba biodiesel. *Energies*, *15*(17), 6282.

Myo, T. (2008). The effect of fatty acid composition on the combustion characteristics of biodiesel. *PhD thesis,* Kagoshima University, Japan.

Ndegwa, G., Moraa, V., & Iiyama, M. (2011). Potential for biofuel feedstock in Kenya. *World Agroforestry Centre (ICRAF)*.

Neupane, D. (2022). Biofuels from Renewable Sources, a Potential Option for Biodiesel Production. *Bioengineering*, *10*(1), 29.

Nguyen, V., & Pham, P. (2015). Biodiesels: Oxidizing enhancers to improve CI engine performance and emission quality. *Fuel*, *154*, 293-300. https://doi.org/10.1016/J.FUEL.2015.04.004.

Ni, P., Wang, X., & Li, H. (2020). A review on regulations, current status, effects and reduction strategies of emissions for marine diesel engines. *Fuel*, *279*, 118477. https://eprints.whiterose.ac.uk/164697/1/Marine%20diesel%20review%20Manuscript-final.pdf.

Niculescu, R., Clenci, A., & Iorga-Siman, V. (2019). Review on the use of diesel–biodiesel–alcohol blends in compression ignition engines. *Energies*, *12*(7), 1194.

Niu, L., *et al*. (2020). "Performance Optimization of Diesel Engine with a Grey-TOPSIS-Based Multi-Objective Optimization Approach." *Energies*, *13*(2), 369.

Nyakundi, D. (2022). Exchange Rates and the Volume of Imports in Kenya (*Doctoral dissertation*, University of Nairobi).

Ogunkunle, O., & Ahmed, N. A. (2019). A review of global current scenario of biodiesel adoption and combustion in vehicular diesel engines. *Energy Reports*, *5*(1), 1560-1579.

Ondimu, S., Raude, J. M., and Wanjala, G. (2019). Personal Computer-Based Control and Monitoring System for Biodiesel Algae Photobioreactor.

Örs, İ., Sarıkoç, S., Atabani, A. E., & Ünalan, S. (2019). Experimental investigation of effects on performance, emissions and combustion parameters of biodiesel–diesel–butanol blends in a direct-injection CI engine. *Biofuels*.

Osawa, W. O., Sahoo, P. K., Onyari, J. M., & Mulaa, F. J. (2015). Experimental investigation on performance, emission and combustion characteristics of *croton endocarps* biodiesel blends in direct injection diesel engine. *International Journal of Science and Technology*, 26-34.

Padmavati, M., Kumar, B. R., & Sıngh, V. K. (2017). Virtual Labs on Secondary Metabolic Pathways in Plants. *International Journal of Biology Education*, *5*(2).

Palani, Y., Devarajan C., Manickam D., & Thanikodi S. (2022). Performance and emission characteristics of biodiesel-blend in diesel engine: *A review*, *Environ. Eng. Res. 27*(1), 1-12

Pandey, G. (2019). Biomass Based Bio-electro Fuel Cells Based on Carbon Electrodes: An Alternative Source of Renewable Energy. *SN Applied Sciences, 5*(1). https://doi.org/10.1007/s42452-019-0409-4.

Pandian, M. S., Palanisamy, K., & Rajakumar, S. (2019). Parameter optimization of biodiesel fueled engine incorporating differential evolution algorithm blended with modulus arithmetic operators. Renewable energy, 132, 186-200.

Nair, J. N., Kaviti, A. K., & Daram, A. K. (2017). Analysis of performance and emission on compression ignition engine fuelled with blends of neem biodiesel. *Egyptian Journal of Petroleum, 26*(4), 927-931.

Patel, V. R., Dumancas, G. G., Kasi Viswanath, L. C., Maples, R., & Subong, B. J. (2016). Castor oil: Properties, uses, and optimization of processing parameters in commercial production. *Lipid insights, 9*, 1-12. https://doi.org/10.4137/LPI.S40233

Paula, R. S., Figueredo, I. M., Vieira, R. S., Nascimento, T. L., Cavalcante, C. L., Machado, Y. L., & Rios, M. A. (2019). Castor–babassu biodiesel blends: estimating kinetic parameters by Differential Scanning Calorimetry using the Borchardt and Daniels method. *SN Applied Sciences, 1*, 1-7.

Pereira, R. C., Pereira, F. M., Oliveira, L. S., Costa Neto, P. R., Oliveira, J. E., Fernandes, H. R., & Scares, C. H. (2019). Fuel properties and emission analysis for blends of selected oils from Amazonian biomass. *Renewable Energy, 141,* 393–405. https://doi.org/10.1016/j.renene.2019.04.021

Peterson, C. L., & Reece, D. L. (1994). Emissions tests with an on-road vehicle fueled with methyl and ethyl esters of rapeseed oil. *ASAE paper.* ASAE, St. Joseph, MI.

Pham, M. T., Hoang, A. T., Le, A. D., Al-Tawaha, A. R., Dong, V. H., & Le, V. V., (2018). Measurement and Prediction of the Density and Viscosity of Biodiesel Blends. *International Journal of Technology, 5(9),* 1015. https://doi.org/10.14716/ijtech.v9i5.1950.

Powell, J. J. (2010). Engine performance and exhaust emissions from a diesel engine using cottonseed oil biodiesel. *Texas A and M University*.

Prabu, S. S. (2019). Experimental investigations on a DI diesel engine fueled with diesel-biodiesel blends and effect of antioxidant additive. *Applied Thermal Engineering, 148,* 1175–1182. https://doi.org/10.1016/j.applthermaleng.2018.11.140

Pulko, B., *et al*. (2018). "Multi-Objective Optimization of a Diesel Engine Using MOGA and NSGA-II Algorithms." *Energies, 11*(3), 603.

Pullen, J., & Saeed, K. (2012). An overview of biodiesel oxidation stability. *Renewable and Sustainable Energy Reviews, 16*(8), 5924-5950.

Rakopoulos, D. C., Rakopoulos, C. D., Papagiannakis, R. G., Giakoumis, E. G., Karellas, S., & Kosmadakis, G. M. (2016). Combustion and emissions in an HSDI engine running on diesel or vegetable oil base fuel with n-butanol or diethyl ether as a fuel extender. *Journal of Energy Engineering*, *142*(2), E4015006.

Ramírez-Verduzco, L. F., Rodríguez-Rodríguez, J. E., & Jaramillo-Jacob, A. D. (2012). Predicting cetane number, kinematic viscosity, density and higher heating value of biodiesel from its fatty acid methyl este composition. *Fuel*, *91*(1), 102-111. https://doi.org/10.1016/j.fuel.2011.06.070

Rao, G., Saravanan, S., Sampath, S., & Rajgopal, K. (2006). Emission characteristics of a direct injection diesel engine fuelled with bio-diesel and its blends. *Paper presented at the Proceedings of the International Conf. on Resource Utilization and Intelligent Systems,* India. Allied publishers private limited.

Rastogi, P. M., Sharma, A., & Kumar, N. (2021). Effect of CuO nanoparticles concentration on the performance and emission characteristics of the diesel engine running on jojoba (Simmondsia Chinensis) biodiesel. *Fuel*, *286*, 119358.

Refaat, A. A. (2009). Correlation between the chemical structure of biodiesel and its physical properties. *International Journal of Environmental Science and Technology*, *6*(4), 677-694. https://doi.org/10.1007/BF03326054

Resitoglu, I. A., Altinişik, K., & Keskin, A. (2014). The pollutant emissions from diesel-engine vehicles and exhaust aftertreatment systems. *Clean Technologies and Environmental Policy*, *17*, 15-27.

Riyadi, T. W., Hernandez, M. S., Herawan, S. G., Idris, M., Paristiawan, P. A., Putra, N. R. & Veza, I. (2023). Biodiesel for HCCI engine: Prospects and challenges of sustainability biodiesel for energy transition. *Results in Engineering*, 100916. https://doi.org/10.1016/j.rineng.2023.100916.

Sagar, S., Udaya Mohanan, K., Cho, S., Majewski, L. A., & Das, B. C. (2022). Emulation of synaptic functions with low voltage organic memtransistor for hardware oriented neuromorphic computing. *Scientific reports*, *12*(1), 3808.

Sajid, Z., Zhang, Y., & Khan, F. (2016). Process design and probabilistic economic risk analysis of bio-diesel production. *Sustainable Production and Consumption*, *5*, 1-15.

Sajjadi, B., Raman, A. A. A., & Arandiyan, H. (2016). A comprehensive review on properties of edible and non-edible vegetable oil-based biodiesel: Composition, specifications and prediction models. *Renewable and Sustainable Energy Reviews*, *63*, 62-92.

Sakthivel, V. P., Goh, H. H., Srikrishna, S., Sathya, P. D., & Rahim, S. K. A. (2020). Multi-objective squirrel search algorithm for multi-area economic environmental dispatch with multiple fuels and valve point effects. *IEEE Access*, *9*, 3988-4007.

Salama, E. S., Kurade, M. B., Abou-Shanab, R. A., El-Dalatony, M. M., Yang, I. S., Min, B., & Jeon, B. H. (2017). Recent progress in microalgal biomass production coupled with wastewater treatment for biofuel generation. *Renewable and Sustainable Energy Reviews*, *79*, 1189-1211.

Saroha, A., Pal, D., Kaur, V., Kumar, S., Bartwal, A., Aravind, J., ... & Wankhede, D. P. (2022). Agro-morphological variability and genetic diversity in linseed (Linum usitatissimum L.) germplasm accessions with emphasis on flowering and maturity time. *Genetic Resources and Crop Evolution*, *69*(1), 315-333.

Senda, J., Okui, N., Tsukamoto, T., & Fujimoto, H. (2004). On-board measurement of engine performance and emissions in diesel vehicle operated with bio-diesel fuel: SAE Paper.

Shahidi, F. (Ed.). (2005). *Bailey's Industrial Oil and Fat Products, Industrial and Nonedible Products from Oils and Fats (Vol. 6).* John Wiley and Sons.

Sharma, A., Sharma, P., Chintala, V., Khatri, N., & Matsakas, L. (2020). Environment-friendly Biodiesel/diesel Blends for Improving the Exhaust Emission and Engine Performance to Reduce the Pollutants Emitted From Transportation Fleets. *International Journal of Environmental Research and Public Health*, *11*(17), 3896. https://doi.org/10.3390/ijerph17113896.

Silitonga, A. S., Masjuki, H. H., Mahlia, T. M. I., Ong, H. C., Chong, W. T., & Boosroh, M. H. (2013). Overview properties of biodiesel diesel blends from edible and non-edible feedstock. *Renewable and Sustainable Energy Reviews*, *22*, 346-360.

Singh, M., Gandhi, S. K., Mahla, S. K., & Sandhu, S. S. (2018). Experimental investigations on performance and emission characteristics of variable speed multi-cylinder compression ignition engine using Diesel/Argemone biodiesel blends. *Energy Exploration and Exploitation*, *36*(3), 535-555.

Singh, R. N., Singh, S. P., & Pathak, B. S. (2007). Performance of renewable fuel based CI engine. *Agricultural Engineering International: CIGR Journal*, *9*(1), 12-19.

Sivaramakrishnan, K., & Ravikumar, P. (2021). Application of hybrid genetic algorithm to optimize the performance and emission parameters of a variable compression ratio diesel engine fuelled with fish oil biodiesel. *Fuel, 301*, 121177.

Solomatine, D. P., & Ostfeld, A. (2008). Data-driven modelling: some past experiences and new approaches. *Journal of Hydroinformatics, 10*(1), 3–22. https://doi.org/10.2166/hydro.2008.015

Soudagar, M. E. M., Mujtaba, M. A., Safaei, M. R., Afzal, A., Ahmed, W., Banapurmath Soudagar, N. R., ... & Taqui, S. N. (2021). Effect of Sr@ ZnO nanoparticles and Ricinus communis biodiesel-diesel fuel blends on modified CRDI diesel engine characteristics. *Energy, 215*, 119094.Strezov, V., and Cho, H. H. (2020). Environmental impact assessment from direct emissions of Australian thermal power generation technologies. *Journal of Cleaner Production*, *270*(1), 122515.

Strong, C., Erickson, C., & Shukla, D. (2004). Evaluation of biodiesel fuel: Literature review: Montana Department of Transportation Research Section.

Su, C., Nguyen, H., Pham, U., Nguyen, M., & Juan, H. (2018). Biodiesel Production from a Novel Nonedible Feedstock, Soursop (Annona Muricata L.) Seed Oil. *Energies, 10*(11), 2562. https://doi.org/10.3390/en11102562.

Subramani, Karthik, & Muralidharan Karuppusamy. (2021) "Performance, combustion and emission characteristics of variable compression ratio engine using waste cooking oil biodiesel with added nanoparticles and diesel blends." *Environmental Science and Pollution Research* 28.45 (2021): 63706-63722.

Subramani, L., & Venu, H. (2018). Evaluation of methyl ester derived from novel Chlorella emersonii as an alternative feedstock for DI diesel engine and its combustion, performance and tailpipe emissions. *Heat and Mass Transfer*, *55*(1), 1513-1534. https://doi.org/10.1007/S00231-018-2530-0.

Tan, P. Q., Ruan, S. S., Hu, Z. Y., Lou, D. M., & Li, H. (2014). Particle number emissions from a light-duty diesel engine with biodiesel fuels under transient-state operating conditions. *Applied Energy*, *113*, 22-31.

Tasic, I., Tomić, M., Aleksić, A., Đurišić-Mladenović, N., Martinovic, F., & Micic, R. D. (2019). Improvement of Low-temperature Characteristics of Biodiesel by Additivation. *Chemical Industry*, *2*(73), 103-114. https://doi.org/10.2298/hemind190117009t.

Taylor, A. H. (2019). Diesel Engine Air Handling Strategies for Fuel Efficient Aftertreatment Thermal Management and Connected and Automated Class 8 Trucks (Doctoral dissertation, Purdue University).

Teixeira, L. S. G., Couto, M. B., Souza, G. S., Filho, M. A., Assis, J. C. R., Guimarães, P. R. B., Pontes, L. A. M., Almeida, S. Q., & Teixeira, J. S. R. (2010). Characterization of beef tallow biodiesel and their mixtures with soybean biodiesel and mineral diesel fuel. *Biomass and Bioenergy*, *34*(3), 418-422. https://doi.org/10.1016/j.biombioe.2009.12.007

Tesfa, B., Mishra, R., Gu, F., & Powles, N. (2010). Prediction Models for Density and Viscosity of Biodiesel and Their Effects On Fuel Supply System in CI Engines. *Renewable Energy*, *12*(35), 2752-2760. https://doi.org/10.1016/j.renene.2010.04.026

Tveit, O. (2015). Study of biodiesel emission characteristics in internal combustion engines (Master's thesis, Norwegian University of Science and Technology).

Vadivelu, T., Ramanujam, L., Ravi, R., Vijayalakshmi, S. K., & Ezhilchandran, M. (2022). An exploratory study of direct injection (DI) diesel engine performance using CNSL–ethanol biodiesel blends with hydrogen. *Energies, 16*(1), 415. https://doi.org/10.3390/en160100415

Van Gerpen, J. (2004). *Biodiesel production technology*. USDA/NCAUR.

Verma, P., & Singh, V. M. (2014). Assessment of diesel engine performance using cotton seed biodiesel. *Integrated Research Advances, 1*(1), 1-4.

Wood, B. M., Kirwan, K., Maggs, S., Meredith, J., & Coles, S. R. (2015). Study of combustion performance of biodiesel for potential application in motorsport. *Journal of Cleaner Production*, *93*, 167-173. https://doi.org/10.1016/j.jclepro.2015.01.074

Xue, J., Grift, T. E., & Hansen, A. C. (2011). Effect of biodiesel on engine performances and emissions. *Renewable and Sustainable Energy Reviews, 15*(2), 1098-1116. https://doi.org/10.1016/j.rser.2010.11.016.

Yaakob, Z., Narayanan, B. N., & Padikkaparambil, S. (2014). A review on the oxidation stability of biodiesel. *Renewable and Sustainable Energy Reviews*, *35*, 136-153.

Yang, C., Zhang, B., Cui, C., Wu, J., Ding, Y., & Wu, Y. (2016). Standards and protocols for characterization of algae-based biofuels. *Trends in Renewable Energy, 2*(2), 56-60. https://doi.org/10.17737/tre.2016.2.2.0023.

Yoshimoto, Y., Onodera, M., & Tamaki, H. (2001). Performance and emission characteristics of diesel engines fueled by vegetable oils (SAE Technical Paper No. 2001-01-1984). *SAE International*. https://doi.org/10.4271/2001-01-1984.

Young, P. C., Pedregal, D. J., & Tych, W. (1999). Dynamic harmonic regression. *Journal of Forecasting, 18*(6), 369-394. https://doi.org/10.1002/(SICI)1099-131X(199911).

Yuan, X., Li, L., Zeng, G., Tong, J., Xie, W., & Wang, L. (2022). Current status and perspective on catalytic conversion of vegetable oils into biodiesel: A state-of-the-art review. *Fuel, 315*, 123487. https://doi.org/10.1016/j.fuel.2022.123487.

Zhang, Q., Pennycott, A., Burke, R., Akehurst, S., & Brace, C. (2015). Predicting the nitrogen oxides emissions of a diesel engine using neural networks (SAE Paper No. 2015-01-1626). *SAE International*. https://doi.org/10.4271/2015-01-1626.

Zhang, Y., Yu, L., Yung, K. F., Leung, D. Y., Sun, F., & Lim, B. L. (2012). Over-expression of AtPAP2 in *Camelina sativa* leads to faster plant growth and higher seed yield. *Biotechnology for Biofuels, 5*(1), 1-10. https://doi.org/10.1186/1754-6834-5-10.

Zhang, Z., Cheng, X., Xing, Z., & Gui, X. (2023). Pareto multi-objective optimization of metro train energy-saving operation using improved NSGA-II algorithms. *Chaos, Solitons and Fractals, 176*, 114183. https://doi.org/10.1016/j.chaos.2023.114183.

Zheng, M., Asad, U., Reader, G. T., Tan, Y., & Wang, M. (2009). Energy efficiency improvement strategies for a diesel engine in low-temperature combustion. *International Journal of Energy Research, 33*(1), 8-28. https://doi.org/10.1002/er.1470.

APPENDICES

Appendix A: NACOSTI approval

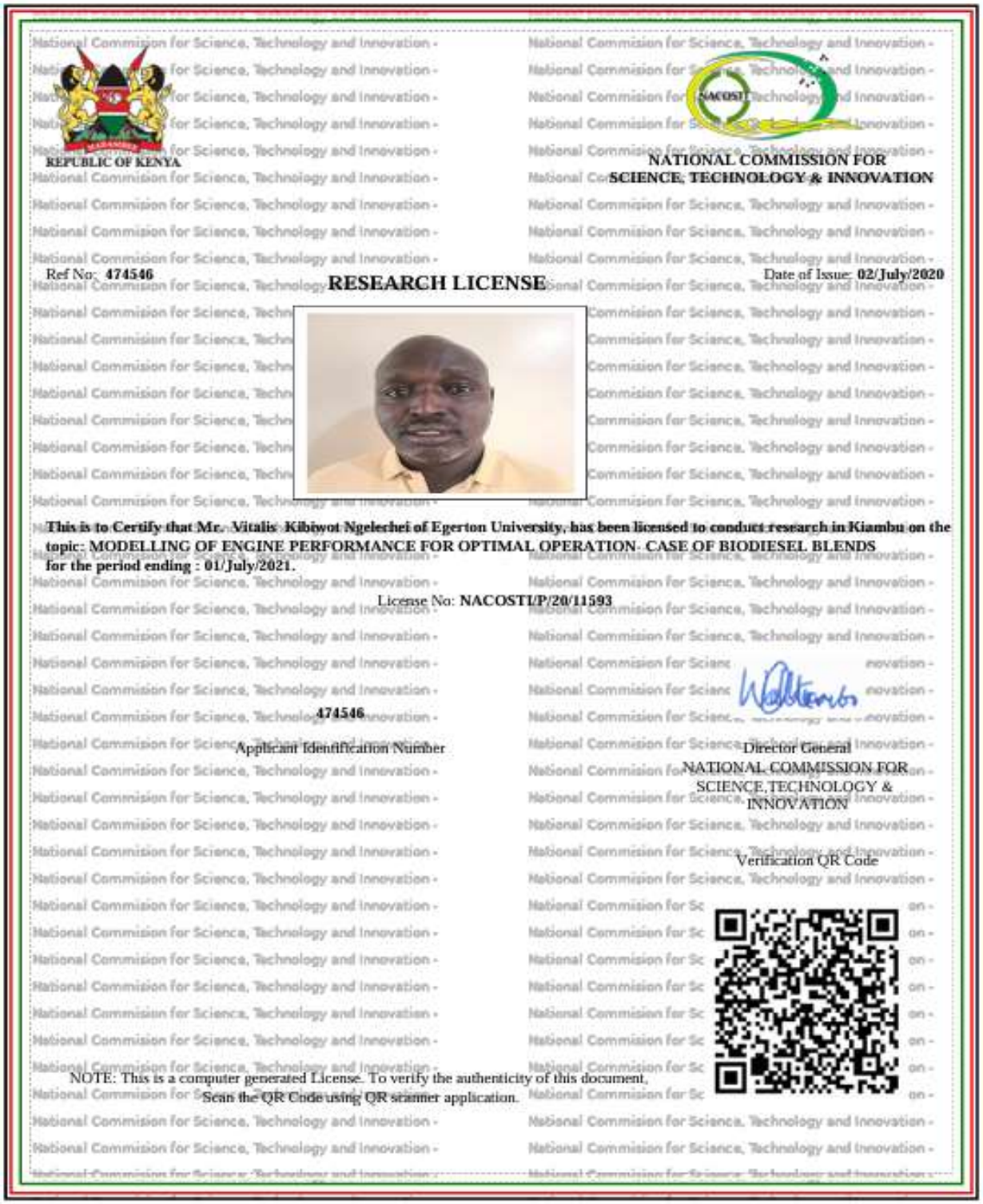

REPUBLIC OF KENYA

NATIONAL COMMISSION FOR SCIENCE, TECHNOLOGY & INNOVATION

Ref No: **474546**

Date of Issue: **02/July/2020**

RESEARCH LICENSE

This is to Certify that Mr. Vitalis Kibiwot Ngelechei of Egerton University, has been licensed to conduct research in Kiambu on the topic: MODELLING OF ENGINE PERFORMANCE FOR OPTIMAL OPERATION- CASE OF BIODIESEL BLENDS for the period ending : 01/July/2021.

License No: **NACOSTI/P/20/11593**

474546

Applicant Identification Number

Director General
NATIONAL COMMISSION FOR SCIENCE,TECHNOLOGY & INNOVATION

Verification QR Code

NOTE: This is a computer generated License. To verify the authenticity of this document, Scan the QR Code using QR scanner application.

Appendix B: Published Papers

Appendix B.1: Published Paper on modelling of engine performance and emissions

Editon Consortium Journal of Engineering and Computer Science [ISSN: 2789 - 9985]

Issue no: 1 | **Vol no:** 1 | **February** 2024: 1-10

Modelling of engine performance and emissions fueled by biodiesel blends

Vitalis N. Kibiwot[1]
Daudi Nyaanga[2]
Musa R. Njue[3]
George O. Owino[4]

(1.2.3.4) Egerton University, Kenya.
Main author email: vkibiwot@egerton.ac.ke

Article History
Received: 2023-10-23
Accepted: 2024-01-21
Published: 2024-02-02

Cite this article in APA
Kibiwot, V. N., Nyaanga, D. M., Njue, M. R., & Owino, G. O. (2024). Modelling of engine performance and emissions fueled by biodiesel blends. *Editon consortium journal of engineering and computer science, 1*(1), 1-10. https://doi.org/10.51317/ecjecs.v1i1.458

Abstract

The aim of this study is to investigate the modelling of engine performance and emissions fueled by biodiesel blends. Biodiesel blended with diesel, were introduced to mitigate its decreased power output, poor fuel atomization and increased nitrogen oxides emissions. Unfortunately, it has been difficult to obtain the best biodiesel blend level for optimal engine performance, since it sourced from a variety of vegetable oils whose fuel parameters and interactions differ considerably, causing variation in their combustion processes. The research has developed mathematical models, using Buckingham pi-theorem analytical method and experimental data to predict CI engine performance parameters {brake thermal efficiency (Bte) and carbon monoxide (CO) emissions, while, specific fuel consumption (sfc) and nitrogen oxides (NOx) emission fueled by different biodiesels' diesel blends. The experimental tests were performed on factorial design method using a 3.5 kW one cylinder four stroke CI engine on a test rig connected to an eddy current electric dynamometer, running on biodiesels (WVO, canola, sunflower, oleander and coconut) with their blends (mixed at ratios by volume of biodiesel: diesel;10:90, 15:85, 20:80, 25:75 and 30:70) using the ASTM procedures. The results showed that engine fueled with biodiesel and their blends had lower Bte and CO emissions, while, sfc and NOx emission were higher, as compared those of diesel fuel. The developed mathematical model predicted Bte, sfc, CO and NOx with error margins of 1.65, 15.98, 4.69 and 2.78 per cent respectively as compared to the experimental results.

Key words: Biodiesel blend, emissions, modelling, performance.

Appendix B.2: Published Paper on optimization of engine performance and emissions

Journal of Computer Science and Technology

[ISSN 2789-9985]
Volume: 02 Issue: 01 | May-2024

JCST

OPTIMISATION OF ENGINE PERFORMANCE AND EMISSIONS FUELED BY BIODIESEL BLENDS

Authors

Kibiwot V. N[1]; Nyaanga D. M[2]; Njue M. R[3]; Owino G. O[4]

Main author email: vkibiwot@egerton.ac.ke

(1.2.3) Egerton University, Kenya; (4) Technical University of Kenya, Kenya.

Cite this article in APA

Kibiwot, V. N., Nyaanga, D. M., Njue, M. R., & Owino, G. O. (2024). Optimisation of engine performance and emissions fueled by biodiesel blends. *Journal of computer science and technology, 2*(1), 10-19. https://doi.org/10.51317/jcst.v2i1.531

OPEN ACCESS
A publication of Editon Consortium Publishing (online)

Article history
Received: 16.02.2024
Accepted: 11.03.2024
Published: 30.04.2024

Scan this QR to read the paper online

Abstract

This study sought to find out the optimisation of engine performance and emissions fueled by biodiesel blends. Compression ignition(CI) engines are most widely used as a power source for many applications, such as automotive and agricultural purposes, as well as portable machines, because of their higher torque, power output, energy content per unit mass, and fuel cost. Unfortunately, CI engines use diesel fuel, which emits greenhouse gases (GHG) and pollutes the environment. Biodiesel has been the preferred alternative fuel due to its benefits of reducing GHG emissions and being used on engines with little or no modification. Biodiesel blends with diesel were introduced to mitigate its decreased engine performance. Unfortunately, it has been difficult to obtain the best blend mix ratios for optimal engine performance and emission since biodiesels are sourced from a variety of vegetable oils whose fuel properties and their interactions differ considerably, causing variation in their combustion processes. The study used non-dominated sorting genetic algorithm II (NSGA II) optimisation to establish the best biodiesel blend to optimise engine performance and emissions. In conclusion, the study found that specific biodiesel blends for various feedstocks (waste vegetable oil, canola, oleander, coconut, and sunflower) achieved the optimal balance between reducing harmful emissions and maintaining engine performance. This study suggests expanding the model's inputs to encompass more fuel properties, engine types, and real-world conditions to improve its applicability, efficiency, and reliability.

Key terms: Biodiesel blends, engine performance, exhaust emission, optimisations.

Appendix C: Map of research site

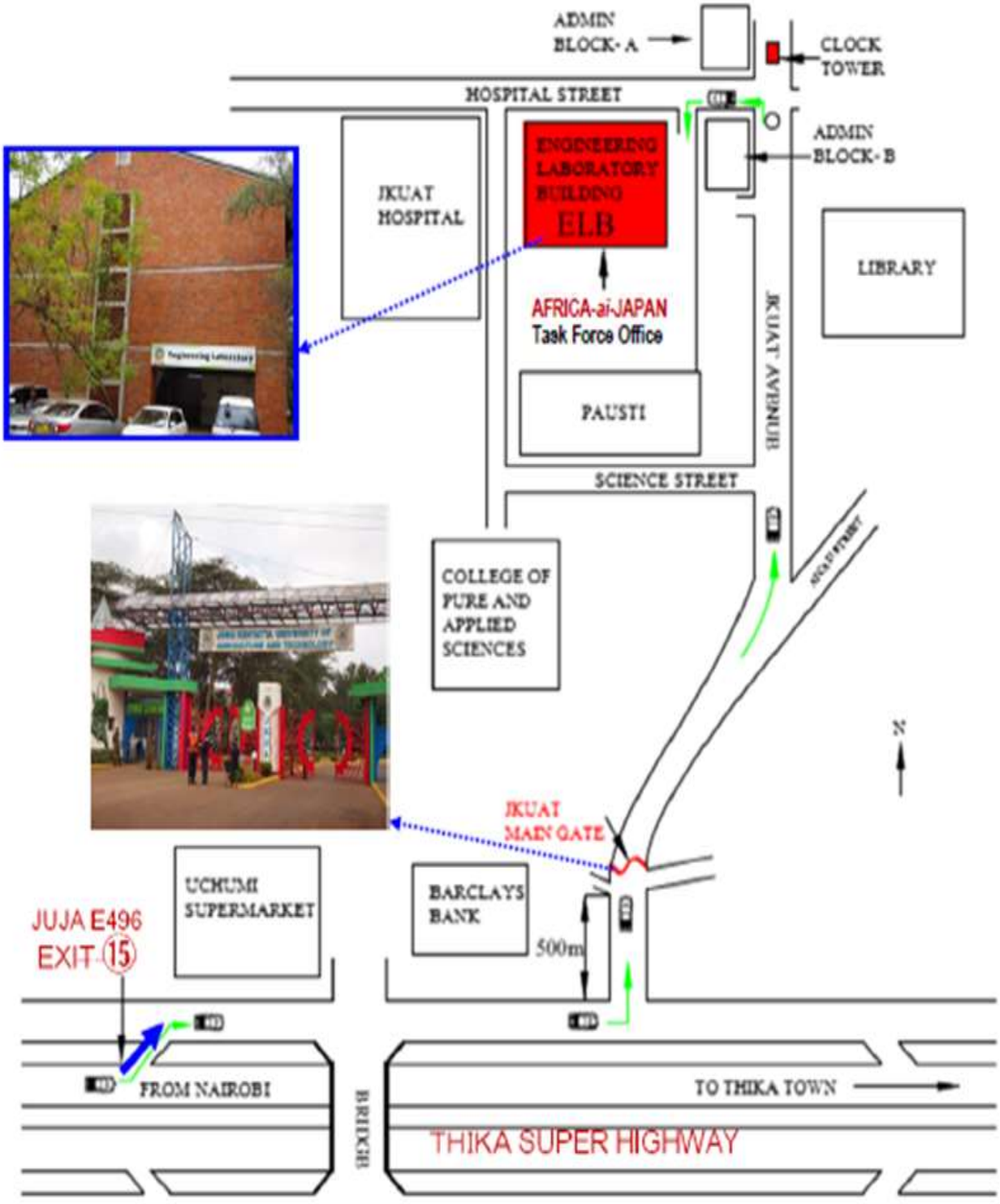

Map of research site engineering Lab at Jomo Kenyatta university of agriculture and technology (JKUAT)

Appendix D: Results and Data Analysis

Appendices D.1: Fuel Properties results

(a). Densities of the fuels:

Densities of diesel was determined using procedure in section 3.1 and given in tables D.1 and figure D1. Density was given as gradient of 'best fit' line of graph.

Table D1: Density of diesel

Volume, ml	Mass, g
25	20.9
50	41.8
75	62.8
100	83.6
125	104.5
150	125.6
175	146.5
200	167.4
225	188.1
250	209.0
Density	837.6

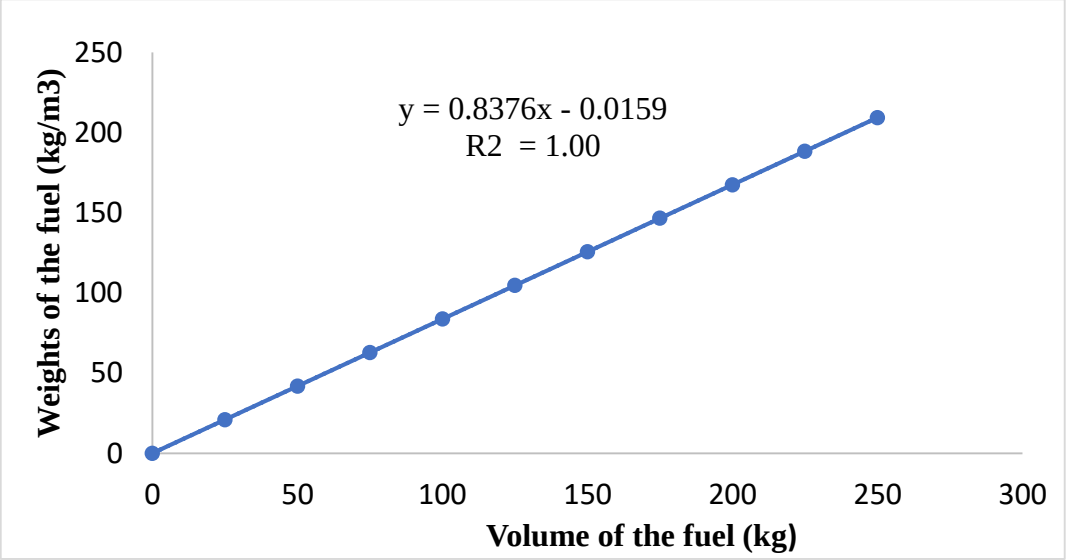

Figure A1: Volume verses weight for diesel

Densities for biodiesel blends given tables A3.1-A3.6 and summarized data in table 3.1 section 3.1;

Table A2: Densities of coconut biodiesel blends

Volume of biodiesel (ml)	Mass of the volume of the biodiesel, g.					
	B100	**B30**	**B25**	**B20**	**B15**	**B10**
25	23.6	21.9	21.9	21.7	21.6	21.4
50	46.1	43.8	43.6	43.4	43.3	43.1
75	69.3	65.1	65.4	65.2	64.9	64.8
100	92.5	87.8	87.3	86.8	86.6	86.1
125	115.6	109.9	109.1	108.4	108.2	107.9
150	138.8	131.0	130.5	130.3	129.8	129.2
175	161.2	153.3	152.1	152.0	151.4	150.6
200	185.2	175.2	174.9	173.8	173.1	172.9
225	208.1	197.4	196.8	195.5	194.8	193.6
250	231.3	219.1	218.2	217.2	216.7	215.5
Density	925.1	876.2	872.6	868.8	865.5	862.1

Table A3: Densities of waste vegetable oil (WVO) biodiesel blends data

Volume of biodiesel (ml)	Mass of the volume of the biodiesel, g.					
	B100	**B30**	**B25**	**B20**	**B15**	**B10**
25	22.0	21.7	21.5	21.8	21.5	21.4
50	43.8	43.1	43.1	43.5	43.0	42.5
75	65.3	64.7	64.9	65.1	64.7	64.3
100	87.9	86.2	86.1	86.9	85.9	85.7
125	109.5	107.9	107.9	108.1	107.5	107.2
150	131.4	129.2	129.5	130.3	128.8	128.7
175	153.4	150.4	151.0	153.6	150.2	150.0
200	175.1	172.3	172.8	173.9	171.7	171.9
225	197.5	194.0	193.6	195.5	193.1	192.5
250	219.5	215.9	215.4	217.0	215.4	214.3
Density	876.6	861.5	860.4	859.4	858.3	857.2

Table A4: Densities of oleander biodiesels' blends

Volume of biodiesel (ml)	Mass of the volume of the biodiesel, g.					
	B100	**B30**	**B25**	**B20**	**B15**	**B10**
25	21.3	21.0	21.5	21.5	21.4	21.4
50	43.5	43.2	42.7	43.0	42.6	42.9
75	65.4	64.6	64.5	64.2	64.3	64.3
100	87.2	86.0	86.6	85.9	85.7	86.1
125	109.0	107.3	107.4	107.3	107.6	107.1
150	130.8	129.0	128.8	128.4	128.7	128.5
175	152.4	150.0	150.3	150.2	150.1	149.9
200	174.2	172.8	171.7	171.8	171.5	171.3
225	196.1	193.5	194.1	193.1	192.6	192.5
250	218.1	215.1	215.1	214.6	214.2	214.2
Density	21.3	21.0	21.5	21.5	21.4	21.4

Table A5: Densities of canola biodiesel blends data

Volume of biodiesel (ml)	Mass of the volume of the biodiesel, g.					
	B100	**B30**	**B25**	**B20**	**B15**	**B10**
25	22.2	21.3	21.7	21.1	21.5	21.7
50	44.5	43.0	43.2	43.1	43.0	42.9
75	66.9	64.9	64.6	64.6	64.3	64.4
100	89.9	86.9	86.4	86.1	86.1	85.0
125	111.4	108.4	108.0	107.1	107.8	107.3
150	133.8	129.8	129.4	129.3	129.8	133.0
175	156.1	151.8	151.3	150.6	150.6	128.5
200	178.3	173.0	172.8	172.4	172.1	171.6
225	200.6	194.1	194.4	193.1	193.5	193.1
250	223.0	216.3	216.6	215.5	216.0	214.7
Density	891.6	865.0	864.2	862.2	860.5	858.6

Table A6: Densities of sunflower biodiesel blends

Volume of biodiesel (ml)	Mass of the volume of the biodiesel, g.					
	B100	**B30**	**B25**	**B20**	**B15**	**B10**
25	22.1	20.2	21.5	21.6	21.6	21.5
50	44.1	43.2	43.2	43.0	43.0	42.9
75	66.1	64.1	64.6	64.5	64.0	64.9
100	88.0	86.3	86.1	86.0	86.0	85.8
125	110.9	107.9	107.7	107.5	107.5	107.1
150	132.3	129.5	129.2	129.0	128.9	128.6
175	154.1	150.9	150.5	150.7	150.4	150.1
200	176.6	172.1	172.2	172.1	172.5	171.5
225	198.6	194.3	193.9	193.7	193.7	192.8
250	220.7	215.9	215.5	215.1	214.7	214.4
Density	882.9	863.6	861.8	860.3	859.2	857.5

Table A7: Densities of linseed biodiesel blends

Volume of biodiesel (ml)	Mass of the volume of the biodiesel, g.					
	B100	**B30**	**B25**	**B20**	**B15**	**B10**
25	22.4	21.7	21.5	21.6	21.6	21.4
50	45.0	43.5	43.3	43.0	43.1	43.0
75	67.2	65.4	65.0	64.8	64.5	64.4
100	89.7	86.9	86.6	86.3	86.1	85.9
125	112.0	108.5	107.9	107.9	107.8	107.1
150	133.9	130.3	129.9	129.8	129.3	128.8
175	156.8	152.0	151.6	151.1	151.0	150.3
200	180.6	173.7	173.1	172.7	172.4	171.8
225	201.9	195.4	195.0	195.2	194.1	193.2
250	223.5	217.1	216.5	216.5	215.4	214.5
Density	896.5	868.5	865.7	863.3	861.8	858.9

(b) Kinematic viscosities

Kinematic viscosities of biodiesels and diesel were determined using redwood viscometer as described in section 3.2.2 and its data in tables A8 – A13 below

Table B1: Kinematic viscosities of Waste vegetable biodiesel (WVO) blends

Biodiesel Blend	viscosity's	Reps of effluent Time (t), s,			
		Average Time (t)	t1	t2	t3
B100	5.24	37.7	37.4	37.7	38.3
B30	3.81	34.1	33.9	34.2	34.4
B25	3.71	33.8	33.8	33.6	33.9
B20	3.61	33.6	33.5	33.9	33.7
B15	3.51	33.3	33.4	33.5	33.2
B10	3.40	33.1	33.2	33.3	32.9

Table B2: Kinematic viscosities for canola biodiesel blends

Biodiesel Blend	Kinematic Viscosity, cst	Reps of effluent Time (t), s,			
		average time (t)	t1	t2	t3
B100	4.95	36.9	36.5	36.9	37.8
B30	3.73	33.9	33.6	33.9	34.4
B25	3.64	33.6	33.3	33.9	34.3
B20	3.55	33.4	33.4	33.2	33.5
B15	3.46	33.2	33.0	33.1	33.0
B10	3.38	33.0	32.7	33.3	33.7

Table B3: Kinematic viscosities of oleander biodiesel blends

Biodiesel Blend	Kinematic viscosity, cst	Reps of effluent Time (t), s,			
		average t	t1	t2	t3
B100	5.84	39.3	40.2	39.6	37.5
B30	3.99	34.5	34.5	34.6	34.6
B25	3.86	34.2	33.8	34.3	35.0
B20	3.73	33.9	33.6	34.5	34.4
B15	3.60	33.5	33.2	33.6	34.2

Table B4: Kinematic viscosities of sunflower biodiesel blends

Biodiesel Blend	Kinematic Viscosity, cst	Reps of effluent Time (t), s,			
		average t	t1	t2	t3
B100	5.36	38.0	37.6	37.9	38.8
B30	3.85	34.2	34.2	33.9	34.1
B25	3.74	33.9	33.6	34.2	34.5
B20	3.63	33.6	33.4	33.5	34.1
B15	3.52	33.4	33.5	33.4	33.1
B10	3.42	33.1	33.1	33.3	33.1

Table B5: Kinematic viscosities for oleander biodiesel blends

Biodiesel Blend	Kinematic viscosity, cst	Reps of effluent Time (t), s,			
		Average Time (t)	t1	t2	t3
B100	6.04	39.8	39.8	33.7	39.9
B30	4.05	34.7	34.7	34.5	34.6
B25	3.91	34.3	34.3	34.5	34.3
B20	3.77	34.0	33.9	34.4	34.1
B15	3.63	33.6	33.9	33.5	33.1
B10	3.48	33.3	33.4	33.1	33.0

Table B6: Kinematic viscosities of Linseed Biodiesel blends

Biodiesel Blend	Kinematic Viscosity, cst	Reps of effluent Time (t), s,			
		average t	t1	t2	t3
B100	5.69	38.9	38.6	40.1	39.5
B30	3.95	34.4	34.3	35.0	34.6
B25	3.82	34.1	33.7	34.3	34.9
B20	3.70	33.8	33.5	33.9	34.4
B15	3.57	33.5	33.7	33.3	33.1
B10	3.45	33.2	33.2	33.0	33.2

c). Lower heat value

Table C1: lower heating value of WVO biodiesel blends

	Reps	Sample Mass (g)	Temp. Rise	mass of burned wire	calory correction	CV cal/g	CV kJ/kg
B100	**R1**	0.61	2.62	0.56	479.39	9443.16	39510.18
	R2	0.69	3.69	0.46		9409.99	39371.4
	R3	0.71	3.35	0.45		9412.4	39381.48
	avg	0.67	3.22	0.49		9421.85	39421
B30	**R1**	0.47	2.1	0.46	383.85	10107.92	42291.54
	R2	0.55	3.17	0.36		10074.75	42152.75
	R3	0.57	2.83	0.35		10077.16	42162.84
	avg	0.53	2.7	0.39		10086.61	42202.38
B25	**R1**	0.51	2.36	0.49	409.44	10169.89	42550.82
	R2	0.59	3.43	0.39		10136.72	42412.04
	R3	0.61	3.09	0.38		10139.13	42422.12
	avg	0.57	2.96	0.42		10148.58	42461.66
B20	**R1**	0.47	2.13	0.46	379.75	10231.48	42808.51
	R2	0.55	3.2	0.36		10198.31	42669.73
	R3	0.57	2.86	0.35		10200.72	42679.81
	avg	0.53	2.73	0.39		10210.17	42719.35
B15	**R1**	0.51	2.39	0.48	403.42	10293.24	43066.92
	R2	0.59	3.46	0.38		10260.07	42928.13
	R3	0.61	3.12	0.37		10262.48	42938.22
	avg	0.57	2.99	0.41		10271.93	42977.76
B10	**R1**	0.47	2.16	0.46	379.75	10355.07	43325.61
	R2	0.55	3.23	0.36		10321.9	43186.83
	R3	0.57	2.89	0.35		10324.31	43196.91
	avg	0.53	2.76	0.39		10333.76	43236.45

Table C2: lower heating value of coconut biodiesel blends

Blend	Reps	Sample mass(g)	Temp. Rise	mass of burned wire	calory correction	CV cal/g	CV kJ/kg
B100	**R1**	0.61	2.57	0.56	480.06	9279.44	38825.16
	R2	0.69	3.64	0.46		9246.27	38686.38
	R3	0.71	3.3	0.45		9248.68	38696.46
	avg	0.67	3.17	0.49		9258.26	38736
B30	**R1**	0.51	2.33	0.49	408.98	10073.02	42145.5
	R2	0.59	3.4	0.39		10039.85	42006.72
	R3	0.61	3.06	0.38		10042.26	42016.8
	avg	0.57	2.93	0.42		10051.71	42056.34
B25	**R1**	0.51	2.36	0.5	417.24	10136.42	42410.8
	R2	0.59	3.43	0.4		10103.25	42272.02
	R3	0.61	3.09	0.39		10105.66	42282.1
	avg	0.57	2.96	0.43		10115.11	42321.64
B20	**R1**	0.46	2.12	0.45	377.31	10206.88	42705.59
	R2	0.54	3.19	0.35		10173.71	42566.81
	R3	0.56	2.85	0.34		10176.12	42576.89
	avg	0.52	2.72	0.38		10185.57	42616.43
B15	**R1**	0.51	2.39	0.49	408.07	10272.6	42980.57
	R2	0.59	3.46	0.39		10239.43	42841.79
	R3	0.61	3.12	0.38		10241.84	42851.87
	avg	0.57	2.99	0.42		10251.29	42891.41
B10	**R1**	0.46	2.15	0.45	370.55	10338.84	43257.7
	R2	0.54	3.22	0.35		10305.67	43118.92
	R3	0.56	2.88	0.34		10308.08	43129
	avg	0.52	2.75	0.38		10317.53	43168.54

Table C3: Lower heating value of Canola biodiesels blends

Blend	Reps	Sample Mass (g)	Temp. Rise(^{0}K)	mass of burned wire	calory correction	CV cal/g	CV kJ/kg
B100	**R1**	0.61	2.48	0.56	484.81	9001.23	37661.16
	R2	0.69	3.55	0.46		8968.06	37522.38
	R3	0.71	3.21	0.45		8970.47	37532.46
	avg	0.67	3.08	0.49		8979.95	37572
B30	**R1**	0.47	2.08	0.46	386.33	10024.52	41942.61
	R2	0.55	3.15	0.36		9991.35	41803.83
	R3	0.57	2.81	0.35		9993.77	41813.91
	avg	0.53	2.68	0.39		10003.21	41853.45
B25	**R1**	0.51	2.34	0.49	408.41	10100.33	42259.76
	R2	0.59	3.41	0.39		10067.16	42120.98
	R3	0.61	3.07	0.38		10069.57	42131.06
	avg	0.57	2.94	0.42		10079.02	42170.6
B20	**R1**	0.61	2.86	0.56	483.51	10175.81	42575.59
	R2	0.69	3.93	0.46		10142.64	42436.81
	R3	0.71	3.59	0.45		10145.05	42446.89
	avg	0.67	3.46	0.49		10154.5	42486.43
B15	**R1**	0.51	2.38	0.49	408.41	10251.55	42892.5
	R2	0.59	3.45	0.39		10218.38	42753.72
	R3	0.61	3.11	0.38		10220.79	42763.8
	avg	0.57	2.98	0.42		10230.24	42803.34
B10	**R1**	0.51	2.4	0.49	407.27	10327.02	43208.26
	R2	0.59	3.47	0.39		10293.85	43069.48
	R3	0.61	3.13	0.38		10296.26	43079.56
	avg	0.57	3	0.42		10305.71	43119.1

Table C4: Lower heating value of sunflower biodiesel blends

Blend	Reps	Sample mass(g)	Temp. Rise (^{0}K)	mass of burned wire	calory correction	CV cal/g	CV kJ/kg
B100	**R1**	0.51	2.06	0.49	412.49	9060.03	37907.16
	R2	0.59	3.13	0.39		9026.86	37768.38
	R3	0.61	2.79	0.38		9029.27	37778.46
	avg	0.57	2.66	0.42		9038.72	37818
B30	**R1**	0.47	2.08	0.46	381.41	10040.96	42011.39
	R2	0.55	3.15	0.36		10007.79	41872.61
	R3	0.57	2.81	0.35		10010.2	41882.69
	avg	0.53	2.68	0.39		10019.65	41922.23
B25	**R1**	0.47	2.1	0.46	379.75	10114.09	42317.34
	R2	0.55	3.17	0.36		10080.92	42178.56
	R3	0.57	2.83	0.35		10083.33	42188.64
	avg	0.53	2.7	0.39		10092.78	42228.18
B20	**R1**	0.51	2.36	0.49	408.41	10186.75	42621.36
	R2	0.59	3.43	0.39		10153.58	42482.58
	R3	0.61	3.09	0.38		10155.99	42492.66
	avg	0.57	2.96	0.42		10165.44	42532.2
B15	**R1**	0.51	2.39	0.49	414.11	10259.52	42925.84
	R2	0.59	3.46	0.39		10226.35	42787.06
	R3	0.61	3.12	0.38		10228.76	42797.14
	avg	0.57	2.99	0.42		10238.21	42836.68
B10	**R1**	0.61	2.92	0.58	504.66	10332.02	43229.16
	R2	0.69	3.99	0.48		10298.85	43090.38
	R3	0.71	3.65	0.47		10301.26	43100.46
	avg	0.67	3.52	0.51		10310.71	43140

Table C5: lower heating value (Cv) of Coconut Biodiesels

Blend	Reps	Sample mass(g)	Temp. Rise(^{0}K)	mass of burned wire	calory correction	CV cal/g	CV kJ/kg
B100	**R1**	0.66	2.59	0.57	515.88	8674.75	36295.16
	R2	0.74	3.66	0.47		8641.58	36156.38
	R3	0.76	3.32	0.46		8643.99	36166.46
	avg	0.72	3.19	0.5		8653.44	36206
B30	**R1**	0.51	2.31	0.49	414.13	9958.31	41665.56
	R2	0.59	3.38	0.39		9925.14	41526.78
	R3	0.61	3.04	0.38		9927.51	41536.86
	avg	0.57	2.91	0.42		9936.98	41576.4
B25	**R1**	0.56	2.57	0.52	442.05	10045.77	42031.48
	R2	0.64	3.64	0.42		10012.62	41892.7
	R3	0.66	3.3	0.41		10015.01	41902.78
	avg	0.62	3.17	0.45		10024.46	41942.32
B20	**R1**	0.47	2.11	0.46	386.22	10132.8	42395.65
	R2	0.55	3.18	0.36		10099.63	42256.87
	R3	0.57	2.84	0.35		10102.04	42266.95
	avg	0.53	2.71	0.39		10111.49	42306.49
B15	**R1**	0.51	2.37	0.49	407.27	10220.04	42760.63
	R2	0.59	3.44	0.39		10186.87	42621.85
	R3	0.61	3.1	0.38		10189.28	42631.93
	avg	0.57	2.97	0.42		10198.73	42671.47
B10	**R1**	0.61	2.9	0.56	482.50	10312.06	43145.66
	R2	0.69	3.97	0.46		10278.89	43006.88
	R3	0.71	3.63	0.45		10281.3	43016.96
	avg	0.67	3.5	0.49		10290.75	43056.5

Appendices D.2: Engine test results

a). Format of ICEngineSoft output

The report was genearted using the ware and store in the computer.

Report Date :1st October, 2020, Time : 12:14:30 PM

Organization : Egerton Univ., Operator : Kibiwot V.N

Data File : EngineSoft DataKIB rpm1000.xlsx, Last Modified Date: Thursday, October 1, 2020,

Config. File : Research Diesel Engine.xls

Engine Details :

ICEngine set up under test is Research Diesel having power 3.50 kW @ 1500 rpm which is 1 Cylinder, Four stroke , Constant Speed, Water Cooled, Diesel Engine, with Cylinder Bore 87.50(mm), Stroke Length 110.00(mm), Connecting Rod length 234.00(mm), Compression Ratio 17.50, Swept volume 661.45 (cc)

Combustion Parameters :

Specific Gas Const (kJ/kgK) : 1.00, Air Density (kg/m^3) : 1.17, Adiabatic Index : 1.41, Polytrophic Index:1.28, Number Of Cycles : 10, Cylinder Pressure Reference:4, Smoothing:2, TDC Reference : 0

Performance Parameters :

Orifice Diameter (mm) : 20.00, Orifice Coeff. Of Discharge : 0.60, Dynamometer Arm Legnth (mm) : 185, Fuel Pipe dia (mm) : 12.40, Ambient Temp. (Deg C) : 27, Pulses Per revolution : 360, Water flow engine: 250 lpHr, Water flow calorimeter: 100 lpHr, Compression ratio: 17.5, Ignition angle: 25.175 degree.

Fuel :Diesel, Properties: Density (Kg/m^3) : 820, Lower Calorific Value (Kj/Kg) : 43906, Kinematic viscosity (mm^2/s): 3.21, Cetane Number (No.): 48

The results of the engine experiments were tabulated as a set of constant speed varying loads, shown in the tables A3 below; {Note the symbols used};

N - Engine speed; W – Engine load; Bp – Equivalent Brake power; m= Fuel flow rate; Sfc – Specific fuel consumption Bte – Brake thermal efficiency NOx = Nitrogen oxide emissions, CO = carbon monoxide emissions; CO_2 = carbon dioxide emissions.

b). Sampled ANOVA (SAS) analysis for brake thermal efficiency

The GLM Procedure: Class Level Information

Class	Level	Values
BP	10	0.83 1.17 1.48 1.74 1.79 2.13 2.25 2.53 2.82 3.43
Blend	1	B10
rep	3	1,2,3
Number of observations		30

The GLM Procedure for dependent variable: Bte

Source	DF	Squares	Mean square	F value	Pr>F
Model	9	404.8988700	44.9887633	449888	<.0001
Error	20	0.0020000	0.0001000		
		Corrected Total	29	404.9008700	

R-Square	Coeff Var	Root MSE	Bte Mean
0.999995	0.049429	0.010000	20.23100

Source	DF	Type I SS	Mean Square	F Value	Pr > F
Blend	0	0.0000000	.	.	.
BP	9	404.8988700	44.9887633	449888	<.0001

Source	DF	Type III SS	Mean Square	F Value	Pr > F
Blend	0	0.0000000	.	.	.
BP	9	404.8988700	44.9887633	449888	<.0001

Least Squares Means Adjustment for Multiple Comparisons: Tukey Standard

BP	Bte LS-MEAN	Error	Pr > |t|	Number
0.83	12.2700000	0.0057735	<.0001	1
1.17	15.6900000	0.0057735	<.0001	2
1.48	18.1200000	0.0057735	<.0001	3
1.74	20.1800000	0.0057735	<.0001	4
1.79	19.7500000	0.0057735	<.0001	5
2.13	23.1000000	0.0057735	<.0001	6
2.25	23.0100000	0.0057735	<.0001	7
2.53	23.0300000	0.0057735	<.0001	8
2.82	23.4100000	0.0057735	<.0001	9
3.43	23.7500000	0.0057735	<.0001	10

Least Squares Means for effect BP; Pr > |t| for H0: LS-Mean(i)=LS-Mean(j)

Turkey Pairwise comparison

REGWQ Grouping	**N**	**Mean**	**Biodiesel**
a	3	0.420000	Coconut
b	3	0.400000	Sunflower
c	3	0.390000	Canola
d	3	0.350000	Oleander
e	3	0.340000	WVO

Dependent Variable: Bte

i/j	1	2	3	4	5	6	7	8	9	10
1		<.0001	<.0001	<.0001	<.0001	<.0001	<.0001	<.0001	<.0001	<.0001
2	<.0001		<.0001	<.0001	<.0001	<.0001	<.0001	<.0001	<.0001	<.0001
3	<.0001	<.0001		<.0001	<.0001	<.0001	<.0001	<.0001	<.0001	<.0001
4	<.0001	<.0001	<.0001		<.0001	<.0001	<.0001	<.0001	<.0001	<.0001
5	<.0001	<.0001	<.0001	<.0001		<.0001	<.0001	<.0001	<.0001	<.0001
6	<.0001	<.0001	<.0001	<.0001	<.0001		<.0001	<.0001	<.0001	<.0001
7	<.0001	<.0001	<.0001	<.0001	<.0001	<.0001		0.3497	<.0001	<.0001
8	<.0001	<.0001	<.0001	<.0001	<.0001	<.0001	0.3497		<.0001	<.0001
9	<.0001	<.0001	<.0001	<.0001	<.0001	<.0001	<.0001	<.0001		<.0001
10	<.0001	<.0001	<.0001	<.0001	<.0001	<.0001	<.0001	<.0001	<.0001	

t Tests (SEM) for Bte

t Grouping	Mean	N	BP
A	23.750000	3	3.43
B	23.410000	3	2.82
C	23.100000	3	2.13
D	23.030000	3	2.53
E	23.010000	3	2.25
F	20.180000	3	1.74
G	19.750000	3	1.79
H	18.120000	3	1.48
I	15.690000	3	1.17
J	12.270000	3	0.83

NOTE: This test controls the Type I comparison wise error rate, not the experiment wise error rate.

Alpha 0.05; Error Degrees of Freedom 20; Error Mean Square 0.0001; Critical Value of t 2.08596; Least Significant Difference 0.017

c). Sampled ANOVA (SAS) results for specific fuel consumption

The GLM Procedure: Class Level Information

Class	Levels	Values				
Blend	1	B15				
Biodiesel	5					
rep		Canola	Coconut	Oleander	Sunflower	WVO
		3	1	2	3	

The GLM Procedure: Dependent Variable: B15

Source	**DF**	**Type I SS**	**Mean Square**	**F Value**	**Pr > F**
Blend	0	0.00000000	.	.	
Biodiesel	4	0.01380000	0.00345000	34.50	<.0001
Source	DF	Type III SS	Mean Square	F Value	Pr > F
Blend	0	0.00000000	.	.	
Biodiesel	4	0.01380000	0.00345000	34.50	<.0001

The GLM Procedure: Adjustment for Multiple Comparisons: Tukey

Biodiesel	Sfc LSMEAN	Error	Pr > |t|	Number
Canola	0.39000000	0.00577350	<.0001	1
Coconut	0.42000000	0.00577350	<.0001	2
Olender	0.35000000	0.00577350	<.0001	3
Sunflwer	0.40000000	0.00577350	<.0001	4
WVO	0.34000000	0.00577350	<.0001	5

Least Squares Means for effect Biodiesel: Pr > |t| for H0: LS-Mean(i)=LS-Mean(j)
Dependent Variable: Sfc

i/j	1	2	3	4	5
1		0.0276	0.0044	0.7385	0.0008
2	0.0276		<.0001	0.1791	<.0001
3	0.0044	<.0001		0.0008	0.7385
4	0.7385	0.1791	0.0008		0.0002
5	0.0008	<.0001	0.7385	0.0002	

The GLM Procedure: t Tests (SEM) for Sfc

Alpha	0.05
Error Degrees of Freedom	10
Error Mean Square	0.0001
Critical Value of t	2.22814
Least Significant Difference	0.0182

NOTE: This test controls the Type I comparison-wise error rate, not the experimental error rate.

Turkey pairwise comparison

Biodiesel	N	t Grouping	Mean
Coconut	3	A	0.420000
Sunflower	3	B	0.400000
		B	
Canola	3	B	0.390000
Oleander	3	C	0.350000
		C	
WVO	3	C	0.340000

The GLM Procedure: Ryan-Einot-Gabriel-Welsch Multiple Range Test for Sfc

Alpha	0.05			
Error Degrees of Freedom	10			
Error Mean Square	0.0001			
Number of Means	2	3	4	5
Critical Range	0.022493	0.0248734	0.0249795	0.0268716

NOTE: This test controls the Type I error rate.

Turkey Pairwise comparison

REGWQ Grouping	**N**	**Mean**	**Biodiesel**
a	3	0.420000	Coconut
ab	3	0.400000	Sunflower
b	3	0.390000	Canola
c	3	0.350000	Oleander
d	3	0.340000	WVO

The GLM Procedure: Class Level Information

Class	Levels	Values
BP	10	0.83 1.17 1.48 1.74 1.79 2.13 2.25 2.53 2.82 3.43
Blend	1	B10
rep	3	1 2 3

The GLM Procedure: Dependent Variable: Bte

		Sum of			
Source	DF	Squares	Mean Square	F Value	Pr > F
Model	9	404.8988700	44.9887633	449888	<.0001
Error	20	0.0020000	0.0001000		
Corrected Total	29	404.9008700			
R-Square	Coeff. Var.	Root MSE	Bte Mean		
0.999995	0.049429	0.010000	20.23100		
Source	DF	Type I SS	Mean Square	F Value	Pr > F
Blend	0	0.0000000	.	.	.
BP	9	404.8988700	44.9887633	449888	<.0001
Source	DF	Type III SS	Mean Square	F Value	Pr > F
Blend	0	0.0000000	.	.	.
BP	9	404.8988700	44.9887633	449888	<.0001

The GLM Procedure: Least Squares Means Adjustment for Multiple Comparisons: Tukey

BP	Bte LS-Mean	Error	Pr > |t|	Number
0.83	12.2700000	0.0057735	<.0001	1
1.17	15.6900000	0.0057735	<.0001	2
1.48	18.1200000	0.0057735	<.0001	3
1.74	20.1800000	0.0057735	<.0001	4
1.79	19.7500000	0.0057735	<.0001	5
2.13	23.1000000	0.0057735	<.0001	6
2.25	23.0100000	0.0057735	<.0001	7
2.53	23.0300000	0.0057735	<.0001	8
2.82	23.4100000	0.0057735	<.0001	9
3.43	23.7500000	0.0057735	<.0001	10

Least Squares Means for effect Bp: Pr > |t| for H0: LS-Mean(i)=LS-Mean(j) Dependent Variable: Bte

i/j	1	2	3	4	5	6	7	8	9	10
1		<.0001	<.0001	<.0001	<.0001	<.0001	<.0001	<.0001	<.0001	<.0001
2	<.0001		<.0001	<.0001	<.0001	<.0001	<.0001	<.0001	<.0001	<.0001
3	<.0001	<.0001		<.0001	<.0001	<.0001	<.0001	<.0001	<.0001	<.0001
4	<.0001	<.0001	<.0001		<.0001	<.0001	<.0001	<.0001	<.0001	<.0001
5	<.0001	<.0001	<.0001	<.0001		<.0001	<.0001	<.0001	<.0001	<.0001
6	<.0001	<.0001	<.0001	<.0001	<.0001		<.0001	<.0001	<.0001	<.0001
7	<.0001	<.0001	<.0001	<.0001	<.0001	<.0001		0.3497	<.0001	<.0001
8	<.0001	<.0001	<.0001	<.0001	<.0001	<.0001	0.3497		<.0001	<.0001
9	<.0001	<.0001	<.0001	<.0001	<.0001	<.0001	<.0001	<.0001		<.0001
10	<.0001	<.0001	<.0001	<.0001	<.0001	<.0001	<.0001	<.0001	<.0001	

The GLM Procedure: t Tests (SEM) for Bte

Alpha	0.05
Error Degrees of Freedom	20
Error Mean Square	0.0001
Critical Value of t	2.08596
Least Significant Difference	0.017

NOTE: This test controls the Type I comparison-wise error rate, not the experimental error rate.

Turkey pairwise comparison for Bte

t Grouping	Mean	N	BP
A	23.750000	3	3.43
B	23.410000	3	2.82
C	23.100000	3	2.13
D	23.030000	3	2.53
E	23.010000	3	2.25
F	20.180000	3	1.74
G	19.750000	3	1.79
H	18.120000	3	1.48
I	15.690000	3	1.17
J	12.270000	3	0.83

d). Sampled ANOVA (SAS) output for Nitrogen oxides

The GLM Procedure Class Level Information

Class	Levels	Values
Bp	10	0.83 1.17 1.48 1.74 1.79 2.13 2.25 2.53 2.82 3.43
Blend	1	B10
rep	3	1 2 3

The GLM Procedure Dependent Variable: NOx

Source	DF	Sum of Squares	Mean Square	F Value	Pr > F
Model	9	15060.30000	1673.36667	1673.37	<.0001
Error	20	20.00000	1.00000		
Corrected Total	29	15080.30000			

R-Square	Coeff. Var.	Root MSE	NOx Mean
0.998674	2.583979	1.000000	38.70000

Source	DF	Type I SS	Mean Square	F Value	Pr > F
Blend	0	0.00000	.	.	.
Bp	9	15060.30000	1673.36667	1673.37	<.0001

Source	DF	Type III SS	Mean Square	F Value	Pr > F
Blend	0	0.00000	.	.	.
Bp	9	15060.30000	1673.36667	1673.37	<.0001

The GLM Procedure Least Squares Means Adjustment for Multiple Comparisons: Tukey

Bp	NOx LSMEAN	Error	Pr > |t|	Number
0.83	9.0000000	0.5773503	<.0001	1
1.17	15.0000000	0.5773503	<.0001	2
1.48	21.0000000	0.5773503	<.0001	3
1.74	27.0000000	0.5773503	<.0001	4
1.79	29.0000000	0.5773503	<.0001	5
2.13	42.0000000	0.5773503	<.0001	6
2.25	45.0000000	0.5773503	<.0001	7
2.53	51.0000000	0.5773503	<.0001	8
2.82	61.0000000	0.5773503	<.0001	9
3.43	87.0000000	0.5773503	<.0001	10

Least Squares Means for effect Bp: Pr > |t| for H0: LS-Mean(i)=LS-Mean(j)

Dependent Variable: of NOx

i/j	1	2	3	4	5	6	7	8	9	10
1		<.0001	<.0001	<.0001	<.0001	<.0001	<.0001	<.0001	<.0001	<.0001
2	<.0001		<.0001	<.0001	<.0001	<.0001	<.0001	<.0001	<.0001	<.0001
3	<.0001	<.0001		<.0001	<.0001	<.0001	<.0001	<.0001	<.0001	<.0001
4	<.0001	<.0001	<.0001		0.3497	<.0001	<.0001	<.0001	<.0001	<.0001
5	<.0001	<.0001	<.0001	0.3497		<.0001	<.0001	<.0001	<.0001	<.0001
6	<.0001	<.0001	<.0001	<.0001	<.0001		0.0381	<.0001	<.0001	<.0001
7	<.0001	<.0001	<.0001	<.0001	<.0001	0.0381		<.0001	<.0001	<.0001
8	<.0001	<.0001	<.0001	<.0001	<.0001	<.0001	<.0001		<.0001	<.0001
9	<.0001	<.0001	<.0001	<.0001	<.0001	<.0001	<.0001	<.0001		<.0001
10	<.0001	<.0001	<.0001	<.0001	<.0001	<.0001	<.0001	<.0001	<.0001	

The GLM Procedure: t Tests (SEM) for NOx

Alpha	0.05
Error Degrees of Freedom	20
Error Mean Square	1
Critical Value of t	2.08596
Least Significant Difference	1.7032

NOTE: This test controls the Type I comparison-wise error rate, not the experimental error rate.

t Grouping	Mean	N	Bp
a	87.0000	3	3.43
b	61.0000	3	2.82
c	51.0000	3	2.53
d	45.0000	3	2.25
e	42.0000	3	2.13
f	29.0000	3	1.79
g	27.0000	3	1.74
h	21.0000	3	1.48
i	15.0000	3	1.17
J	9.0000	3	0.83

e). Sampled ANOVA (SAS) output for Carbon monoxide

The GLM Procedure: Class Level Information

Class	Levels	Values
Biodiesel	5	Canola, Coconut, Sunflower, Oleander and WVO
Blend	1	B10
rep	3	1 2 3

The GLM Procedure: Dependent Variable: C-mono

Source	DF	Sum of Squares	Mean Square	F Value	Pr > F
Model	4	95888.40000	23972.10000	23972.1	<.0001
Error	10	10.00000	1.00000		
Corrected Total	14	95898.40000			
R-Square	Coef. Var.	Root MSE	C-mono Mean		
0.999896	0.047569	1.00000	2102.200		
Source	DF	Type I SS	Mean Square	F Value	Pr > F
Biodiesel	4	95888.40000	23972.10000	23972.1	<.0001
Blend	0	0.00000	.	.	.

The GLM Procedure: Adjustment for Multiple Comparisons: Tukey Standard

Biodiesel	C-mono LSMEAN	Error	Pr > |t|	Number
Canola	2088.00000	0.57735	<.0001	1
Coconut	2001.00000	0.57735	<.0001	2
Oleander	2175.00000	0.57735	<.0001	3
Sunflower	2036.00000	0.57735	<.0001	4
WVO	2211.00000	0.57735	<.0001	5

Least Squares Means for effect Biodiesel Pr > |t| for H0: LS-Mean(i)=LS-Mean(j)

Dependent Variable: C-mono

i/j	1	2	3	4	5
1		<.0001	<.0001	<.0001	<.0001
2	<.0001		<.0001	<.0001	<.0001
3	<.0001	<.0001		<.0001	<.0001
4	<.0001	<.0001	<.0001		<.0001
5	<.0001	<.0001	<.0001	<.0001	

The GLM Procedure: t Tests (SEM) for C-mono

Alpha	0.05
Error Degrees of Freedom	10
Error Mean Square	1
Critical Value of t	2.22814
Least Significant Difference	1.8193

NOTE: This test controls the Type I comparison wise error rate, not the experiment wise error rate.

Turkey Pairwise comparison

t Grouping	Mean	N	Biodiesel
a	2211.0000	3	WVO
b	2175.0000	3	Oleander
c	2088.0000	3	Canola
d	2036.0000	3	Sunflower
e	2001.0000	3	Coconut